Patrycja Dzianok

Imaging genetics: *APOE*/*PICALM* genes are associated with mild alterations in brain function in healthy, middle-aged individuals

PhD thesis
completed in the Laboratory
of Emotions Neurobiology
of the Nencki Institute of Experimental Biology
Polish Academy of Sciences

SUPERVISOR
Ewa Kublik, Ph.D., D.Sc.

Warsaw, 2023

NATIONAL SCIENCE CENTRE
POLAND

The research was funded by the Polish National Science Center (NCN) PRELUDIUM grant no. 2018/31/N/HS6/03551: “Executive attention, genetic risk of Alzheimer's disease and cingulate cortex: an EEG and fMRI study”
(principal investigator: Patrycja Dzianok).

Acknowledgments

To begin, I express my gratitude to my thesis supervisor, **Ewa Kublik**, Ph.D., D.Sc., who has been a true source of inspiration, guiding me to delve into the topics that captivate my interest.

My appreciation extends to Professor **Urszula Wojda** for her collaborative efforts and to all the people at the Laboratory of Preclinical Testing of Higher Standard who contributed to the miRNAs analysis of the collected samples.

Special thanks are due to **Tomasz Wolak**, Ph.D., D.Sc., who permitted the execution of MRI/fMRI experiments in his laboratory, and to everyone at the Bioimaging Research Center (Institute of Physiology and Pathology of Hearing, Poland) who played a role in their execution. I particularly acknowledge **Jakub Wojciechowski**, MSc, for his involvement in processing the experimental MRI data and for all consultations.

I also extend my gratitude to **Ingrida Antonova**, Ph.D., and all the students and interns (especially **Olga Stefańska**), who help in collection of experimental EEG data.

Lastly, I extend my gratitude to all the participants for actively participating in the experiments and generously contributing their time.

And a special thanks, for everyday support, go to Miłosz (my partner) & Floki (my dearest four-legged friend).

With a dedication to my mother — Joanna.

Abstract

The process of aging is a complex biological phenomenon that results in a decline in cellular function and tissue degeneration. The aging of the brain has clear implications for cognitive functioning. Neurodegenerative diseases are associated with increased damage and loss of nerve cells and excessive cognitive decline. Although the main risk factor for these diseases is age, it remains uncertain to what extent they are an inevitable aspect of the aging process or pathology which could possibly be prevented. Late-onset Alzheimer's disease (LOAD), the most prevalent cause of dementia, is a neurodegenerative disease that is often diagnosed in advanced stages. The etiology of LOAD is multifaceted and includes lifestyle, environmental, and genetic factors. Due to the global (especially noticeable in post-industrial and developed countries) problem of aging populations and increasing life expectancy, late-life diseases are becoming a growing burden on countries, societies, and healthcare systems. Detecting neurodegenerative diseases early is crucial for global healthcare and for affected individuals, as it enables the potential for early prevention and treatment. Therefore, understanding how Alzheimer's disease risk genes impact the brain function of healthy individuals is crucial in advancing this process.

This dissertation describes a study on the relationship of LOAD risk genes and brain function/structure and basic health indicators in middle-aged individuals without symptoms of dementia. A genetic screening involving 200 participants was conducted to assess two LOAD risk genes: *APOE* (encoding apolipoprotein E) and *PICALM* (encoding phosphatidylinositol binding clathrin assembly protein). A comprehensive demographic data was collected, along with a battery of psychometric tests assessing intelligence, memory, depression, and personality traits, among other factors. Based on the screening results, distinct groups were defined including individuals with no risk (N), carriers of risk variant exclusively in the *APOE* gene (A+P-), and carriers of risk variants in both the *APOE* and *PICALM* genes (A+P+). The groups differences were studied with neuroimaging techniques, involving both structural methods (magnetic resonance imaging, MRI) and functional approaches (electroencephalography, EEG; and functional MRI, fMRI). Protocols were employed to examine resting-state brain activity and cognitive functions with use of the memory (Sternberg Task) and executive function/cognitive control tasks (Multi-Source Interference Task, MSIT). Extended blood tests were also performed, including microRNA panel associated with Alzheimer's disease.

The groups were similar in demographic characteristics, and most psychometric tests yielded comparable results. Importantly, no differences between control and risk groups

were found in memory abilities as assessed by The California Verbal Learning Test (CVLT). In terms of health indicators, the at-risk groups differed from control group in standard blood test parameters, showing slightly elevated levels of eosinophils and hemoglobin content in red blood cells. Analysis of circulating miRNAs in plasma revealed downregulation of miR-29b-3p, a trait reported in scientific literature as characteristic of Alzheimer's disease (AD) patients. Changes in the brain function were also observed in individuals who carried risk variants of the specified genes. The findings indicated a reduction in the complexity of the EEG signal and a phenomenon termed “slowing” of the EEG. These two characteristics are recognized as key signal features distinguishing individuals with LOAD from healthy participants in existing literature. Behavioral data from cognitive tasks showed minimal difference in behavior – at-risk subjects showed increased reaction times for challenging task variants, while maintaining correct responses. Analysis of brain responses during MSIT showed differences between the study groups in the components related to the attention and cognitive control (N2 event-related potential component) and during response execution phase (late sustained potential, LSP). In terms of brain structure, a reduced thickness of the cerebral cortex is one of the symptoms of Alzheimer's disease; our study showed similar changes in the right temporal pole for individuals with risky gene variants. Examination of the brain connectivity within selected frequency bands, revealed no significant differences between groups (with results corrected for multiple comparisons). However, a trend (at the uncorrected level) indicated a comparable pattern of changes, reminiscent of those observed in individuals with dementia. fMRI connectivity showed significant alterations in small clusters within some areas (e.g., posterior cingulate cortex) linked to the default mode network (DMN). Furthermore, task-related fMRI revealed differences in brain activation between the groups in areas partially associated with this network. Disruption of the DMN is frequently observed in the neurodegenerative diseases. Moreover, alterations in regions linked to the so-called signature of Alzheimer's Disease, such as the angular gyrus, inferior temporal gyrus, and supramarginal gyrus, were also found.

An important finding is the absence of a linear accumulation of effects along the risk level axis. *APOE* and *PICALM* seem to influence the organism in a complex way. Obviously, only some of health-related and neuroimaging-related parameters may be associated with the studied genetic variants and their impact on Alzheimer's disease development. These features should be explored in the future and possibly be incorporated into the pool of potential “biomarkers” for Alzheimer's disease, aiding in early diagnosis and/or risk assessment of the disease. Longitudinal studies are essential to identify individuals from our experimental groups, who will eventually develop symptoms of the disease.

Streszczenie

Starzenie się jest skomplikowanym procesem biologicznym prowadzącym do utraty funkcji komórkowych i degeneracji tkanek. Starzenie się mózgu ma oczywisty wpływ na funkcjonowanie poznawcze. Choroby neurodegeneracyjne są związane z postępującym uszkodzeniem i utratą komórek nerwowych oraz ze znacznym pogorszeniem funkcji poznawczych. Mimo, że głównym czynnikiem ryzyka tych chorób jest zaawansowany wiek, to nie wiadomo w jakim stopniu są one nieuniknionym elementem starzenia, a w jakim patologią, której być może da się uniknąć. Choroba Alzheimera o późnym początku (LOAD), będąca chorobą neurodegeneracyjną, jest najczęstszą przyczyną demencji i często jest diagnozowana dopiero w zaawansowanych stadiach. LOAD charakteryzuje się złożoną etiologią, uwzględniającą styl życia, czynniki środowiskowe i genetyczne. Ze względu na globalny (szczególnie zauważalny w postindustrialnych i rozwiniętych krajach) problem starzejących się społeczeństw, oraz wydłużenie średniej długości życia, choroby wieku późnego będą coraz większym obciążeniem dla państw, społeczeństw czy systemów opieki zdrowotnej. Wczesne wykrywanie chorób neurodegeneracyjnych, a tym samym możliwość stosowania wczesnej profilaktyki i terapii, jest więc istotnym aspektem ochrony zdrowia na świecie i jest kluczowe dla pacjentów. Poszerzenie wiedzy na temat wpływu genów ryzyka choroby Alzheimera na funkcjonowanie mózgu osób zdrowych jest kluczowe w tym procesie.

Niniejsza rozprawa opisuje badania dotyczące zależności genów ryzyka LOAD i funkcji/struktury mózgu oraz podstawowych wskaźników zdrowia u osób w średnim wieku bez objawów demencji. Wykonano przesiewowe badanie genetyczne (N = 200) w kierunku dwóch genów ryzyka LOAD: *APOE* (ang. *apolipoprotein E*) oraz genu *PICALM* (ang. *phosphatidylinositol binding clathrin assembly protein*). Dodatkowo zebrano dane dotyczące demografii oraz wykonano serię testów psychometrycznych (między innymi z wykorzystaniem narzędzi do badania inteligencji, pamięci, osobowości i depresji). Na podstawie badania przesiewowego wybrano osoby bez ryzykownych wariantów genów (N), osoby z ryzykownymi wariantami tylko w zakresie genu *APOE* (A+P-) i osoby z ryzykiem dotyczącym genów *APOE* oraz *PICALM* (A+P+). Do przeprowadzenia badania wykorzystano metody neuroobrazowe: strukturalne (magnetyczny rezonans jądrowy, MRI) i funkcjonalne (elektroencefalografia, EEG; oraz funkcjonalny MRI, fMRI). W trakcie badań neuroobrazowych wykorzystano protokół badania spoczynkowej aktywności mózgu (tzw. *resting-state*) oraz dwa zadania poznawcze badające pamięć (zadanie Sternberga) oraz funkcje wykonawcze/kontrolę poznawczą (zadanie *Multi-Source Interference Task*).

Przeprowadzono również rozszerzone badania krwi, w tym badania panelu mikroRNA dla choroby Alzheimera.

Badane grupy były jednolite pod względem miar demograficznych i większości wyników w testach psychometrycznych. Co ważne, nie wykazano różnic w zdolnościach pamięciowych w wykonaniu Kalifornijskiego Testu Uczenia się Językowego (CVLT). Również w zakresie miar dotyczących zdrowia, grupa osób z ryzykiem różniła się od grupy osób bez ryzyka choroby w zakresie parametrów standardowego badania krwi (nieznacznie podwyższony poziom eozynofilii, oraz zawartość hemoglobiny w krwinkach czerwonych). Ponadto, badania krążących miRNA w osoczu wykazały obniżenie poziomu (ang. *downregulation*) miR-29b-3p, co również jest opisywane w literaturze naukowej jako jedna z cech charakteryzująca pacjentów z AD. Zaobserwowano również zmiany w funkcjonowaniu mózgu osób z ryzykownymi wariantami opisanych genów. Wyniki wskazują na mniejszą złożoność sygnału EEG oraz jego tzw. „spowolnienie". Te dwie cechy sygnału EEG opisywane są w literaturze jako odróżniające osoby chore na LOAD od osób zdrowych. Dane behawioralne z zadań poznawczych wykazały niewielkie różnice w zachowaniu – u osób z ryzykiem zaobserwowano wydłużone czasy reakcji dla trudnych wariantów zadań, przy zachowaniu poprawności odpowiedzi. Analiza funkcjonowania mózgu podczas wykonywania zadania poznawczego (MSIT) wykazała różnice pomiędzy badanymi grupami na poziomie potencjałów wywołanych związanych z uwagą i kontrolą poznawczą (w szczególności dla fali N2) oraz w późniejszym oknie, kiedy badani udzielali odpowiedzi (LPP). W zakresie anatomii mózgu zmniejszenie grubości kory mózgu jest jednym z objawów w przebiegu choroby Alzheimera; w naszym badaniu wykazano podobne zmiany w prawym biegunie skroniowym dla osób z ryzykownymi wariantami genów. Badanie połączeń funkcjonalnych w mózgu (ang. *connectivity*) w zakresie wybranych pasm sygnału EEG nie wykazało istotnych różnic statystycznych pomiędzy grupami na poziomie z poprawką na wielokrotne powtórzenia. Zauważalny był jednak trend (na poziomie bez poprawki) wskazujący na podobne wzorce zmian, które obserwuje się u osób chorych na demencje. Analiza połączeń funkcjonalnych, przeprowadzona na danych fMRI, wykazała między innymi istotne zmiany na poziomie niewielkich klastrów w obszarach (np. tylna część zakrętu obręczy) łączonych z siecią aktywności spoczynkowej (DMN). Również analiza danych fMRI zebranych podczas wykonywania zadania poznawczego ujawniła różnice w aktywacji mózgu między grupami w obszarach częściowo związanych z tą siecią. Zaburzenia w sieci DMN są często obserwowane podczas chorób neurodegeneracyjnych. Ponadto stwierdzono zmiany aktywacji w regionach kluczowych dla choroby Alzheimera, takich jak zakręt kątowy, zakręt skroniowy dolny czy zakręt nadbrzeżny.

Ważnym odkryciem jest brak liniowej kumulacji efektów wzdłuż osi poziomu ryzyka. *APOE* i *PICALM* wydają się wpływać na organizm w złożony sposób. Wydaje się, że tylko niektóre parametry zdrowia i dane neuroobrazowe mogą być ściśle związane z badanymi wariantami genetycznymi i ich wpływem na rozwój choroby Alzheimera. Ten zestaw parametrów powinien zostać zbadany dogłębniej, a część czynników być może powinna wejść do zestawu „biomarkerów" choroby Alzheimera pomagających we wczesnej diagnozie i/lub ocenie ryzyka zachorowania. Potrzebne są do tego między innymi badania podłużne, które pomogą w ustaleniu, które osoby z przebadanych grup ostatecznie zachorują.

Table of contents

Abbreviations

AUDIT	Alcohol Use Disorders Identification Test
AD	Alzheimer's disease
APOE	gene coding Apolipoprotein E
ApoE	Apolipoprotein E (protein)
BDI	Beck's Depression Inventory
BMI	Body mass index
CVLT	California Verbal Learning Test
DMN	Default Mode Network
EEG	Electroencephalography
ERP	Event-related potentials
EOAD	Early-onset Alzheimer's diseases
fMRI	Functional magnetic resonance imaging
GWAS	Genome wide association studies
ICA	Independent component analysis
LSP	Late sustained potential
LOAD	Late-onset Alzheimer's disease
MCI	Mild cognitive impairment
MRI	Magnetic resonance imaging
MSIT	Multi-Source Interference Task
NFT	Neurofibrillary tangle
PICALM	gene for Phosphatidylinositol Binding Clathrin Assembly Protein
ROI	Region of interest
RPM	Raven's Progressive Matrices
SES	Rosenberg's Self-Esteem Scale
STM	Sternberg Memory Task

1 Introduction

1.1 Aging

Aging is considered as the progressive and time-dependent degeneration of biological systems. This complex process can be discussed in the context of molecular, cellular and systems biology. Several biological components of aging include: accumulation of DNA damage (due to impairment of DNA repair mechanisms), telomere shortening, mitochondrial dysfunction, and changes in cell signaling pathways, including pro-inflammatory pathways (DiLoreto & Murphy, 2015). In the phenotype of animals (including humans), aging contributes to the decline in their sensory, motor, and cognitive performance. Gradual decline in brain functions is a natural aspect of aging, but it sometimes aggravates to the level of neurodegeneration when the severe loss of functions (dementia) dramatically impacts the animal overall behavior (Alzheimer's Association, 2022). The best-known and most common neurodegenerative diseases are Alzheimer's disease (AD, firstly described in 1906 by Alois Alzheimer; the history of this finding is described in Hippius & Neundörfer, 2003) and Parkinson's disease (Alzheimer's Association, 2022).

The aging brain undergoes a series of structural and functional changes. Neurons are susceptible to oxidative stress, mitochondrial dysfunction and degeneration of synapses (Peters, 2006). Ultimate loss of neurons, particularly in regions associated with memory and executive functions (Peters, 2006), is visible as an atrophy and thinning of cerebral cortex. Neuronal communication is disrupted due to white matter changes, such as reduced myelin integrity and/or white matter lesions (Kövari et al., 2004). These structural alterations are accompanied by a decline in various cognitive domains, such as processing speed, executive functions, working memory, and episodic memory. Changes in neuromodulatory systems (especially dopaminergic and serotoninergic ones) impact the cognitive functions and the mood further reducing the quality of life (Peters, 2006). Neurodegeneration, on the cellular level involves loss of neuronal cells and dendritic simplification (decrease in density and shape of dendritic spines). Specifically, the hippocampus, temporal lobes, parietal lobes, partially frontal lobes, and the cingulate cortex are globally affected (DeTure & Dickson, 2019).

Despite these age-related changes, the brain still demonstrates remarkable plasticity, allowing for adaptation and compensation. This ability can be explained by the concepts of brain reserve and cognitive reserve.

1.1.1 Brain/cognitive reserve and resilience

As the brain ages, it exhibits a degree of resilience in coping with age-related changes and external stressors. This resilience is influenced by a combination of genetic, environmental, and lifestyle factors (Stern et al., 2020). Brain reserve is a concept that reflects the inherent, passive capacity of an individual's brain to tolerate age-related changes and pathological conditions without displaying clinical symptoms (it refers to brain structure: size and number of neurons and synapses) (Katzman, 1993; Stern, 2009). Brain reserve can be understood as an individual threshold at which brain damage triggers perceptible decline in functioning (Barulli & Stern, 2013; Stern, 2009). Cognitive reserve, on the other hand, pertains to the dynamic capacity of the brain to optimize its performance in response to environmental or neurodegenerative challenges. It encompasses the utilization of cognitive strategies, intellectual engagement, and adaptive processes that enable individuals to effectively maintain cognitive function even when confronted with brain damage (Whalley et al., 2004). Cognitive reserve can be built over a lifetime through education, mental stimulation, and intellectual pursuits (Stern et al., 2020; Whalley et al., 2004). Individuals with high cognitive reserve may experience the same level of brain pathology but show milder cognitive decline compared to those with lower cognitive reserve. This concept emphasizes the importance of continuous learning and cognitive engagement as a means of preserving cognitive function and quality of life throughout the aging process. Another concept related to neural reserve points to the compensatory flexibility of brain networks – the ability to use alternative brain circuits (structures, pathways) not typically employed for a specific task, to compensate for neuronal loss and maintain (or enhance) performance (Stern, 2009). This concept is related to mechanisms of neuroplasticity.

The evidence that brain/cognitive reserve can prevent or postpone effects of neurodegeneration first came from observations that not all individuals with deposits of β-amyloid (Aβ) plaques (pathological proteins believed to underlie dementia in Alzheimer's disease), exhibited symptoms of the disease (Katzman et al., 1988). Those who remained asymptomatic despite the accumulation of β-amyloid proteins were distinguished by having larger brains and a greater number of neurons (Katzman et al., 1988). On the other hand, individuals with lower levels of education or those lacking formal education were more prone to show signs of dementia (Katzman, 1993; Stern et al., 1994). Brain size (whole-brain volume, and the size of specific regions measured e.g., by MRI method) was even proposed to serve as an indicator of brain reserve and a predictor of cognitive efficacy/resilience in aging (Farias et al., 2012). Factors such as physical activity, social engagement, cognitive stimulation, and a healthy diet can enhance resilience and brain reserve by promoting neural

plasticity and improving brain health (Phillips, 2017). Understanding the specific factors responsible for a personal level of brain and cognitive reserves are especially important in the context of neurodegenerative disease, as they define susceptibility or resistance to aging-related decline and the development of dementia.

1.2 Alzheimer's disease overview

Alzheimer's disease stands out as one of the most prevalent neurodegenerative diseases and late onset variant constitutes 95% of all AD cases (Alzheimer’s Association, 2022; Barber, 2012)). The LOAD and the early-onset Alzheimer's Disease (EOAD) represent distinct types of this disease, differentiated by the age of onset and etiology. LOAD typically does not manifest before the age of 65. EOAD is a less prevalent disease, impacting individuals below the age of 65, with symptoms typically emerging in their 40s or 50s (Barber, 2012). While EOAD constitutes a smaller proportion of overall Alzheimer's cases, its progression is often more rapid.

Alzheimer's disease is a global health concern, with millions of people affected worldwide. According to the World Health Organization (WHO), approximately 55 million people worldwide were living with dementia in 2023, and its global cost was estimated at 1.3 trillion US dollars in 2019 (WHO, 2023). At the same time, AD is the most prevalent type of dementia, accounting for 60-70% of cases (WHO, 2023). The prevalence of LOAD can vary across different studies and populations. In the United States (USA), the Alzheimer's Association reported that over 6.5 million Americans were living with Alzheimer's disease in 2022 (Alzheimer’s Association, 2022). It is the sixth leading cause of death in the USA (Alzheimer’s Association, 2022). In Poland, as of 2016, there were over 300 000 individuals with AD diagnosis (Raport RPO, 2016). The average survival time for individuals with probable AD is 11 years from the onset of symptoms and 5.7 years from the time of diagnosis (Waring et al., 2005). LOAD impacts not only individuals who are affected but also their caregivers, who are often spouses, children, or other family members (Alzheimer’s Association, 2022; Laakkonen et al., 2008).

Most common symptoms related to AD are memory impairment, confusion with time or place, trouble understanding spatial relationships, poor judgment, withdrawal from work and social activities, mood and personality changes, changes in hygiene and personal care, problems with adapting to change, problems with creative and abstract thinking, repetitive behaviors, loss of initiative or wandering and getting lost (Alzheimer’s Association, 2022). The symptoms can vary among individuals, and not everyone with Alzheimer's will experience all these symptoms. Additionally, the severity and progression of symptoms can differ over time. Based on psychometric testing conducted on individuals with Alzheimer's disease, it has been observed that personality traits (impulsivity, neuroticism), and mood changes (depression, anxiety, agitation, apathy), may be associated with the disease or could

potentially contribute to its development (Alzheimer's Association, 2022; Balsis et al., 2005; Low et al., 2013; Wang et al., 2009).

This progressive disorder manifests through a continuum of stages, each characterized by distinct cognitive and functional changes. Understanding this continuum is crucial for early detection, intervention, and management of the disease. The stages include preclinical AD, mild cognitive impairment (MCI), and mild, moderate, and severe stages of Alzheimer's disease (Figure 1) (Alzheimer's Association, 2022). Preclinical stage occurs before any noticeable symptoms are visible (cognitive functions remain intact), although some early biological changes may occur. MCI represents a transitional stage between preclinical stage and dementia due to AD. Individuals with MCI experience noticeable cognitive changes but can still perform daily activities. Memory loss and other cognitive deficits are more prominent than expected for age but do not meet the criteria for a dementia diagnosis. MCI may progress to Alzheimer's disease, remain stable, or, in some cases, even improve (Blumenthal et al., 2019). In the mild stage, symptoms become more apparent, and patients may struggle with some everyday activities. The moderate stage is marked by a more significant decline in cognitive function, while everyday activities become challenging, and assistance is often (but not always) needed. The severe stage is characterized by profound cognitive and functional impairment, including compromised mobility (Alzheimer's Association, 2022). Symptoms influence most everyday activities, even communication may become severely limited. The time of the progression trough these stages show some variability (and different rates of decline may occur) which is moderated by age, sex, *APOE* genotype, and level of chosen biomarkers (Alzheimer's Association, 2022; Vermunt et al., 2019).

Figure 1. Alzheimer's disease continuum: from preclinical to severe stages

Demographic predictions (increasing life expectancy due to medical advancements and improvements of quality of life, along with increasing global population levels) suggest that future generations will face a significant healthcare capacity crisis. Over 153 million of people will be affected by AD by 2050 worldwide (GBD 2019 Dementia Forecasting Collaborators, 2022).

1.2.1 Genetic basis of Alzheimer's Disease

Mutations in specific genes, including *APP* (amyloid precursor protein; chromosome 21), *PSEN1* (presenilin 1, chromosome 14), and *PSEN2* (presenilin 2, chromosome 1), have been identified in cases of early AD (Barber, 2012; Liu et al., 2019). Mutations in these genes disrupt the pathways of protein processing in the brain, resulting in the accumulation of Aβ plaques and neurofibrillary tangles (NFTs; aggregated hyperphosphorylated tau proteins), which are hallmark features of Alzheimer's disease (Alzheimer's Association, 2022; Ertekin-Taner, 2007). Genetic variations related to EOAD are inherited in an autosomal dominant manner and are causative for the disease.

This is different for the late form of Alzheimer's disease (the more common one), where genetic factors were also indicated but among many other proposed causes of the disease. Genes associated with an elevated risk of developing specific diseases or conditions are referred to as risk genes. While these genes may heighten susceptibility to a particular disease, they do not directly cause it. Initially identified through candidate gene studies, the exploration of risk genes has evolved with the advancements of genome-wide association studies (GWAS). The *APOE* gene (located on chromosome 19) is a best known and the strongest genetic risk factor for LOAD (Alzheimer's Association, 2022; Corder et al., 1993; Michaelson, 2014; Saunders, Strittmatter, et al., 1993). There are three known variants: *APOE*-ε2 – (possibly) protective variant that may decrease the risk of AD (or have no impact) (Corder et al., 1994), *APOE*-ε3 – the most common variant with no known effect on AD (neutral one), *APOE*-ε4 – risk allele increasing the risk and associated with earlier onset of the disease (in certain populations) (Lehtovirta et al., 2000). *APOE*-ε4 has the capability to accelerate the progression of the disease, also in individuals with a familial form of AD associated with mutations in the *PSEN1* gene (Pastor et al., 2003). This allele elevates the risk of the disease by 3-4 fold in heterozygotes and 9-15 in homozygotes (Farrer et al., 1997; Neu et al., 2017). More than 60% of Alzheimer's patients in Europe carry at least one *APOE*-ε4 allele (Crean et al., 2011). The impact of *APOE* differs across different populations; for instance, certain Nigerian populations display no correlation between the presence of *APOE*-ε4 and the incidence or timing of the disease manifestation (Crean et al., 2011; Gureje et al., 2006; Osuntokun et al., 1995).

Another interesting gene (named as the most significant AD risk gene after *APOE* and *BIN1* (Ando et al., 2022)) is *PICALM*, which has been associated with Alzheimer's disease through various specific single nucleotide polymorphisms (SNPs): rs3851179, rs541458, rs59229 and many more (which some are in linkage disequilibrium) (Ando et al., 2022; Bellenguez et al., 2022; Harold et al., 2009; Jun et al., 2010). Among them, rs3851179 is the most extensively researched. The A allele is considered to be neutral, while the G allele is regarded as the potentially risky one. However, only GG genotype exhibits a significant risk impact, whereas heterozygous GA genotype is generally considered neutral. The link to Alzheimer's disease has been confirmed in both (*APOE* and *PICALM*) genes through GWAS studies (Alzheimer's Association, 2022; Bellenguez et al., 2022; Harold et al., 2009).

Additional well-known risk genes include the clusterin (*CLU*) gene and the bridging integrator 1 (*BIN1*) gene (Karch & Goate, 2015). However, recent genome-wide association studies have identified many other loci correlated with the incidence of the disease. These include *ABCA7*, *CASS4*, *CD33*, *CD2AP*, *CELF1*, *CR1*, *DSG2*, *EPHA1*, *FERMT2*, *HLA-DRB5-DBR1*, *INPP5D*, *MS4A*, *MEF2C*, *NME8*, *PTK2B*, *SLC24H4-RIN3*, *SORL1*, and ZCWPW1 (Karch & Goate, 2015). Another 42 new loci discoveries were made in 2022 (Bellenguez et al., 2022). These genes are involved in various biological processes such as inflammatory response, autophagy of damaged organelles, intracellular transport of beta-amyloid precursor, and cholesterol metabolism (Rosenthal & Kamboh, 2014). Despite being clustered across a few common pathways, the precise involvement of many of these genes in the pathogenesis of diseases remains unknown (Rosenthal & Kamboh, 2014).

1.2.1.1 *APOE* and *PICALM* functions and possible role in AD etiology

APOE is expressed in many organs, including liver, spleen, kidney and brain (Mahley, 1988). In the brain it is mainly expressed by microglia and astrocytes (Fernandez et al., 2019). ApoE protein in a physiological state mainly participates in lipid (particularly cholesterol) metabolism and transport (Mahley, 1988). It is important for neuronal homeostasis in the brain (Huang & Mahley, 2014). Moreover, it is implicated to take part in tissue injury (including peripheral nerve injury and regeneration), immunoregulation, impacting cell growth and differentiation (Mahley, 1988). While the mechanisms responsible for the pathogenic role of *APOE* gene in Alzheimer's disease are not fully understood, recent findings indicate that they may be both related to the Aβ-dependent and Aβ-independent pathways (Fernandez et al., 2019). It is (mostly) a disruption in Aβ metabolism and clearance (also mediated by ApoE) that leads to pathological aggregates and to neurodegeneration. Glial cells are responsible for Aβ degradation (primarily by proteases, and endothelin-converting enzymes), and *APOE*-ε4 allele was considered to alter the physiological function of these cell types (Fernandez et al., 2019; Ries & Sastre, 2016). Research indicated a link between *APOE*-ε4 and accumulation of Aβ and (to a lesser extent, as some research do not confirm that) tauopathy (measured through PET) in all symptomatic stages of Alzheimer's disease (Baek et al., 2020; Barthel et al., 2011; Dincer et al., 2022). Other ApoE associated mechanisms related to AD, include tau pathology, inflammation, oxidative stress, and other contributing factors (Michaelson, 2014; Yu et al., 2014). Elevated cholesterol level was also proposed (but it is still under debate) to be a risk factor for the development of Alzheimer's disease (Wood et al., 2014), and *APOE*-ε4 allele disrupts physiological metabolism and transport of cholesterol. *APOE*-ε4 allele was also linked to the dysfunction in the blood-brain barrier (BBB) (Montagne et al., 2020). This BBB dysfunction, as indicated, serves as an early predictor of cognitive impairment (Nation et al., 2019). As astrocytes and microglia are mainly responsible for *APOE* expression, the main function of these cells is managing inflammation in the brain. AD patients with the *APOE*-ε4 allele exhibit more pronounced inflammation compared to those with neutral alleles

(Egensperger et al., 1998). *APOE*-ε4 allele has been linked to a heightened risk also of cardiovascular disease, encompassing conditions such as coronary artery disease, stroke, and atherosclerosis (Mahley, 2016; Michaelson, 2014).

PICALM (phosphatidylinositol binding clathrin assembly protein) is expressed widely, both in neurons, in microglia, oligodendrocytes and other cells like endothelial cells in the brain (Ando et al., 2022; Xu et al., 2015). It plays a crucial role in various cellular functions and homeostasis, particularly in clathrin-mediated endocytosis, autophagy, erythroid maturation, lipid homeostasis, neuritic prolongation, synaptic vesicle turnover, and transferrin uptake (Ando et al., 2022; Xu et al., 2015). PICALM was also associated with amyloid clearance and aggregation. It is engaged in the transport and processing of amyloid precursor protein (APP), a key factor in the formation of Aβ plaques (Ando et al., 2022; Xu et al., 2015). Although, there are some contradictory observations in that matter (Ando et al., 2022). It is also linked to AD by other pathways as well, including, but not limited to, influencing glutaminergic neurotransmission and neurotoxicity, cellular homeostasis, glial lipid transport and synaptic function (Ando et al., 2022; Xu et al., 2015)

Both discussed genes share a common link to the development of AD, primarily influencing the Aβ pathology (Robinson et al., 2018). Jun and colleagues (Jun et al., 2010) revealed a genetic interaction between them in conferring AD risk. The authors reported – that *PICALM* influenced the AD risks primarily in *APOE*-ε4 carriers. Another study reported that both genes have combined negative effect on carriers performance and brain atrophy in AD patients (on early stages of the disease) (Morgen et al., 2014).

1.2.2 Etiology: widely recognized hypotheses

The first hypothesis regarding Alzheimer's disease was centered on a disruptions within the cholinergic system (Davies & Maloney, 1976). It was based on the fact that acetylcholine plays significant role in learning and memory functions and supported by the results from AD patients showing the degeneration of cholinergic neurons particularly dramatic in the nucleus basalis of Meynert. In a healthy adult brain, this region typically contains approximately 500 000 cholinergic neurons, and in AD patients – only 100 000 neurons remain intact (Ferreira-Vieira et al., 2016; Schliebs & Arendt, 2006). The levels of acetylcholine are reduced mostly in the forebrain regions including the cortex, hippocampus, and amygdala (Liu et al., 2019). The key elements of cholinergic turnover impaired in the course of AD include functions of choline acetyltransferase (ChAT) and acetylcholinesterase (AChE), or changes within cholinergic receptors (both muscarinic, mAChR and nicotinic, nAChR) (Ferreira-Vieira et al., 2016). The ChAT is responsible for producing acetylcholine, so a decrease in its activity is associated with diminished levels of the transmitter. AChE catalyzes the degradation of acetylcholine. A reduction in AChE activity indicates a decline in acetylcholine levels. Moreover, studies have shown that AChE can interact with Aβ and promote the formation of amyloid fibrils (Ferreira-Vieira et al., 2016). Simultaneously, the

expression of AChE may be influenced by Aβ and abnormally hyperphosphorylated tau (García-Ayllón et al., 2011). Consequently, acetylcholinesterase inhibitors (AChEIs) were introduced as a treatment to improve deteriorated cholinergic function and they still remain the most used therapeutics for AD (Aupperle, 2006). However, their effectiveness is limited, and therefore other theories are being developed to better explain AD etiology.

Presently, the most recognized is the amyloid hypothesis (first introduced in 1991, (Hardy & Allsop, 1991; Selkoe, 1991)), which suggests that the buildup of amyloid plaques (composed of amyloid beta – Aβ) within the intercellular space (between neurons) is a primary factor in the development of Alzheimer's disease. Among other, the hypothesis is supported by the fact that in individuals with Down's syndrome, LOAD is more frequent and its onset is earlier than in general population (Lott & Head, 2019). Down's syndrome results from the trisomy of chromosome 21 on which amyloid precursor protein (*APP*) gene is located.

The trans-membrane APP protein undergoes proteolysis by beta and gamma secretases, leading to the formation of individual Aβ units. These units undergo modifications and aggregate to create senile plaques. In normal conditions, alpha and gamma secretases break down the APP protein, preventing the formation of Aβ deposits (Liu et al., 2019). The enzyme alpha-secretase plays a role in removing APP, resulting in the production of sAPP-alpha (a soluble form of APP with neuroprotective effects), along with a peptide called p3 and a carboxyl group referred to as c83. In the amyloidogenic pathway, sAPP-beta is formed, and instead of the p3 peptide, Aβ is generated (Liu et al., 2019). Initially, Aβ exists in the form of oligomers that induce neuronal apoptosis and later accumulates as senile plaques. The subunits of P1 and P2 proteins (coded by *PSEN1/PSEN2* genes) are components of gamma-secretase. As mentioned above, *PSEN1* and *PSEN2* mutations are recognized genetic causes of early onset, familiar AD. Under normal physiological conditions, Aβ is produced at a relatively low rate, leading to the predominant processing of APP through the non-amyloidogenic pathway. Two primary isoforms of Aβ exist: the 42-residue (Aβ42) and the 40-residue (Aβ40) (Gu & Guo, 2013). Amyloid plaques in the brains of Alzheimer's patients primarily consist of Aβ42, with some plaques exclusively containing Aβ42, despite Aβ40 being present at concentrations several times higher than Aβ42 (Gu & Guo, 2013). It is suggested that these plaques directly disrupt communication between nerve cells.

Another protein, which abnormal accumulation was detected in AD, is a microtubule-associated protein tau, forming neurofibrillary tangles (NFTs) that aggregate within the neurons itself and disrupt their internal structure (Frost et al., 2009; Liu et al., 2019). According to this hypothesis (named as tau propagation hypothesis) the tau undergoes abnormal hyperphosphorylation, resulting in the impairment of microtubules' ability to maintain their structure (Frost et al., 2009). This disruption of microtubules can impair the transport within neurons, leading to cell dysfunction and, ultimately, cell death. The presence of neurofibrillary tangles is a hallmark pathological feature of Alzheimer's disease, but they can also be found in other neurodegenerative disorders collectively known as tauopathies

(Kovacs, 2017). These disorders include Pick disease, frontotemporal dementia with tau pathology (FTDP-17), progressive supranuclear palsy (PSP), and corticobasal degeneration (CBD), among others (Kovacs, 2017). Both, *APOE* and *PICALM*, were link to Aβ and NFTs formation and clearance. The relationship with tau pathology is not as straightforward, but there is some evidence linking *APOE*-ε4 allele to an increased risk of NFTs formation.

Yet another hypothesis that is gaining attention relates to the role of neuroinflammation in provoking dementia (Kinney et al., 2018; Liu et al., 2019; Snellman et al., 2023). It proposes that chronic inflammatory state, which can be triggered in the brain by several factors through life, slowly leads to neurodegeneration and may cause symptoms of Alzheimer's. In particular, some indications exist associating pathogenesis of AD with so-called low-grade systemic inflammation (Holmes et al., 2009; Xie et al., 2021). It is a chronic, subtle, and persistent state of inflammation in the body. It is characterized by slightly elevated levels of inflammatory markers such as C-reactive protein (CRP), interleukin-6 (IL-6), and tumor necrosis factor-alpha (TNF-alpha) (Holmes et al., 2009; Xie et al., 2021). Unlike acute inflammation, which is a normal and essential response to injury or infection, chronic low-grade inflammation is a persistent, pathological (often autoimmunological) process provoking adverse responses in multiple organs including the brain. The immune system in the brain is responsible for elimination of pathogens, cell debris, and misfolded proteins. Specialized glial cells, (microglia and astrocytes) are activated early in AD and are found to “surrounds” Aβ plaques (Britschgi & Wyss-Coray, 2007; Dickson, 1997) which may be part of a healthy defensive response. However, inflammatory cytokines can intensify immune response and lead to tissue degeneration. In this context it is important to note that glial cells’ functions were shown to be altered in carriers of a risky ε4 variant *APOE* gene (Fernandez et al., 2019).

Other proposed AD pathomechanisms include: mitochondrial cascade hypothesis, calcium homeostasis hypothesis, neurovascular hypothesis, metal ion hypothesis, neurotransmitters disruption hypothesis (linked also to the cholinergic hypothesis), and lymphatic system hypothesis (Liu et al., 2019). The issues that are being discussed and addressed are also related to the influence of oxidative stress, neurotrophic factors, glutamate excitotoxicity and other.

Among the listed hypotheses, the most frequently addressed in clinical trials for new therapeutics for Alzheimer's disease are the amyloid hypothesis (22.3%, development of drugs that targets aggregated forms of Aβ), neurotransmitter hypothesis (19.0%), tau propagation hypothesis (12.2%), and those associated with mitochondrial dysfunctions (17%) (Liu et al., 2019)

As mentioned at the beginning – LOAD ethology is exceedingly complex. Described hypotheses are not mutually exclusive, but rather complementary, and none of them alone adequately captures the mechanisms underlying the development and symptoms of the disease. Numerous factors, including immunological influences, can instigate the creation

of Aβ plaques or tauopathy. These, in turn, result in the damage/death of neurons and synapses within different brain systems, including cholinergic, dopaminergic, and glutamatergic systems. The disruption of dopaminergic transmission is considered a significant factor linked to neuropsychiatric symptoms of AD. Impairment of glutaminergic system (especially the function of NMDAR receptors, and the availability of glutamate), leads to further complications related to glutamate excitotoxicity (Wang & Reddy, 2017). The emergence of pathologically structured proteins leads to the activation of glial cells. Their activation should clean pathological deposits, however it initiates inflammation, including the release of free radicals, excitatory amino acids, inflammatory interleukins, and nitric oxide. All these factors, in turn, lead to neuronal damage and brain atrophy.

1.2.3 LOAD risk and protective factors

The exact causes of LOAD are not fully understood, but it is believed to be influenced by a combination of genetic, environmental, health related and lifestyle factors (Armstrong, 2019). The most significant risk factor for LOAD is age – over 65 years of age the risk of developing the disease doubles every 5-6 years (Ziegler-Graham et al., 2008). The second most significant risk factor for LOAD is the family history of the condition. Other risk factors can be categorized into several groups (Armstrong, 2019) and some of the most known are presented on the diagram (Figure 2). Almost two-thirds of Alzheimer's disease patients are women. This is thought to be due to biological factors (like hormonal changes) and the fact that women live longer (Andrew & Tierney, 2018; Chêne et al., 2015). It has been estimated that for a person aged 65, the risk of developing Alzheimer’s disease over the remaining life-period is 21.1% for women and 11.6% for men (Chêne et al., 2015). Certain dietary changes may exert a protective effect against AD. The key dietary guidelines involve minimizing the consumption of saturated fats, primarily present in dairy products and meats, as well as avoiding trans fats (Barnard et al., 2014). Additionally, substituting meat and dairy products with vegetables, legumes (such as beans or lentils), fruits, and whole grains is crucial (Barnard et al., 2014). Lastly, diet (or supplementation) should ensure adequately high levels of important vitamins, including vitamins E and B12 (Barnard et al., 2014). The Mediterranean diet is frequently mentioned, highlighting the importance of incorporating fruits, vegetables, whole grains, fish, and olive oil, while minimizing the intake of red meat and saturated fats. This diet has been associated with a decreased risk of cognitive decline and Alzheimer's disease (Scarmeas et al., 2006). Diets rich in antioxidants, which are abundant in fruits and vegetables, play a crucial role in mitigating oxidative stress. There are also reports that a caffeine intake can reduce risk of dementia (Eskelinen et al., 2009). On the other hand, deficiencies in vitamins such as C, E, and notably B12 can accelerate the risks (Armstrong, 2019). An unhealthy diet can elevate levels of cholesterol and homocysteine, both influencing neuronal functioning directly and via cardiovascular system (Armstrong, 2019).

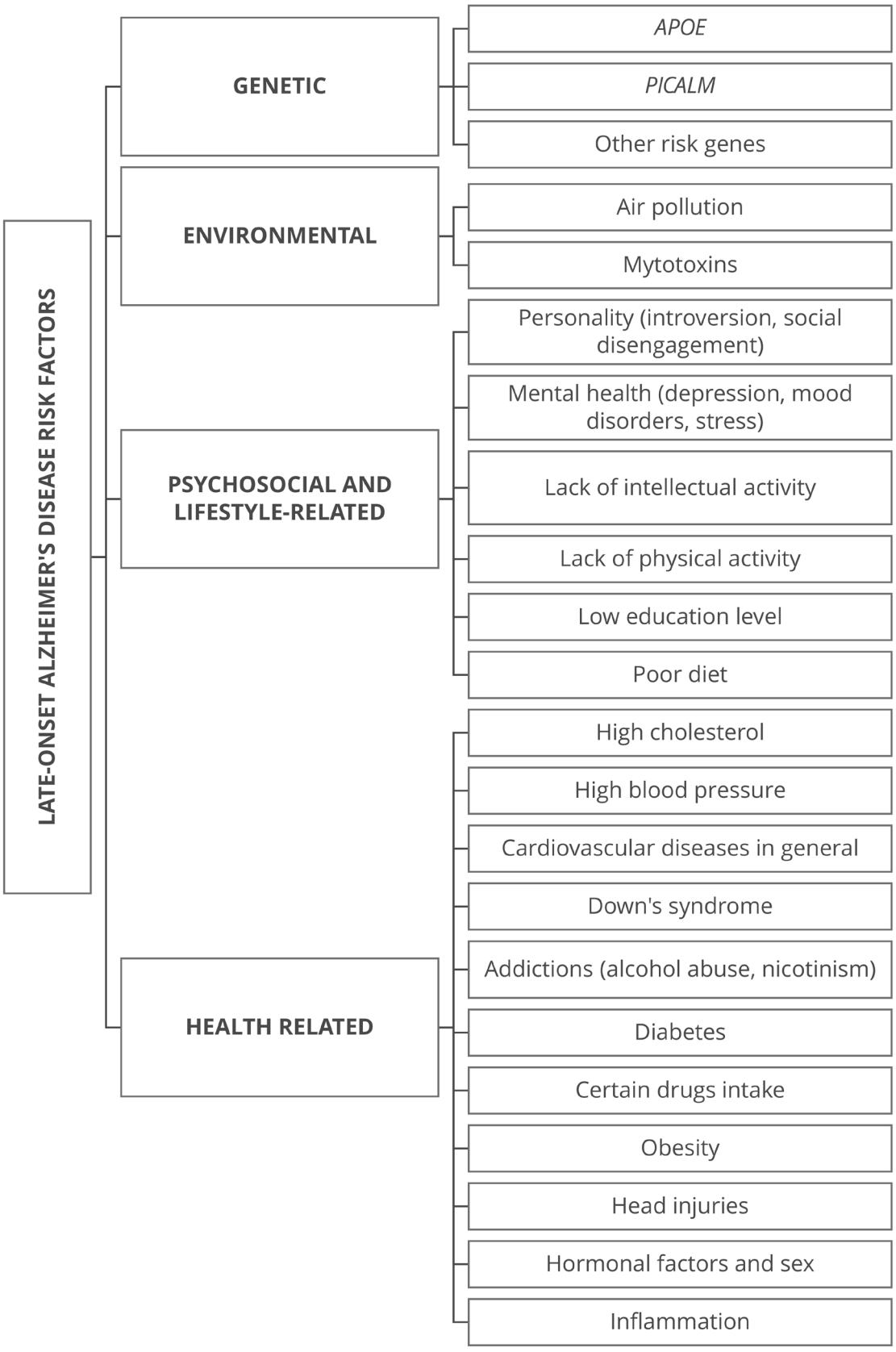

Figure 2. Diagram showing some of the known risk factors for late-onset Alzheimer's disease.

Exposure to environmental pollutants, including heavy metals, can also impact the risk of disease (Armstrong, 2019). Current studies consistently demonstrate a robust correlation between early neurodegenerative changes in the brain and air pollution (Block & Calderón-Garcidueñas, 2009; Tan et al., 2022). A review of epidemiological studies indicates that prolonged stress, particularly in combination with genetic factors, may influence the development of Alzheimer's disease through the hypothalamic-pituitary-adrenal (HPA) axis (Milligan Armstrong et al., 2021). Stress activates the HPA pathway, which regulates levels of stress hormones (cortisol). Elevated cortisol levels are frequently observed in AD patients and are link to poor overall cognitive functioning (including episodic and spatial memory, executive functions, processing speed or language) (Ouanes & Popp, 2019). Lifestyle factors and personality factors are commonly linked to AD development (Low et al., 2013; Wang et al., 2009).

The risk of developing Alzheimer's disease increases because of interplay of many specific factors. Some of them cannot, but others can be modified by preventive or therapeutic interventions. Obviously, genetic risk cannot be changed, however individuals carrying high-risk alleles can reduce their cumulative disease contingency through informed modifications of other factors through lifestyle changes and healthcare. Consequently, it would be reasonable to test AD related genes variants along with other health measures to estimate and monitor individual risk level of developing symptomatic dementia. Valid biomarkers reliably predicting the disease are essential for predicting the overall risks.

1.3 LOAD possible biomarkers

A biomarker is a measurable factor (such as substance, gene, physiological properties, or behavioral characteristic) within an organism that can serve as an indicator of a particular condition e.g., disease or infection. Biomarkers may play a crucial role in diagnosing diseases, identifying health risks and monitoring responses to treatment.

Alzheimer's Disease is usually diagnosed at late stage, when evident cognitive and behavioral decline impact everyday functioning and the neurodegeneration is irreversible. Hoverer, the changes in the brain start several decades before the manifestation of symptoms (Alzheimer’s Association, 2022; Dubois et al., 2016) (referred as asymptomatic, “preclinical” stage as described in previous sections). This asymptomatic stage was initially identified and described in 1990 (Hubbard et al., 1990) and it is a proper stage to initiate interventions preventing transition to symptomatic phases. This required introducing an innovative disease model that begins with the assessment of risk factors and early detection through screening, followed by the diagnosis and implementation of intervention and treatment (Dubois et al., 2016). Initial screening should utilize tests characterized by high sensitivity and cost-effectiveness, with subsequent diagnosis involving more specific (but more expensive) tests. It is noteworthy that the preclinical (“silent”) phase of the disease

remains underexplored. It is thus necessary to find biomarkers allowing for the earliest possible risk assessment and diagnosis. There already are validated biomarkers for Alzheimer's, namely the Aβ plaques and NFTs (Gunes et al., 2022), which classically are detected through neuroimaging techniques (like positron emission tomography), or by analyzing cerebrospinal fluid. However, these methods are expensive and/or invasive. Recently, these hallmarks of Alzheimer's disease have also been identified through blood tests, which are more broadly available and cost-effective (Gunes et al., 2022). However, there are also individuals who test positive for Aβ plaques and/or NFTs but do not display symptoms of Alzheimer's disease. A single biomarker cannot function as a dependable method for screening the disease, given that LOAD is such a multifaceted condition.

Apart from these well-established traditionally used biomarkers, new indicators are emerging that have the potential to detect changes preceding symptomatic Alzheimer's disease. In this context, I will now outline some lesser-known characteristics related to blood tests and neuroimaging techniques, although other novel biomarkers are also being discussed (Gunes et al., 2022). While not classified as clear biomarkers of AD, these traits are being more commonly associated with the disease and may (in the future) build comprehensive, multivariate sets of features for screening or identifying Alzheimer's risk. Due to the complex nature of the AD, it will be necessary to use multiple biomarkers sets alongside artificial intelligence methods (machine/deep learning classification methods), to improve diagnostic accuracy and characterize individual phenotypes.

1.3.1 Blood tests and circulating miRNAs

Blood tests are a cost-effective and common diagnostic method employed to assess the overall health, and can be used to easily obtain AD biomarkers (Wojsiat et al., 2017). Research has indicated that individuals with Alzheimer's disease and those at an elevated risk for the disease may exhibit alterations in blood counts (Shad et al., 2013; Zhang et al., 2022), including platelets, lymphocytes or erythrocytes (Wojsiat et al., 2017). However, the results are not consistent. Among other characteristics, changes in granulocyte profiles were noted in AD patients (Chen et al., 2017; Järemo et al., 2013; Lunnon et al., 2012; Stock et al., 2018) and a higher likelihood of history of herpes simplex virus (HSV) infection, which can also be verified from a standard blood sample (Dobson & Itzhaki, 1999; Ge & Yuan, 2022; Itzhaki, 2021; Itzhaki et al., 1997).

MicroRNAs (miRNAs) are short, single-stranded non-coding RNAs that are typically 20-22 nucleotides in length. They play a crucial role in regulation of gene expression. Novel approaches allowed studying miRNA circulating within the blood (not CSF) and they also reliably differentiate AD patients from control subjects (Nagaraj et al., 2017, 2019). Consequently more than 20 miRNA have been reported as candidates for Alzheimer's disease blood derived biomarkers (Nagaraj et al., 2017) .

1.3.2 Neuroimaging of brain structure and functions in AD

1.3.2.1 MRI/fMRI

Magnetic resonance imaging (MRI) has been used to examine the brain structure in AD patients. MRI provides the capability to detect very subtle and early abnormalities in the brain structure and function, potentially allowing for the initiation of prevention/therapy before the onset of symptomatic disease. The advantages of MRI include good spatial resolution, precise localization of active brain areas during tasks (fMRI), and the ability to predict the transition from prodromal stages, such as mild cognitive impairment, to the disease (Ficiarà et al., 2021). A notable structural change detected by MRI is the atrophy of brain tissue, particularly in crucial areas such as the hippocampus and other regions within medial temporal lobe associated with memory processing (Rao et al., 2022). Cortical abnormalities (named as the “cortical signature of Alzheimer's disease”) are mainly detected in: medial temporal cortex, inferior temporal gyrus, temporal pole, angular gyrus, superior frontal gyrus, superior parietal lobule, supramarginal gyrus, superior frontal lobule, supramarginal gyrus, precuneus, and inferior frontal sulcus (Dickerson et al., 2009). Cortical thinning in these areas was shown to corelate with the severity of symptoms even at the earliest stages of the disease; and of course it intensifies with the course of the disease, from incipient AD to the severe AD (Dickerson et al., 2009). MRI diagnostic estimating cortical thickness has been demonstrated to serve as a predictor for the conversion from questionable Alzheimer's disease dementia to mild AD (Bakkour et al., 2009).

Functional magnetic resonance imaging (fMRI) can also be used to study possible biomarkers. It detects the modifications of MRI signal related to changes in the levels of oxyhemoglobin in the tissue (blood oxygenated level-dependent signal, BOLD). Thanks to neurovascular coupling oxyhemoglobin is supplied to small domains of activated brain tissue and fMRI scans can illustrate their spatial patterns. It allows to monitor activation of specific brain regions both during resting state and during different tasks. Resting state protocol is a neuroimaging technique that measures brain activity in the absence of a specific task or stimulus, used to measure functional connectivity (FC) (Biswal et al., 1995). FC serves as a metric for the statistical relationship or correlation between the activities of distinct brain regions, or within known hubs or networks. Various functional brain networks have been identified, primarily associated with specific cognitive functions such as motor control, visual processing, attention, and executive functions. Additionally, there is a network known as the default mode network (DMN), which becomes active when the brain disengages from external tasks, indicating a state of introspection or self-reflection (Raichle et al., 2001; Shulman et al., 1997). Aging, neurodegeneration and various genetic factors were shown to be linked to alterations in functional connectivity (Foo et al., 2020). In AD, a significant disruptions in brain neural networks are evident, particularly within the DMN (Damoiseaux, 2012; Vemuri et al., 2012). Similar alterations are observed in individuals with mild

cognitive impairment (Eyler et al., 2019). The DMN has been shown to be involved in a range of functions, encompassing memory, introspection, mind-wandering, generation of spontaneous thought, and the integration of information across different cognitive domains (Eyler et al., 2019; Raichle et al., 2001). Core regions of DNM include the medial prefrontal cortex (mPFC), posterior cingulate cortex (PCC), angular gyrus and precuneus (Raichle et al., 2001). The thinning of angular gyrus and precuneus is considered one of the hallmarks of AD (Dickerson et al., 2009). In fMRI studies of AD, functional connectivity is commonly assessed through either seed-based mapping or independent component analysis (ICA). In seed-based analysis, a small, specific region is selected (the seed) as a reference point, and correlations in activity between that seed region and other brain regions are computed. In ICA, the data is decomposed into statistically independent spatial components representing different patterns of connectivity across the brain. Seed-based correlation studies involve *a priori* assumptions about the nodes or regions of interest, whereas ICA is a data-driven method. ICA has been extensively utilized in resting-state fMRI studies focusing on AD or individuals at risk (Cacciaglia et al., 2020; Filippini et al., 2009; Greicius et al., 2004; Mentink et al., 2021; Sorg et al., 2007).

1.3.2.2 EEG

Electroencephalography (EEG) is a non-invasive method used to assess the electrical activity of the brain. There is a growing need to identify biomarkers that can be widely employed across diverse settings and populations, and EEG presents a promising option. It is a low-cost, globally available, and non-invasive tool (particularly in comparison to MRI, PET, or CSF tests). Several EEG-derived features have been suggested as potential future candidates for Alzheimer's disease biomarkers (Rossini et al., 2020). Both, event-related potential (ERP) and spectral analysis of EEG revealed specific patterns that can differentiate Alzheimer's disease patients from healthy controls (Horvath et al., 2018; Jackson & Snyder, 2008).

EEG has poor spatial precision (when compared to fMRI) but excellent time resolution allowing to study the dynamics of brain activity. Ongoing EEG signal can be separated into basic frequency bands which characterize current brain state (e.g., sleep versus wakefulness, cognitive effort versus relaxation) and health. Cholinergic neurons originating in the basal forebrain project widely to the thalamus and neocortex and modulate the overall level of arousal and attention (Riekkinen et al., 1991). A decrease in cholinergic activity (for example through cholinolytics) is associated with an increase in slower frequency EEG patterns, such as delta waves (0.5-4 Hz), which are often prominent during sleep (Riekkinen et al., 1991). Persistent shift in the power spectrum of brain waves towards slower frequencies is a noticeable functional EEG characteristic in AD patients (Cecchetti et al., 2021; Jelic et al., 1996; Jeong, 2004; Letemendia & Pampiglione, 1958; Lizio et al., 2011; Meghdadi et al., 2021; Soininen et al., 1989; Weiner & Schuster, 1956). It is called “slowing of EEG” and is typically measured within delta, theta (4-8 Hz) and alpha (8-12 Hz) waves. Faster EEG bands

as beta (15-35 Hz) or gamma (>35 Hz) are rarely investigated or do not show evident changes in this regard (Benz et al., 2014; Jelic et al., 1996; Soininen et al., 1989). EEG slowing, coupled with a decrease in signal complexity (Al-Nuaimi et al., 2018; Jeong, 2004; Sun et al., 2020), is believed to mirror neuronal degeneration and disruptions in the cholinergic system. Functional connectivity can also be examined using EEG signals recorded from multiple electrodes overlying the whole brain. Studies indicate that Alzheimer's disease patients exhibit heightened spectral coherence in the delta and theta bands (Meghdadi et al., 2021). The changes observed in AD patients are enhanced in individuals with the *APOE*-ε4 genotype (Lehtovirta et al., 2000).

EEG features can serve as a proxy of neuronal loss and synapse damage (Colom-Cadena et al., 2020) and be used, along with blood derived biomarkers, to accurately predict AD and/or monitor the brain function and health during clinical trials. It can be utilized to monitor prodromal phases of cognitive decline and, could be incorporated, along with other biomarkers, into routine medical assessments of middle-aged and elderly at risk of dementia (Gaubert et al., 2020; Rossini et al., 2020). It has been demonstrated that incorporating ERP EEG features can enhance the effectiveness of CSF biomarkers in diagnosing AD (Babić Leko et al., 2018). The strongest correlation with CSF biomarkers was shown for P3 and N2 ERP waves, where P3 latency was prolonged in Alzheimer's disease patients (Babić Leko et al., 2018; Polich et al., 1990). The P3 wave is believed to reflect attention and cognitive effort and changes within this wave can be used to monitor the reduction in cognitive efficiency (Polich & Corey-Bloom, 2005) or its recovery during therapy (Chang et al., 2014). N2 wave have some specific functional affiliations generally related to various aspects of attention, conflict monitoring and response inhibition (Folstein & Van Petten, 2008).

1.4 Importance of studying presymptomatic individuals

Even though the *APOE* gene was the first one associated with late-onset sporadic Alzheimer's disease, and despite over 30 years of research into its functions (first publication in 1993) (Corder et al., 1993; Saunders, Strittmatter, et al., 1993; Strittmatter et al., 1993), the precise mechanism of its action remains elusive. Even before (1991), *APOE* was linked to amyloid plaques and NFTs within the brain (Namba et al., 1991). Daniel M. Michaelson correctly stated in 2014 (and this remain true nowadays) that *APOE* is “the most prevalent yet understudied risk factor for AD” (Michaelson, 2014). Most importantly, the reason why certain individuals with the identical *APOE* risk alleles develop the disease while others do not remain unknown. Contemporary research is emphasizing necessity of studying of healthy individuals to explore how risk genes impact the functioning of individuals without the disease. This approach aims to discern additional factors that ultimately influence the susceptibility or resilience to the disease, potentially aiding in predictive measures.

Changes in behavior and mood can precede signs of dementia and clinical diagnosis of AD (Balsis et al., 2005). Cortical thinning in regions associated with the "cortical signature of Alzheimer's Disease" has been identified even in healthy individuals who test positive for amyloid, suggesting that structural changes may manifest prior to the onset of clinical symptoms (Dickerson et al., 2009). Individuals at risk are also characterized by changes in blood counts (Zhang et al., 2022), that we have also shown for the cohort that will be described in this thesis (Dzianok & Kublik, 2023). Present findings on the influence of *APOE* on aspects such as healthy aging, cognitive function, or brain function occasionally yield inconclusive outcomes (which may be partially explained by resource-modulation and antagonistic pleiotropy hypotheses, which are described in the next section). Two general mechanisms are proposed to explain how *APOE* may affect healthy adults: the phenotype hypothesis, suggesting *APOE* itself contributes to individual variations in cognition and brain health, and the prodromal hypothesis, suggesting the gene impact may be associated with early-stage, presymptomatic dementia. Obviously, they are not mutually exclusive (O'Donoghue et al., 2018). It was shown that *APOE*-ε4 allele is associated with episodic memory changes (Bondi et al., 1995), worse cognitive functions and prolonged reaction times (Staehelin et al., 1999) in older adults. Healthy carriers (young and middle-aged) of the *APOE*-ε4 gene variant demonstrate changes of connections particularly in DMN network (Kucikova et al., 2021). In a fMRI study involving young *APOE*-ε4 carriers, a reduction was observed in activation of the right hippocampal formation during a task requiring sustained attention and vigilance, compared to a control task (Evans et al., 2018). Importantly, despite this altered brain activity, the level of task performance did not significantly differ from the group without the genetic risk. The same authors subsequently demonstrated that individuals in the middle-aged group carrying the *APOE*-ε4 variant exhibit functional disparities related to memory and disruptions within hippocampal regions (although the performance in the memory task did not differentiate the groups) (Evans et al., 2020). Functional connectivity between the hippocampus and precuneus/posterior cingulate cortex was also shown to be disrupted in female *APOE*-ε4 carriers (Heise et al., 2014). Recently it was shown that healthy, older *APOE*-ε4 carriers do not show any compensatory patterns (as assessed by cerebellar EEG source localization), in comparison to *APOE*-ε4 non-carriers; once again this particular study did not show any differences in task performance between the groups (using stop-signal task) (Paitel & Nielson, 2023). General health changes related to *APOE*-ε4 shown increased cholesterol levels in ε4 and ε3 carriers in comparison to the ε2 carriers (Staehelin et al., 1999).

As highlighted above, there are multiple AD risk factors which must interact with each other. Contemporary research tries to estimate their interactions. The interplay between the *APOE*-ε4 variant and *CLU*-C in young carriers was described by Green and colleagues (Green et al., 2014). Specifically, during tasks involving executive control and cognitive conflict resolution, these individuals exhibited diminished brain activity in the medial temporal lobe, posterior cingulate cortex, and parahippocampal gyrus (Green et al., 2014).

The impact of *PICALM* on healthy individuals has been less extensively studied compared to the influence of *APOE*. The A allele of the *PICALM* gene (rs3851179) has been linked to enhanced cognitive performance, including higher scores on cognitive tests such as the Mini-Mental State Examination (MMSE), particularly among individuals in the oldest age group (92-93 years at the beginning of the study) (Mengel-From et al., 2011). The differences in functional connectivity between carriers of GG and AA/AG genotypes was also demonstrated, both as measured by EEG (Ponomareva et al., 2020), and in fMRI (Liu et al., 2018; Zhang et al., 2015). Later authors also showed changes within brain structure and an interaction between the cognitive performance and functional connectivity (Liu et al., 2018). Hippocampal degeneration was also associated with both *PICALM* and *CLU* genes in both young and elderly adults (Yang et al., 2016).

The interaction between the *APOE* and *PICALM* genes was, as mentioned earlier, assessed before in GWAS studies (Jun et al., 2010), but the functional mechanisms of this possible interaction is still not known. The effects of both genes were never tested in healthy adults.

1.4.1 The resource-modulation and antagonistic pleiotropy hypotheses

The resource-modulation hypothesis states that age-related changes that affect brain functions and resources can modulate genetic influences on cognitive functioning. This hypothesis suggests that the relationship between genetics and cognitive functioning is not static but can be influenced by the context of aging (the hypothesis was also proposed for *APOE* gene (Lindenberger et al., 2008). When analyzing the impact of risk genes in research, it is crucial to study populations across different age groups and consider as many covariates as possible. In case of AD, most studies involve elderly and clinical population, and studies with healthy participants tend to concentrate on younger risk carriers.

The impact of *APOE*-ε4 variant on young carriers is complex, revealing sometimes improved cognitive performance in executive function, memory, or verbal fluency tasks (Di Battista et al., 2016; Jochemsen et al., 2012; Mondadori et al., 2006; Rusted et al., 2013). While the impact on older population is related with lower cognitive performance, worse spatial memory and object recognition, as well as executive attention (Berteau-Pavy et al., 2007; Luck et al., 2015). This findings are in line with antagonistic pleiotropy hypothesis (which was introduced and reviewed for the *APOE* gene (Rusted & Carare, 2015; Tuminello & Han, 2011)). This hypothesis suggests that the same genetic variant can have opposing effects on certain traits or functions, contributing to trade-offs in evolutionary fitness across different life stages. In other words, a gene may provide an advantage early in life, promoting survival and reproduction, but may also be associated with negative effects (for example causing the disease) later in life. The effects of risk-gene on brain structure/function may be then age and sex dependent.

1.4.2 Imaging genetics

The combination of genetics and neuroimaging emerged as (neuro)imaging genetic/genomics, a new discipline(s) seeking a deeper understanding of how genetic variations impact both the structure and function of the brain (Bigos et al., 2016; Hariri & Weinberger, 2003; Thompson et al., 2010). Imaging genomics and imaging genetics are terms that are often used interchangeably, but they can have subtle differences in emphasis depending on the context. Imaging genetics typically refers to the study of individual genes, while imaging genomics is a broader term that may encompasses the entire genome and the interactions within it. A critical challenge within imaging genetics/genomics is the integration of information from different analytical levels: from genes to brain structure and function, and behavior. This approach can be used to identify novel disease biomarkers, which later can be used for earlier diagnosis or focused therapies. Imaging genomics studies more accurately model the transition from MCI to AD compared to the conventional clinical-cognitive model (Kong et al., 2015). Machine learning analyses reveal that incorporating SNPs information correlated with neuroimaging findings enhances the accuracy of classification between AD and MCI patients (Zhang et al., 2014).

In the realm of AD related research there are not many reports with task-related fMRI and EEG data from the clinical population. Most of the studies rely on a resting-state protocol, which is easier to perform with cognitively and behaviorally impaired participants, who often cannot perform complex tasks that demand prolonged focus, attention, and numerous repetitions of stimuli. Nevertheless, such studies are crucial for understanding the impact of risk genes on brain function, and they can be effectively carried out with healthy participant (or those in prodromal stage) clustered to experimental groups based on their genetic characteristics.

There is currently no cure for Alzheimer's disease, and the existing (and currently tested) drugs can only slow the neurodegeneration progression (Alzheimer’s Association, 2022). Pharmacological treatment would be most beneficial in the prodromal stages of the disease; however, the delayed diagnosis often results in medication starting too late (Rossini et al., 2020). Apart from the evident endeavors to discover a cure for AD, a crucial objective in modern science involves identifying early biomarkers associated with the condition – symptoms or traits that can predict its onset before irreversible pathological changes in the brain result in substantial cognitive deficits. Identifying individuals at a heightened risk of developing Alzheimer's disease may enable them to access new interventions and treatments. Understanding the roles of risk genes, and their effects on the brains and interaction with other health and lifestyle factors, in healthy individuals across all age groups is essential.

2 Aims

The primary objective of the study was to determine 1) whether middle-aged healthy individuals with LOAD genetic burden exhibit any changes in health, brain (on both, anatomical and functional level) and cognitive functions compared to matched individuals without the genetic risk; and 2) if the presumed changes resemble the symptoms observable in AD patients when compared to healthy controls. Based on the available literature, the following specific questions and hypotheses were proposed.

Specific questions:

I How does the presence of the *APOE*-ε4 allele and specific alleles of the *PICALM* gene influence cognitive function in healthy, middle-aged individuals?

II Are there identifiable blood-based biomarkers and miRNA profiles that correlate with the presence of studied genetic variants in healthy individuals?

III Are there any brain activity features associated with *APOE* and *PICALM*, as measured by EEG and fMRI during resting state protocol and cognitive tasks related to memory and cognitive control?

IV Are there structural changes in the brain, as measured by anatomical MRI scans, related to the presence of specific *APOE* and *PICALM* alleles?

V Should any alterations be observed (as in questions I-IV), do they result from the combined influence of both genes, or are these changes typically linked to the most widely recognized risk gene, *APOE*? How do *PICALM* alleles modify the risk associated with *APOE*?

Main hypotheses:

Hypothesis I: Healthy middle-aged individuals at genetic LOAD risk differ significantly from matched group without the risk in terms of: health – blood counts, lipid profile, health questionnaires, psychometric tests results, miRNA levels; behavior in cognitive tasks – reaction times/accuracy measured in two tasks regarding memory (STM) and cognitive control/executive attention (MSIT); neuroimaging (both during resting-state

protocol and during cognitive tasks) – EEG power spectrum and complexity, EEG ERP, integrity of fMRI networks and structural brain alterations.

Hypothesis II: The observable differences will resemble the pattern previously described for LOAD patients. Individuals carrying the risk alleles will exhibit blood and psychometric tests results with signs of reduced health and mood; will demonstrate lower cognitive performance compared to non-carriers; will present miRNA AD-related pattern; will exhibit aberrant patterns in resting-state connectivity and altered neural responses during the cognitive tasks, indicating early disruptions in functional brain networks. We expect that individuals with the risk alleles will demonstrate reduced cortical thickness in the key brain regions associated with AD (parahippocampal gyrus, supramarginal gyrus, temporal pole, superior parietal lobule and inferior temporal gyrus)

Hypothesis III: The magnitude of anticipated changes is expected to be greater in individuals carrying a double genetic LOAD risk compared to those carrying a single risk.

Given the complex LOAD etiology the methodology was extended to gain relevant information about the study groups in terms of health, psychometric tests results, neuroimaging biomarkers (either EEG and MRI/fMRI) and additional genetic information (miRNA) (described in detail in *Methods* section).

3 Methods

3.1 Outline of the study methodology

To validate the proposed hypotheses and address the research questions, a two-phase study was undertaken, encompassing several experiments. The diagram depicting the stages is presented in Figure 3.

Phase I: Screening tests (N = 200; sex distribution, F/M: 109/91; age range: 50-63 years old). This stage encompasses the following components:

- Genetic screening of *APOE*/*PICALM* genes.
- Administration of a battery of psychometric tests.
- Completion of health and demographic questionnaires.
- Collection of information regarding family history of dementia.

Phase II: Neuroimaging and blood tests (N = ~80; sex distribution, F/M: 41/39, age range: 50-63 years old). Participants were divided into three groups with various LOAD genetic risks. This phase included following experiments:

- Electroencephalography (EEG).
- Functional magnetic resonance imaging (fMRI) and structural MRI (T1/T2-weighted images).
- Blood tests, including a complete blood count, lipid profile, and HSV-1 IgG antibodies; miRNA diagnostic panel.

Neuroimaging sessions included three protocols: Sternberg Memory Task (in this thesis only the behavior data are shown), Multi-Source Interference Task, and a resting-state protocol (eyes-closed condition). The initial one-on-one meetings for the study were conducted in a separate, quiet room in the Nencki Institute of Experimental Biology PAS.

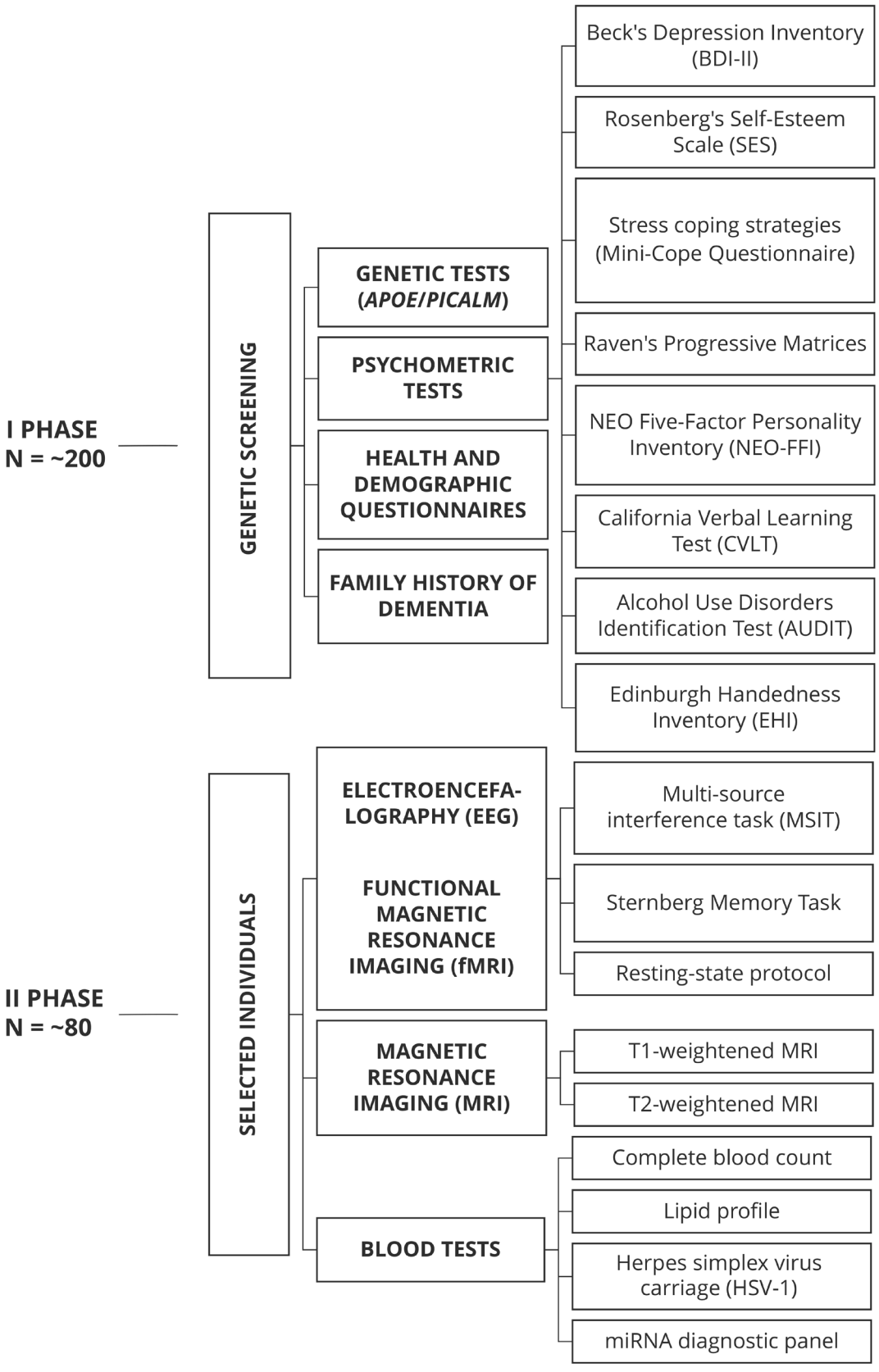

Figure 3. Diagram of study methodology: main study phases and conducted experiments.

Except for the CVLT test, which required the researcher's assistance, the subjects self-administered all other tests. Following the testing session, a buccal swab sample was obtained for genetic screening (participants were instructed on how to collect the sample themselves).

In the Phase II of the experiment, individuals possessing risk alleles for *APOE*/*PICALM* genes and a matched group with neutral alleles were invited to take part in the neuroimaging sessions and blood testing. EEG recordings and fMRI scans were conducted on separate days. The EEG session took place at the EEG laboratory in the Nencki Institute of Experimental Biology PAS, while the MRI/fMRI session was held at the Bioimaging Research Center in the Institute of Physiology and Pathology of Hearing in Poland. To prevent any potential task learning bias in either design, an approximately equal number of subjects underwent an EEG session followed by an fMRI session, and vice versa (N = 31 for EEG session first, N = 40 for fMRI session first). Blood samples were collected on a separate day in a professional medical facility.

3.2 Recruitment criteria, ethics, and study groups

Conventional methods (such as flyers or posters) and social media advertisements were employed in the participant recruitment process. Both strategies directed individuals to a website containing study information and an online survey where they were provided with details about conditions that would disqualify them from participating. Only individuals without contraindications were contacted and recruited. Additionally, three times throughout the study: first before the psychometric and questionnaire session, then before the EEG, and finally just prior to the MRI test, participants were reminded of the same list of contraindications.

This study received approval from the Bioethics Committee of the Nicolaus Copernicus University in Toruń at the Ludwik Rydygier Collegium Medicum in Bydgoszcz, Poland (approval number: KB 684/2019). Written informed consent was obtained from all participants, who also signed a document containing detailed study information. All participants were given the option to receive the results of genetic and other tests. To prevent bias in successive stages of the study, the results were distributed after the final experimental session for those recruited for the Phase II of the experiments. Participants included in the second stage of the study also received a cash remuneration (100 PLN) and a CD with their individual MRI data.

The exclusion criteria for the study included recent or ongoing infections, significant health issues, epilepsy, known mental illnesses or brain damage, chronic headaches, sleep disorders, skin allergies and diseases, metal objects/implants in the body, and pregnancy. Many of these exclusions were implemented due to the MRI/fMRI session requirements. Despite repeated presentations of these contraindications, and the subjects' acknowledgment

through their signatures, situations arose where, for instance, an individual was found to have metal objects in the body just before the fMRI/MRI session (refer to the *Missing Data* section).

Participants were requested to discontinue medication use 24 hours before the neuroimaging sessions, unless it was necessary (e.g., prescribed for a chronic condition). Additionally, subjects were advised to abstain from alcohol, stimulating and caffeinated beverages, and psychoactive substances for 24 hours prior to the experiments. However, if the consumption of a morning cup of coffee was a regular part of the subject's routine, they were encouraged to maintain their natural daily rhythm. Participants were also instructed to ensure they were well-rested before either experimental session.

Ultimately, data from N = 79 out of the initially recruited N = 80 participants for the second stage of the study were analyzed. One participant was excluded from the analysis due to having a rare and ambiguous *APOE*-ε2/ε4 genotype. The groups were selected according to *APOE*/*PICALM* risk alleles, specifically *APOE*-ε4/*PICALM* GG non-carriers (denoted as "N" group), single-risk individuals (*APOE*-ε4 carriers without *PICALM* risky GG alleles, labeled as "A+P-" group), and double-risk individuals (*APOE*-ε4 carriers with *PICALM* risky GG alleles, labeled as "A+P+" group). The distribution of subjects in each group is presented in Table 1.

Table 1. Study groups: Phase II of the study

Group	Frequency [N]	Valid percent [%]
N	31	39.24
A+P-	27	34.18
A+P+	21	26.58

The data are shown for all N = 79 participants from the Phase II of the experiment. Although, not all participants undergone all sessions (*Missing Data* section).

No participants with the *APOE*-ε2 allele were included in the "N" group, which exclusively comprised participants with homozygous *APOE*-ε3/ε3 genotype. The risky *APOE* variants were *APOE*-ε3/ε4 and *APOE*-ε4/ε4, though most participants were homozygous for the ε4 allele. Concerning the *PICALM* gene, GG was regarded as a risky variant, while AA and AG were considered neutral variants.

3.2.1 Statistical power

An appropriate level of statistical power is needed to avoid type II error in statistical analysis (i.e., acceptance of the null hypothesis of no effect when it is false). The statistical power does not influence the type I error, i.e., acceptance of alternative hypothesis (that the relationship between the sets of data exist). On the other hand, high statistical power in the study may lead to overly sensitive results, finding minor differences in the data, which are not meaningful.

A *priori* power analyses were conducted using G*Power version 3.1.9.7 (Faul et al., 2007) to determine the minimum sample size required to test the study hypotheses.

— Results indicated the required sample size to achieve 80% power for detecting a medium effect (0.6), at a significance criterion of α = .05, was N = 36 for t-tests difference between two independent means and to achieve 70% power with the same criteria, was N = 27 for t-tests difference between two independent means.

— Results indicated the required sample size to achieve 80% power for detecting a medium effect (0.3), at a significance criterion of α = .05, was N = 37 for one-way ANOVA and to achieve 70% power with the same criteria, was N = 30. Within the same criteria for two-way ANOVA (considering sex as an additional factor): to achieve 70% power N = 30 participants are needed in each group

Thus, the obtained sample size (Table 1) for N group is for most comparisons adequate to test the study hypothesis, although obtained sample size especially for A+P+ group is relatively small, and so the comparisons with this group would held less statistical power (only this number of participants could be recruited to this group through the Phase I genetic screening of N = 200).

3.3 Genetic screening

Genomed S.A, an external company, was tasked with conducting genetic testing. The samples were collected during the initial meeting with participants (at the Nencki Institute of Experimental Biology PAS) and transferred to the company. For this purpose, COPAN eNat® Cheek Swabs, specifically designed for the collection and long-term storage of nucleic acids, were utilized. The specimens were collected from the buccal mucosa (the interior surface of the cheek). To identify the risk genes *PICALM* (rs3851179) and *APOE* (rs429358/rs7412, necessary for identifying major variants ε2, ε3, and ε4), the conventional Sanger sequencing protocol was employed within Genomed S.A facility. This approach is widely acknowledged for its precision and has been employed in genetic analysis for several decades.

3.4 Statistics

Standard statistical analyzes (results outlined in tables, ANOVA statistics, post-hoc tests and tests assumptions validation) were performed using R (R Core Team, 2023) with RStudio (Posit team, 2023) self-written scripts. Used packages included: tidyverse (Wickham et al., 2019), ggpubr (Kassambara, 2023a), rstatix (Kassambara, 2023b), and broom (Robinson et al., 2023).

3.4.1 Basic testing assumptions

Due to the variety of data, different statistical methods and assumptions were used. For convenience, I describe here the basic statistical assumptions made in the dissertation for standard statistical analyzes.

I For quantitative variables, an ANCOVA test (with age as a covariate and sex as a fixed factor) or two-way ANOVA test (with sex as a fixed factor) was used which was chosen based on the assumptions of tests and if age/gender where previously shown to have an important influence. ANCOVA/two-way ANOVA approaches could increase statistical power by reducing error variance and provide more statistical control. If all the assumptions failed, then the Kruskal-Wallis test was used.

   a. ANCOVA: First, linearity between the covariate (age) and the dependent variable was assessed. If no linearity was assumed, then either one-way or two-way ANOVA test was used checking other ANOVA assumptions.

   b. ANCOVA: secondly, the homogeneity of regression slopes was checked.

   c. Both ANOVA/ANCOVA: Homoscedasticity measured by homogeneity test (Levene's test with criterium of $p < .05$; note: there are several versions of the Levene's test, and here the median based one was used, which is considered generally more robust)

      — If the assumption was violated when the ANCOVA was meant to be calculated, the ANOVA was calculated instead, with Welch's homogeneity correction (which is generally recommended over Brown-Forsythe test and is more robust (Glantz et al., 2016)).

   d. Both ANOVA/ANCOVA: Normality of residuals was assessed by Shapiro-Wilk test, and the quantile (Q-Q) plots (standardized residuals vs. theoretical quantiles) were inspected.

      — ANOVA/ANCOVA is robust to the violation of this assumption with relatively bigger sample sizes (Blanca Mena et al., 2017; Lumley et al., 2002); recent research showed instead that in terms of Type I errors the F-test is robust (Blanca Mena et al., 2017) even with smaller sample sizes (group sizes ranged from 5-100; it is also worth noting that this simulation was tested on 3 groups, which corresponds to study design showed in this dissertation).

      — Additionally, if a deviation from the normality was shown, natural log transformation $\log(x)$ was used for the EEG relative power and behavioral (reaction time) data.

— Data outliers were investigated if the data were not normally distributed. Data entry errors were checked at the level of building a valid database for further statistical testing and removed or corrected. Otherwise, valid (a natural part of the studied population) unusual values (> 3SD) were not removed in any of the analysis as there is no consensus if this method should be used in experimental/research procedures in natural sciences, as it may lead to misinterpretation and inference errors (Altman & Krzywinski, 2016; Karch, 2023).

II For nominal variables, the chi-square test was used.

III For ordinal variables, the non-parametrical Kruskal-Wallis test was used.

ANOVA/ANCOVA were accompanied with standard post-hoc tests with Tukey correction for multiple comparisons. If the ANOVA test with Welch's homogeneity correction was used, then the Games-Howell post-hoc approach (and Tukey's correction) was applied. For Kruskal-Wallis test the Dunn's post-hoc tests were used instead.

Statistical significance was defined as follows: a p-value ≤ 0.05 was considered significant, and p-value > 0.05 and ≤ 0.09 was considered as a trend. All data, where it was possible, were presented as mean (M) ± standard deviation (SD). Annotation on the figures: a p-value ≤ 0.05 is mark with *, < .01 with **, and < .001 with ***. Trend level differences are marked with ~ and exact p value.

3.4.2 Neuroimaging data statistics

Some neuroimaging statistics were computed within software specifically designed for such tasks and were not delegated to R. EEGLAB (Delorme & Makeig, 2004) was employed to compute event-related potential (ERP) statistics, using false discovery rate (FDR) corrected levels (main conditions differences in MSIT). Final ERP amplitude and latency measures were exported to R and followed already described rules. Parametric statistics were used within the EEGLAB toolbox, which utilizes specific functions of the MATLAB (version 2022a was used) (The MathWorks Inc., 2022) environment for statistical calculations. Resting-state protocol and MSIT fMRI data were processed using dedicated software, and the statistical information in the results tables is derived from the SPM12 toolbox (Wellcome Centre for Human Neuroimaging, 2020), with FDR corrected values provided. Statistical analysis of coherence results was conducted in MATLAB utilizing two-sample t-tests, as coherence was calculated within the Fieldtrip toolbox (Oostenveld et al., 2011). For t-test coherence results, FDR correction was applied using the Benjamini & Hochberg method (Benjamini & Hochberg, 1995) with a custom MATLAB function (Groppe, 2015). Statistics on fMRI data connectivity (within resting-state protocol) were conducted at the cluster level (groups of contiguous voxels). These cluster-level inferences

relied on parametric statistics derived from Gaussian Random Field theory (Nieto-Castanon, 2020; Worsley et al., 1996). The results were subjected to a thresholding approach that involved a combination of a voxel-level threshold of $p < 0.001$ for cluster formation and a familywise corrected cluster-size threshold of p-FDR < 0.05 (Chumbley et al., 2010).

3.4.3 Data visualization

Data visualizations (boxplots, barplots, lineplots, circle charts) were created using Python self-written scripts, with use of the seaborn (Waskom, 2021), matplotlib (Hunter, 2007) and a part of statannot (Weber, 2022) libraries. Specific figures for EEG and MRI/fMRI results were prepared using dedicated programs for the analysis or visualization of neuroimaging data and self-written scripts: EEG topographical plots – EEGLAB (Delorme & Makeig, 2004), EEG connectograms and connectivity matrix representations – MNE (Gramfort et al., 2014), MRI Destrieux atlas data – BrainPainter with use of self-written Linux shell scripts (Marinescu et al., 2019), fMRI data – CONN toolbox (Whitfield-Gabrieli & Nieto-Castanon, 2012) and BrainNet Viewer (Xia et al., 2013). All supplementary graphics (such as the arrangement of electrodes with cluster markings, EEG connectivity head plots), and the compilations of individual graphs into comprehensive figures were prepared by hand using Adobe graphics programs.

3.5 Demographic and psychometric questionnaires

During the Phase I of the study (the first meeting), participants completed a set of health, demographic and psychometric questionnaires, the summary of which is presented in the *Results* section. This comprehensive approach aimed to gather essential information about participants' health, demographics, and cognitive functioning.

The demographic and health questionnaires contained the questions regarding following information:

— Demographic data: age, gender, marital status, employment status, education level, place of residence.

— Health data: learning difficulties, height and weight (later used to calculate body mass index, BMI), diabetes, allergies, thyroid diseases, hypertension, other ongoing diseases, ongoing medication use, amount of NSAID intake, smoking status, caffeine intake, alcohol consumption, handedness, physical activity (subjective question), social activity (subjective question), family history of dementia.

Alcohol consumption was measured by the Alcohol Use Disorders Identification Test (AUDIT) (Saunders, Aasland, et al., 1993) and handedness with use of Edinburgh

Handedness Inventory (EHI) (Oldfield, 1971). Other demographic/health characteristics were included in an additional, specially prepared questionnaire with separate questions corresponding to each measure/item (responses were subjective, not medically validated).

Moreover, participants underwent a battery of psychological tests, which included:

— Beck Depression Inventory (BDI) (Beck et al., 1996, 2019): a widely used self-report questionnaire designed to assess the severity of depressive symptoms and mood changes (such as sadness, guilt, fatigue, loss of interests). The test consists of twenty-one items. Total scores range from 0 to 63. Interpreting BDI scores involves considering the total score obtained, where more points are equal to worse functioning. While the BDI provides valuable information about the severity of depressive symptoms, it is not a diagnostic tool.

— Rosenberg Self-Esteem Scale (SES) (Dzwonkowska et al., 2008; Rosenberg, 1989): a widely utilized self-report questionnaire developed by sociologist Morris Rosenberg to measure an individual's overall self-esteem. The test consists of ten items. Scores range from 0 to 30 points. Interpreting SES scores involves considering the total score obtained, where more points suggest higher self-esteem.

— Mini-Cope Questionnaire (Coping Orientation to Problems Experienced Questionnaire) (Carver, 1997; Juczyński & Ogińska-Bulik, 2012): assess various coping strategies individuals employ when faced with stressors. The test consists of twenty-eight items. The items were summarized in seven subscales, as provided by the test handbook: active coping, hopelessness, support seeking, avoidance behavior, turning to religion, acceptance, and humor (each subscale: 0-3 points).

— NEO-FFI Personality Inventory (Costa & McCrae, 1985, 1989; Zawadzki et al., 2010): a widely used personality assessment tool that measures five major personality traits: neuroticism, extraversion, openness to experience, agreeableness, and conscientiousness. Based on the Five-Factor Model of personality, the NEO-FFI provides a concise and reliable measure for evaluating these fundamental dimensions, offering valuable insights into an individual's typical patterns of behavior, emotions, and thought. The test consists of sixty items. The items were recalculated to obtain scores for the described five personality traits (more points mean higher intensity of a given trait).

— Standard/Classic version of Raven's Progressive Matrix (RPM) (Jaworowska & Szustrowa, 2010; Raven et al., 1996): a non-verbal fluid intelligence test designed to assess abstract reasoning and problem-solving abilities. It consists of a series of visual patterns where the participant must identify the missing piece from a set of options, providing insights into cognitive reasoning skills independent of language or cultural influences. We modified the duration allowed to complete the assessment, setting it to 30 minutes, as opposed to the unlimited time given in the classic version.

The test consists of sixty items. The scoring and interpretation involve assessing the number of correct responses and this reflects the performance.

— California Language Learning Test (CVLT) (Delis et al., 1988; Łojek & Stańczak, 2010): designed to evaluate an individual's verbal learning and memory skills. This test involves the presentation of a list of words to the participant, who is then asked to recall and recognize the words over several learning trials, providing valuable insights into memory processes and potential cognitive deficits. An additional benefit of the CVLT test lies in its ecological approach, as the word lists used for memory assessment are related to everyday activities, such as shopping. The test points were calculated and summarized in 12 scales: list A (task 1-5, total points), list A (task 1), list B (total points), short-term delay free recall, short-term delay cued recall, long-term delay free recall, long-term delay cued recall, perseverations, intrusion errors (free recall), intrusion errors (cued recall), recognition (total hits), recognition (false alarms).

The raw scores from the psychometric tests were uniformly recalculated according to the guidelines provided in the test handbooks. This involved necessary adjustments, such as reversing scales when required, to derive the final scores. All psychometric tests used in this study were adaptations and standardized versions in Polish, obtained from the Psychological Test Laboratory of the Polish Psychological Association.

3.6 Blood tests

Blood testing was outsourced to a commercial, certified medical facility, where a certified nurse collected blood samples in a clinical setting (in the morning, after an 8-12 hour fasting period). Table 2 shows the list of parameters covered in the blood cell count and lipid profile tests, along with the corresponding laboratory norms. In addition to morphology and biochemical tests, IgG antibodies for herpes simplex virus (HSV) were assessed with the ELISA method (Euroimmun Kit).

3.6.1 miRNA panel

Additional miRNA tests were performed in the Laboratory of Preclinical Testing of Higher Standard, led by prof. Urszula Wojda, at the Nencki Institute of Experimental Biology PAS. Blood samples were subjected to RT-qPCR analysis to measure the levels of circulating miRNAs previously identified by the prof. Urszula Wojda team as a potential set of Alzheimer's disease biomarkers in blood plasma (including those within patent EP3449009) (Nagaraj et al., 2017, 2019). miRNA panel included: miR-29b-3p, miR-30-5p, miR-34a-5p, miR-125b-5p, miR-135a-5p, miR-142-3p, miR-146-5p, miR-200a-3p, miR-

483-5p, miR-486-5p, and miR-502-3p. To perform differential expression analysis fold change was calculated (log2 fold change), which allows for the interpretation if selected genetic variant is up-regulated or down-regulated. Additionally, the scores were age adjusted, therefore age was not considered as a covariate in the statistical analysis.

Table 2. Blood tests laboratory norms

Parameter	**Laboratory norm [K/µl]**	
	Females	Males
Leukocytes [K/µl]	3.98-10.4	4.23-9.07
Erythrocytes [K/µl]	3.93-5.22	4.63-6.08
Hemoglobin [K/µl]	11.20-15.70	13.70-17.50
Hematocrit [%]	34.10-44.90	40.10-51.0
MCV [fl]	79.40-94.80	79-92.20
MCH [pg]	25.60-32.20	25.70-32.20
MCHC [g/dl]	32.20-35.50	32.30-36.50
RDW-CV [%]	11.70-14.40	11.60-14.40
Platelets [K/µl]	150-400	
PDW [fl]	9.80-16.20	9.80-16.10
MPV [fl]	9.40-12.50	9.40-12.60
P-LCR [%]	19.10-46.60	19.20-47
Neutrophils [K/µl | %]	2-7 (40-80%)	
Lymphocytes [K/µl | %]	1-3 (20-40%)	
Monocytes [K/µl | %]	0.2-1 (2-10%)	
Eosinophils [K/µl | %]	0.02-0.5 (1-6%)	
Basophils [K/µl | %]	0.02-0.10 (0-2%)	
Total cholesterol [mg/dl]	115-190	
HDL cholesterol [mg/dl]	>=45	>=40
Non-HDL cholesterol [mg/dl]	< 145*	
LDL cholesterol [mg/dl]	< 115*	

* Values for healthy people at low or intermediate risk of death from cardiovascular disease

3.7 Neuroimaging

3.7.1 Study environment and procedures details

Participants had the flexibility to select a session time that best suited their schedule (neuroimaging experiments were conducted both in the morning and afternoon). Detailed experimental methods for EEG and MRI/fMRI sessions are provided in Table 3 and Table 4, respectively. The high-density EEG cap was prepared prior to each session to reduce the amount of time participants had to spend in the laboratory. During the EEG session, participants were comfortably seated in a quiet room, facing a monitor. The experiment was overseen from a separate room using a remote desktop connection to an experimental computer and a LAN camera observing the EEG laboratory.

Table 3. Experimental procedure details: EEG session

No.	Task	Duration time
1.	Fill in the laboratory documents	~5-15 minutes
2.	EEG cap preparation, impedance reduction	~60-80 minutes
3.	Resting state protocol instruction and recording: eyes-closed condition	~8 minutes (6 minutes for the recording)
4.	MSIT instruction and training	~5-8 minutes
5.	MSIT recording	~10 minutes
6.	Sternberg memory task instruction and training	~5-8 minutes
7.	Sternberg memory task recording	~ 13 minutes
8.	CapTrak session	~30 minutes

Table 4. Experimental procedure details: MRI/fMRI session

No.	Task	Duration time
1.	Fill in the laboratory documents and an additional consent for fMRI/MRI study	~5-15 minutes
2.	Participant preparation in the scanner	~5-8 minutes
3.	MSIT instruction and training	~5-8 minutes
4.	Sternberg memory task instruction and training	~5-8 minutes
5.	Resting state protocol instruction and recording	~10–12 minutes (7.5 minutes for the recording)
6.	MSIT recording	~10 minutes
7.	Sternberg memory task recording	~13 minutes
8.	T1 and T2-weighetend images collection	~15 minutes

3.7.2 EEG device and recording parameters

EEG data were recorded using a Brain Products system: an actiCHamp amplifier and an actiCAP-slim high-density electrode cap with 128 mounted electrodes (Brain Products GmbH, Munich, Germany). The Brain Products standard electrode configuration file was used (Figure 4). The online reference was set at FCz electrode. The sampling frequency was set to 1000 Hz. No notch filter or high pass filter was used during recording, only the low pass filter was set to 280 Hz. The lowest possible impedance was maintained during the recording, on average 5-10 kΩ (MSIT task: 7.79±3.17 kΩ, minimal value: 1.86 kΩ, maximal value: 19.19 kΩ; resting-state: 7.30±3.12 kΩ, minimal value: 1.76 kΩ, maximal value: 19.19 kΩ), by gently rubbing the skin and by EEG gel application. At the end of each session, actual electrode positions were detected using a CapTrak handheld 3D scanner (Brain Products GmbH, Munich, Germany).

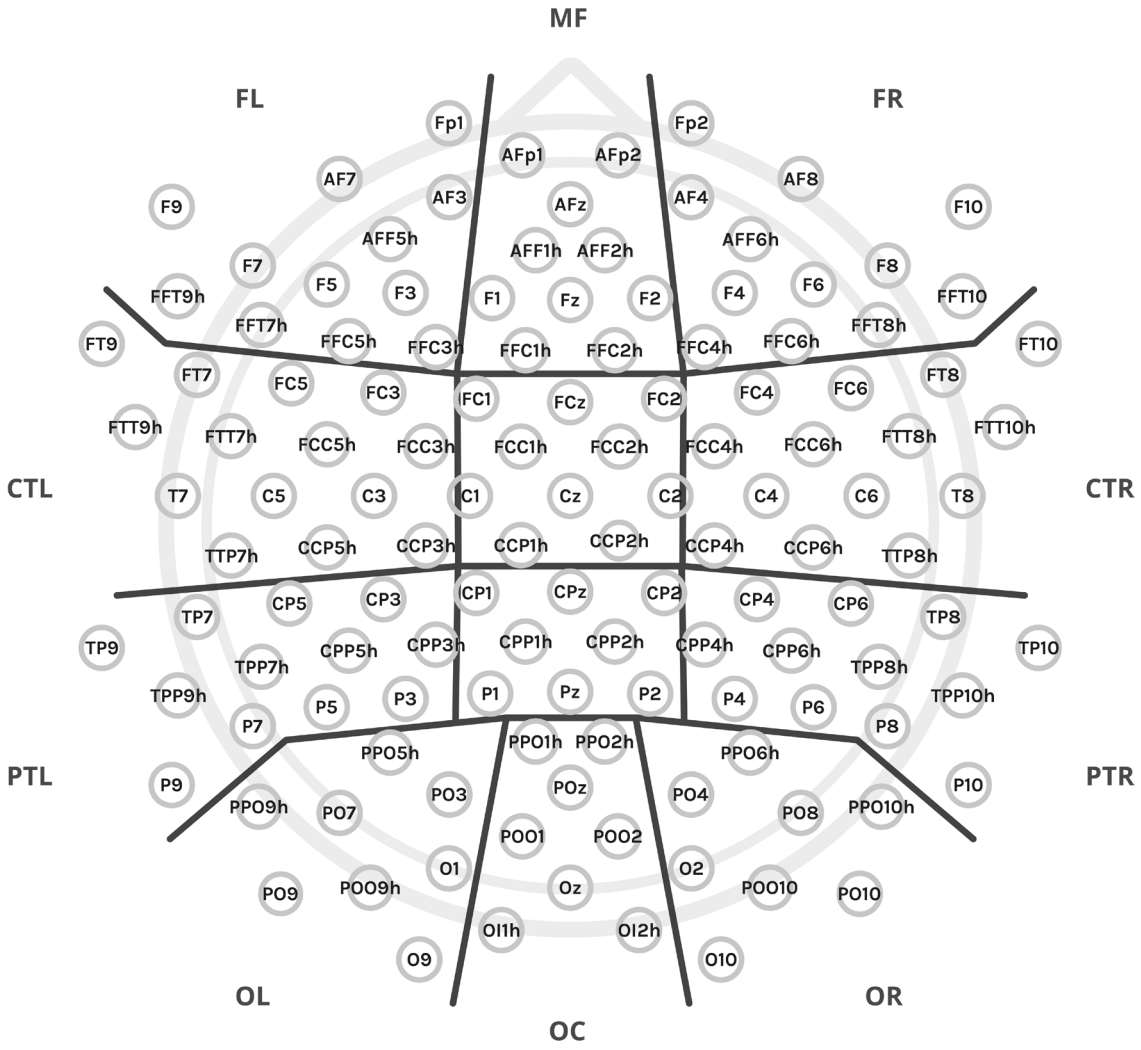

Figure 4. The electrode setup employed in the experiment consisted of 128 electrodes. Their division into anatomical clusters used for data analyses is marked by a thick black line: MF – midfrontal, FL – frontal left, FR – frontal right, C – central, CTL – central-temporal left, CTR – central-temporal right, PR – parietal central, PTL – parietal-temporal left, PTR – parietal temporal right, OC – occipital central, OL – occipital left, OR – occipital right. Two midline clusters are not marked in the figure: C – central (with FCz, Cz and neighboring electrodes), CP – central-parietal (with CPz, Pz and neighboring electrodes).

3.7.3 MRI/fMRI device and acquisition parameters

MRI/fMRI experiments were conducted at Bioimaging Research Center in the Institute of Physiology and Pathology of Hearing in Poland, using a Siemens Prisma FIT 3T scanner (Siemens Medical Systems, Erlangen, Germany), equipped with a 64-channel phased-array RF head coil. The acquisition parameters included a multi-band (slice acceleration factor=8) EPI sequence, a repetition time (TR) of 0.8 seconds, an echo time (TE) of 0.038 seconds, a slice thickness of 2 mm, 72 slices, IPAT=1, a field of view (FOV) measuring 216x216 mm,

a flip angle of 52 degrees, a voxel size of 2x2x2 mm. For each subject, two sequences were obtained for each task, one with an Anterior-Posterior encoding phase and the other with a Posterior-Anterior encoding phase. Structural T1-weighted 3D MP-Rage images were acquired with the following parameters: a TR of 2400 ms, a TI of 1000 ms, a TE of 2.74 ms, a flip angle of 8 degrees, a FOV of 256x256 mm, a voxel size of 0.8x0.8x0.8 mm, and a total acquisition time (TA) of 6 minutes and 52 seconds.

3.7.4 Task details

All cognitive tasks and the resting-state protocol designed for the study were implemented using Presentation software v.20.0 (Neurobehavioral Systems, Inc. Berkeley, CA, n.d.) separately for EEG and fMRI experiments. This software was also employed to present the tasks to the participants and to record the logfiles with procedure metadata including the coding of stimuli and participant's responses (i.e., behavioral data). The stimuli were presented in gray color (RGB: 206, 206, 206) against a dark background (RGB: 58, 58, 58). During EEG session the stimuli were displayed on a computer monitor and during fMRI session on a scanner-compatible goggles (VisualSystem HD, NNL, nordicneurolabs inc.), which allowed monitoring of participants' engagement and wakefulness. In the EEG session, responses were recorded using a keyboard, while in the fMRI session, a response grip (Smitlab response grip) was used. Prior to the main experiment, participants underwent brief training to familiarize them with the tasks. If participants frequently answered incorrectly during the training session, the process was repeated until they fully understood the instructions. Participants were instructed to provide responses as quickly as possible, but without compromising accuracy for the sake of speed.

3.7.4.1 Resting state protocol

The resting-state protocol was employed to explore spontaneous brain activity in the absence of specific tasks. Among others, this protocol allows for the investigation of the functional connectivity of the brain. Participants were directed to stay still and quiet with their eyes closed. Additionally, they were instructed not to focus on any specific thoughts but rather to let their minds rest and allow different thoughts to emerge.

3.7.4.2 Multi-Source Interference Task

The Multi-Source Interference Task (MSIT) serves as a cognitive assessment to gauge attention and cognitive control in a face of cognitive interference (Bush & Shin, 2006; Bush et al., 2003). This task evaluates the ability to disregard distracting information and concentrate on task-relevant data. MSIT is widely used in cognitive neuroscience research,

reliably activating areas such as the dorsal anterior cingulate cortex, medial prefrontal cortex, and supplementary motor area (Deng et al., 2018). It has been applied in clinical populations to assess various disorders (Bush et al., 2008; Mao et al., 2014) and in studies on healthy aging (Kwan et al., 2022).

Participants are presented with a sequence of three digits (e.g., "221") and are tasked with identifying the unique digit (target) while ignoring two other identical digits (distractors). The correct response involves pressing the button corresponding to the target digit value, not its position (e.g., "1" in the example given above). The task introduces congruent, low-demanding condition (named 00, where the target digit and its position are the same) and incongruent, high-demanding condition (named FS, where the target digit location and the response button location differ), creating cognitive interference.

The list of possible trials included:

— Low-demanding condition, congruent (00): 100, 020, 003.
— High-demanding condition, incongruent (FS): contingency-equalized design presenting each unique stimulus equally often. Several parallel subsets of stimuli were used for different sets, such as 221, 233, 131, or 212, 332, 311, or 313, 112, 322, or 331, 211, 232. For each individual experiment, a set of incongruent stimuli was randomly drawn to avoid potential contingency learning bias (Braem et al., 2019) which can occur in the original MSIT task.

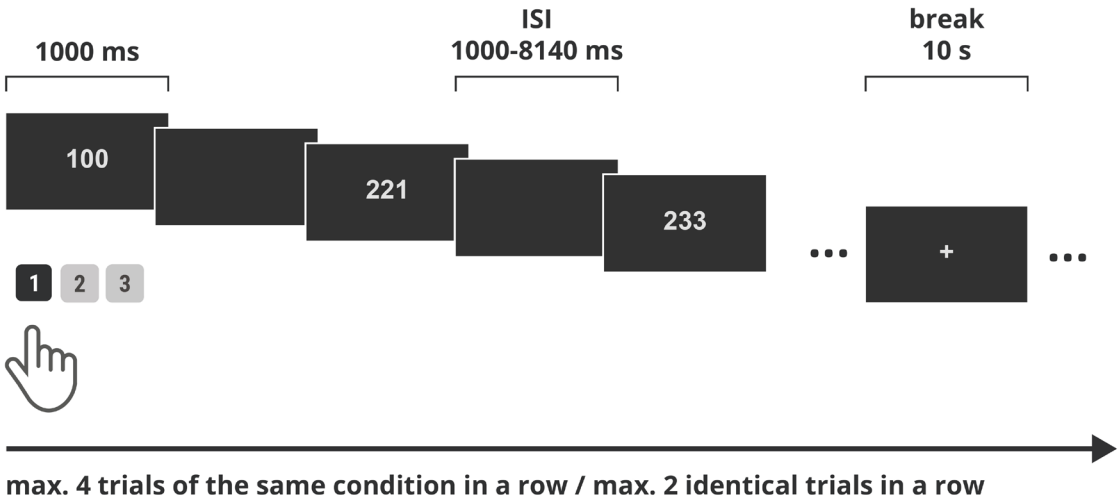

Figure 5. Multi-Source Interference Task design. ISI: interstimulus interval. 100 – an example of low-demanding 00 stimulus; 221 and 233 – examples of high-demanding FS stimuli.

Sixteen sets of predefined stimuli sequences were generated using the OptimizeX algorithm (Spunt, 2016) to minimize collinearity in the event-related task design, particularly for fMRI purposes (Mumford et al., 2015). The orthogonality of regressors in a general linear model (GLM) is crucial for reliable fMRI analysis, as collinearity may impact the estimated

contrasts of parameters and, consequently, the obtained results (Mumford et al., 2015; Poline et al., 2007). Each set displayed a maximum of four trials of the same condition in a row and a maximum of two identical stimuli consecutively (during the initial part of the experiment five recordings from fMRI session did not follow this rule). Among the sixteen stimulus sets, the correlation between both conditions ranged from 0.14 to 0.19. The task was divided into two runs, each containing 83 stimuli (166 trials for full MSIT recording). Stimuli were presented for 1000 ms, and the interstimulus interval (ISI) varied between approximately 1000–8140 ms, with an average ISI of approximately 1804 ms across all sets. During the ISI, a dark, blank screen was displayed. A 10-second break, marked with "+", was included in the middle of each run. The task design is depicted in Figure 5.

3.7.4.3 Sternberg's Memory Task

The Sternberg Memory Task, a widely utilized psychological paradigm developed by Saul Sternberg in 1966 (Sternberg, 1966), serves as a tool to investigate short-term memory. The participants were presented with memory sets containing lists of letters followed by individual single-letter probes. Participants were expected to indicate whether the probe was a part of the original list.

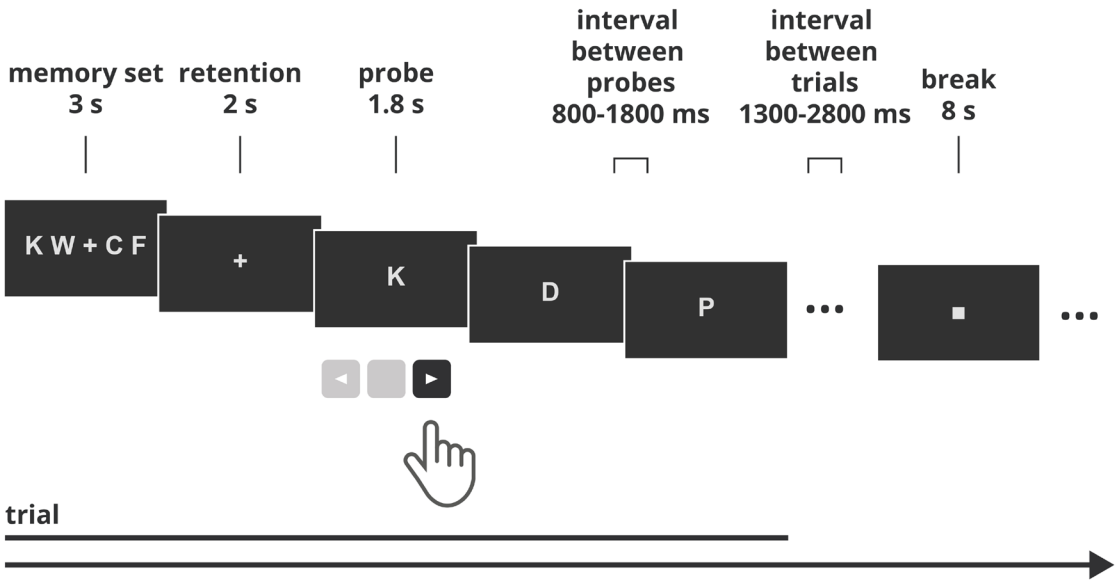

Figure 6. Sternberg's task design. A sample trial of non-demanding condition with four-letter set is shown.

The task was scripted to use predefined letter combinations containing only consonants. It consisted of 24 low-demanding memory sets with 4 letters (e.g., "K W + C F", "P Z + D J") and 24 highly-demanding memory sets with 8 letters (e.g., "R T G L + D F B Z", "W T H J + C F L R"). After each memory set, three probes were presented, each including one letter from the consonant set (B, C, D, F, G, H, J, K, L N, P, R, S, T, W, Z). The retention

period was marked by a "+" sign displayed on the screen. The interval between probes presentations ranged from 800 to 1800 ms, while the interval between whole trials (memory set, retention, probes) ranged from 1300 to 2800 ms. Breaks lasting 8 seconds were introduced in the task, marked by a black square ("■"). The number of target (letter included in the memory set) and non-target (letter not included in the memory set) probes was balanced throughout the task. The task design is illustrated in Figure 6.

3.7.5 Analytical methods

3.7.5.1 Behavioral data

Reaction time and accuracy data for the MSIT and Sternberg's Memory tasks were extracted from raw Presentation logfiles and calculated using custom written MATLAB scripts. Incorrect trials, defined as those with a wrong response, no response, more than one response or a reaction time shorter than 200 ms, were identified and subsequently excluded from the reaction time analysis. This information was also integrated into the EEG and fMRI analyses, both of which were conducted only on correct trials.

3.7.5.2 Structural data (MRI) – cortical thickness

The processing of the MRI/fMRI data was conducted in the Bioimaging Research Center in the Institute of Physiology and Pathology of Hearing in Poland (laboratory head: Tomasz Wolak, Ph.D., D.Sc., and performed by Jakub Wojciechowski, MSc).

The thickness analysis was conducted using CAT12 software (Gaser et al., 2022) (surface-based morphometry, SBM) with a Destrieux atlas-based (Destrieux et al., 2010) approach, based on T1-weighted MR images. The CAT12 employs the SBM approach, incorporating the projection-based thickness method proposed by Dahnke and colleagues (Dahnke et al., 2013), along with topology correction and spherical mapping. Five specifically chosen regions of interest (ROIs), identified as indicative of progression from subjective cognitive decline (in healthy individuals) to Alzheimer's disease (AD) (Verfaillie et al., 2016), and based on nine AD-related areas (Bakkour et al., 2009; Dickerson et al., 2009), were compared between the study groups. These ROIs included the parahippocampal gyrus (a component of the medial temporal cortex), supramarginal gyrus, temporal pole, superior parietal lobule, and inferior temporal gyrus.

3.7.5.3 fMRI – resting-state protocol

The data preprocessing was conducted using SPM12 (SPM, Wellcome Trust Centre for Neuroimaging, London, UK) (Penny et al., 2011) and FSL software. Initially, the functional data underwent realignment, and spatial distortions resulting from the encoding phase were corrected using FSL's topup() function. Subsequently, the structural T1-weighted image was co-registered with the functional images, segmented, and normalized to a common 1-mm isometric MNI space. The obtained transformation parameters were then applied to the functional images after resampling them to a 2-mm isometric voxel size. Spatial smoothing was implemented using a Gaussian kernel with a full width half maximum (FWHM) of 6 mm. The functional data were filtered within the 0.008 to 0.09 Hz band range and denoised using ArtToolbox, as implemented in CONN (Whitfield-Gabrieli & Nieto-Castanon, 2012) with "intermediate settings" (global-signal z-value < 5; motion < 0.9 mm) to eliminate samples with excessive movement or intensity signal changes. Additionally, the COMPCOR approach was applied to white matter and cerebrospinal fluid signals to generate nuisance regressors related to physiological artifacts, incorporating 6 PCA components for each of the masks.

The analysis of functional resting state was carried out utilizing the CONN toolbox (version 21.a) (Whitfield-Gabrieli & Nieto-Castanon, 2012). Group-level independent component analyses (group-ICA) were performed to estimate 21 temporally coherent networks from the combined fMRI data of all subjects. The methodology employed was in line with prior research on *APOE* function, utilizing 21 components, with the aim of replicating and comparing the results (Li et al., 2022). The use of approximately 20 components in ICA-based rsFC studies is also widely considered reasonable (Vemuri et al., 2012). The choice of 21 components was further validated for its suitability in distinguishing between networks of interest through visual inspection. As a subject-specific dimensionality reduction, a singular value decomposition of the z-score normalized BOLD signal was employed, with 64 components applied separately for each subject. Group-level analyses were conducted using a General Linear Model (GLM) (Nieto-Castanon, 2020). The assignment of neural networks to components was automated by the CONN software using the spatial match to template algorithm. This algorithm computed the correlation between each group-level spatial map and CONN's default networks (the table is presented within the *Results* section) with varying levels of spatial correlation coefficient. Despite matching the groups by age and sex, these variables were used as nuisance regressors because of the strong age and gender-related variability in rs-fMRI data. All regions exhibiting statistical significance are documented, accompanied by the corresponding MNI coordinates of peak activity within each cluster, along with the respective cluster sizes, presented in the corresponding tables.

3.7.5.4 EEG – resting state protocol

The data were preprocessed using the EEGLAB toolbox (Delorme & Makeig, 2004) within MATLAB 2022a (The MathWorks Inc., 2022). For each participant, standard electrode positions in EEG data-files were substituted with individual positions obtained from CapTrak localizer). The data were downsampled to 250 Hz and filtered within the range of 0.1-40 Hz (using standard filter parameters from the used toolbox). Additional files were saved with filtering specifically set to 1-40 Hz for subsequent Independent Component Analysis. Channels with excessive noise were removed based on EEGLAB *clean raw data* algorithm (utilizing criteria such as no-signal/flat line, channel correlation, and line noise) and through visual inspection. On average 5.33 channels out of 127 were removed in each participant from resting-state EEG data. Removed channels were interpolated and re-order of interpolated channels was performed. Average reference was applied, and the initial reference electrode (FCz) was restored and included in the dataset. The data were segmented into non-overlapping epochs and those containing excessive artifacts were removed using the ASR algorithm (artifact subspace reconstruction bad burst correction) and further visual inspection. On average, 2.68 epochs were removed per participant from resting-state protocol data. ICA was applied to detect/separate components with evident artifacts (e.g., eye-blink, muscle, ECG artifacts), resulting in the removal of an average of 5.81 components per participant. The data were once again visually inspected, and if necessary, additional cleaning of epochs was conducted, with an average of 1.65 additional epochs removed per participant.

Data analysis was conducted in the MATLAB environment (The MathWorks Inc., 2022) using custom written scripts. For each participant and at each channel, Welch's power spectral density estimate was computed using a 4-second window with a 50% overlap (pwelch MATLAB function; spectral resolution 0.25 Hz). Subsequently, the average power was determined using the bandpower MATLAB function for the following frequency bands: delta (0.5-4 Hz), theta (4-7 Hz), alpha-1 (7.5-9.5 Hz), and alpha-2 (10-12 Hz). Relative average band power was calculated by dividing the band scores by the total power of the signal in the 1-30 Hz range. Both global relative band powers (averaged across all 128 electrodes) and regional relative band powers were computed. For the regional power estimation, electrodes were clustered into 12 anatomical regions of interest (ROIs) (Figure 4): midfrontal (MF), left and right frontal (FL, FR), left and right central-temporal (CTL, CTR), left and right parietal-temporal (PTL, PTR), and left and right occipital (OL, OR). To facilitate statistical analysis and achieve an approximately normal distribution of data, the results were logit-transformed using the $t(x) = log\big(x(1-x)\big)$ function (Gasser et al., 1982), a common approach in similar analyses.

The complexity of the EEG signal was determined using Higuchi's fractal dimension algorithm (Higuchi, 1988; Monge-Álvarez, 2015). This computationally efficient algorithm has been demonstrated to offer accurate estimations of signal fractal dimension in electrophysiological signals (Esteller et al., 1999, 2001; Raghavendra & Narayana Dutt,

2009) and has proven effective in distinguishing between Alzheimer's disease patients and healthy subjects (Al-Nuaimi et al., 2018; Smits et al., 2016). The fractal dimension value ranges between 1 and 2, where 2 signifies a more complex signal. The determination of the algorithm's tuning parameter k_{max}, is crucial for the calculation, and can be approached in many ways. I chose the plateau criterion, which has been demonstrated to be efficient for EEG data (Smits et al., 2016), even though it may not always be recommended for other data types (Wanliss & Wanliss, 2022). The approach of selecting k_{max}, representing the best discrimination between predefined groups, has been employed for other data types as well (Gomolka et al., 2018) and is considered a valid method. To determine the appropriate k_{max} for calculating group differences, first the absolute percentage change between the average HFD on consecutive k values to identify the plateau was calculated. A threshold of 0.1% was employed (horizontal dashed line on the plot) and the starting points of these function minima were identified (Figure 7). The second local minimum on (k_{max} = 62) starts the function plateau, as the percentage change after this value is stabilized below 0.1%. Subsequently, the distance metric (pairwise difference) between the three groups on the plateau values was calculated, and the sum of differences was determined for each k_{max}. The k_{max} = 82 corresponded to the largest sum of differences for the given groups, indicating the point at which the groups were most distinct from each other.

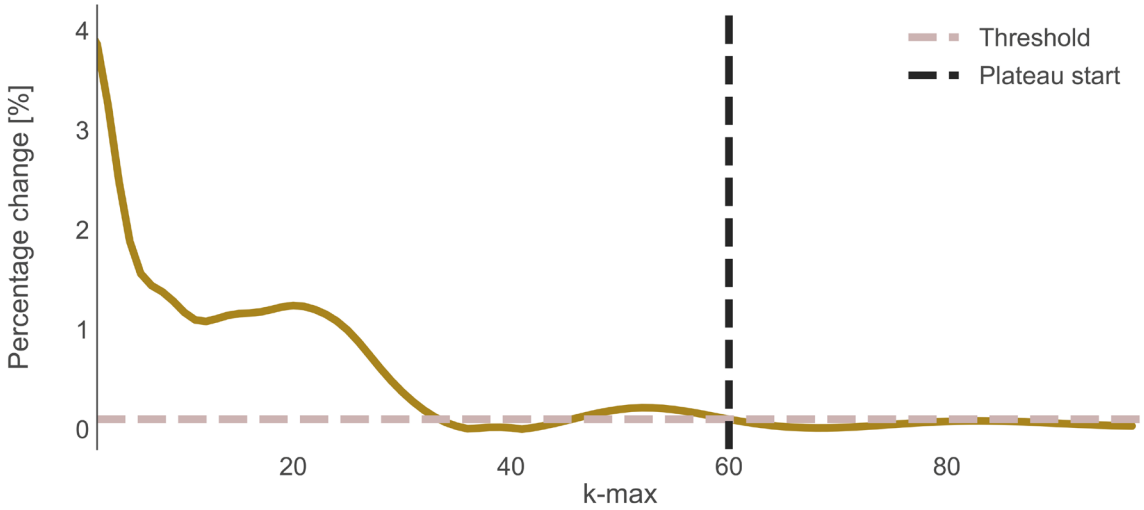

Figure 7. Selection of k_{max}. The absolute percentage change between average HFD for consecutive k values.

Connectivity (coherence) was computed using build-in Fieldtrip functions (Oostenveld et al., 2011) with *mtmfft* method (implementing multitaper frequency transformation; taper: dpss) and previously described parameters (4-second segments and chosen bands of interest). Coherence values for two signals range between 0 and 1, with 1 indicating maximally correlated signals. For the statistical analysis, a subset of electrodes following the standard 10–20 montage commonly used in studies on Alzheimer's disease patients was used (Jelic et al., 1997; Locatelli et al., 1998). However, graphical results, including

connectograms and matrix representations, are also presented for the high-density montage (128 electrodes) (see the *Appendix* section).

3.7.5.5 EEG – Multi-Source Interference Task

The same steps of data preprocessing (as described for the resting-state protocol) were used for the MSIT EEG data (with this statistics regarding the signal cleaning/preprocessing: on average 6.76 channels out of 127 were removed and interpolated; on average 3.67 epochs were removed from first automatic cleaning step and 4.14 from last cleaning step (visual inspection); and on average 10.08 ICA components with artifacts were removed).

Event related data epochs (from -200 to 1200 ms around each stimulus onset) were extracted from continuous EEG data. Only epochs with accurate responses were used for analysis. The data were segregated into trials corresponding to the 00 and FS conditions. Subsequently, the data prepared in this manner were loaded into the EEGLAB STUDY, where ERP group analyses were conducted.

ERP data were baseline corrected (baseline from -200 to 0 ms). Point-to-point amplitude differences were computed within EEGLAB only for comparison between task conditions. For group statistics, peak amplitudes and latencies were measured for N2 (negative peak within 200-400 ms window at the Cz electrode), P3 (positive peak within 400-700 ms window at the Pz electrode) waves. Average amplitude in window of 800-900 ms (at Pz electrode) was also calculated to estimate the level of so-called late sustained potential (LSP) wave. Subsequently the subject level measures were exported to R for the statistical group comparison of these selected ERPs components/waves.

3.7.5.6 fMRI – Multi-Source Interference Task

Mostly the same steps (and parameters) of data preprocessing (as described for the resting-state fMRI protocol; including realignment, normalization, smoothing) were used for the MSIT fMRI data. Here, the data were not subject to the denoising with ArtToolbox (from CONN software) and the COMPCOR approach was not applied.

Functional images were subjected to analysis using the general linear model in SPM12 (Wellcome Centre for Human Neuroimaging, 2020). BOLD responses elicited by each of trial types (either 00 or FS) were individually modeled as regressors. Regressors representing incorrect trials were introduced and subsequently excluded from analyses. The model further encompassed six nuisance regressors associated with motion-related artifacts and an additional regressor accounting for pauses in the task. Whole-brain group-level analyses were conducted following the standard SPM analysis protocol. First level results were masked using the MNI template brain mask. Contrasts of estimated parameters (beta values)

from the first level were subjected to a second-level analysis using a 2-sample t-test to differentiate between the groups.

All regions demonstrating statistical significance are presented in tables along with their respective MNI coordinates indicating peak activity within each cluster, accompanied by information on the cluster size.

3.8 Missing data

The variability in the number of subjects within each group for specific comparisons is associated with the exclusion of data of low quality from analysis. Additionally, the absence of data may occur in instances of participant withdrawal or exclusion from the study, such as due to MRI contraindications. In the fMRI experiment, nine participants failed to complete the study, and the results of one individual were omitted from the group analysis due to minor abnormalities detected in the structural MRI image (though neuropsychological tests were within the normal range, and the participant did not exhibit any subjective or objective symptoms). Moreover, there is a lack of data for just one participant in the Sternberg's Memory Task and another in the resting state protocol within the EEG dataset, attributed to acquisition and technical issues. Additionally, electrode localization with CapTrack was not obtained for two participants, and some participants do not have blood testing results. Due to these reasons, the group allocation for the final analyses was as follows: blood tests (N group: N = 31, A+P- group: N = 24, A+P+ group: N = 21), EEG Sternberg's Memory Task and resting state protocol (N group: N = 31, A+P- group: N = 27, A+P+ group: N = 20), MRI/fMRI experiments (N group: N = 27, A+P- group: N = 24, A+P+ group: N = 18).

4 Results

4.1 Genetic, health, and psychometric screening

4.1.1 Genetic data

Genetic results i.e., the incidence of individual alleles and real and expected genotype frequencies were calculated and tested for Hardy-Weinberg equilibrium (HWE) using the Pearson chi-square test. For the full group of participants (N = 200) *APOE* and *PICALM* distributions were in Hardy-Weinberg equilibrium (*APOE,* $X^2 = 1.27$, $p = 0.94$; *PICALM,* $X^2 = 3.79$, $p = 0.15$). Hardy-Weinberg equilibrium is a fundamental concept in genetics that describes the theoretical distribution of allele frequencies in a stable (not evolving) population. Thus, if a studied sample is in Hardy-Weinberg equilibrium, it indicates that the sample is representative of the general population. *APOE* frequency in our sample was similar to reports from other white European-descent ethnic populations (Tang et al., 1998): ε2/ε3 (11% in our data vs 12% in Tang report), ε2/ε4 (1 vs 2%), ε3/ε4 (23.5 vs 22%), and ε4/ε4 (1 vs 2%). The distribution of *APOE* and *PICALM* genes for Phase I (N = 200) is shown on Figure 8 and genetic data frequency for both phases in Table 5.

Table 5. Genetic variants frequency

	Frequency	
***APOE* haplotype**	**Phase I (N = 200)**	**Phase II (N = 80)***
ε2/ε2	1 (0.5%)	0
ε2/ε3	22 (11%)	0
ε2/ε4	3 (1.5%)	1 (1.25%)
ε3/ε3	125 (62.5%)	31 (38.75%)
ε3/ε4	47 (23.5%)	46 (57.5%)
ε4/ε4	2 (1%)	2 (2.5%)
***PICALM* rs3851179**		
A/A	16 (8%)	11 (13.75%)
A/G	101 (50.5%)	47 (58.75%)
G/G	83 (41.5%)	22 (27.5%)

* The data is shown for all N = 80 participants from the Phase II of the study. Although not all participants underwent all experimental sessions. ε2/ε4 individual (Phase II) was not finally attributed to any of the groups.

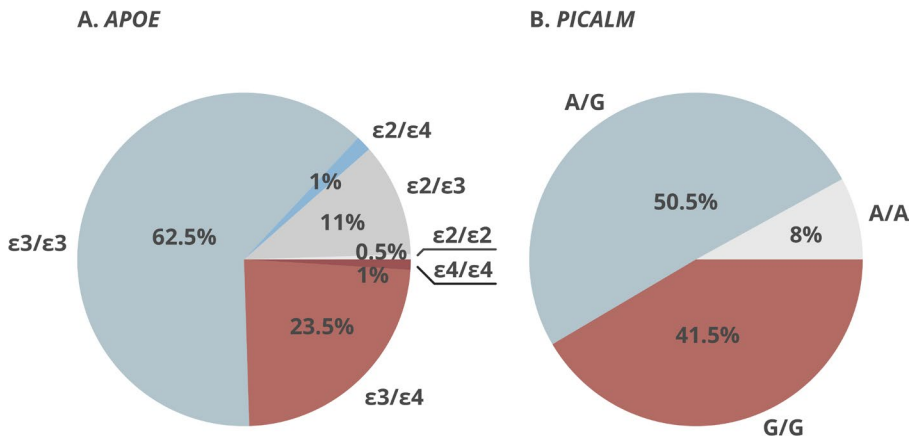

Figure 8. *APOE* and *PICALM* allele distribution for Phase I (N = 200)

4.1.2 Demographic and health data

The study participants were right-handed middle-aged adults (equal frequency of females and males: 109/91 in Phase I, and 41/39 in Phase II, respectively). All demographic data for both study phases are shown in Table 6. Phase I included all participants recruited for the genetic screening. Phase II included a subgroup of participants from Phase I that were chosen for further experiments based on their genetic traits and balanced psychometric and demographic characteristics. Almost all participants with risky *APOE* alleles were recruited for the Phase II, along with a representative, corresponding group of participants without the risk (exact numbers of participants with different genetic test results are presented in Table 5). Phase II sample comprised a homogenic cohort of participants (41 females, 39 males; mean age: 55.36±3.13). Most Phase II participants were in relationships, including marriage or partnership (76.25%), and were professionally active having permanent or part-time jobs (83.75%). Only 8.75% of the respondents were already retired. Most of the participants were highly educated and had a university degree (83.33%) and were coming (70%) from large cities defined as those over 100 000 residents.

The enrolled participants were generally in good health (see the contraindications for study participation detailed in the *Methods*). The following summary applies to the Phase II of the study (note, that general information about health is provided in Table 7, also for the Phase I of the study). Participants had BMI values (27.40±5.05) slightly higher than the norm ranges (18.5 to 24.9). Despite this, the median BMI was 26.44, indicating that nearly half of the subjects still fell within the normal weight range. It is important to note that the assessment does not account for body fat distribution, which is relevant in evaluating health risks. On average, the subjects also had AUDIT (Alcohol Use Disorders Identification Test) test scores that were within normal limits (4.00±2.80; although some individuals had elevated scores). Most subjects (89.20%) reported no learning difficulties (such as dyslexia)

and no allergies (77.03%), and half were on regular medication (55%). Concerning non-steroidal anti-inflammatory drugs, most participants (71.25%) either did not use them or used them very infrequently (a few times a year). Furthermore, most respondents did not have thyroid disease (91.14%), hypertension (75%), diabetes (98.75%), or other chronic illnesses (77.22%). A substantial proportion were non-smokers (83.61%) but consumed caffeinated beverages (73.75%). Additionally, many participants reported no family history of dementia (62.5%), indicating that neither parent had the disease. The majority also claimed engagement in light physical activity (e.g., walking 1-2 times a week; 61.25%) and identified themselves as socially active individuals (63.75%).

Table 6. Demographic characteristics: descriptive statistics for Phase I and Phase II respectively

	Phase I (N = 200)		**Phase II (N = 80) ***	
Parameter	**Mean ± SD**	**Median**	**Mean ± SD**	**Median**
Age (years)	55.05 ± 3.10	55.00	55.36 ± 3.14	56.00
	Frequency N (%)		**Frequency N (%)**	
Sex (females/males)	109/91 (54.5%/45.5%)		41/39 (51.25%/48.75%)	
Marital status: 0	116 (58%)		49 (61.25%)	
Marital status: 1	30 (15%)		12 (15.0%)	
Marital status: 2	8 (4%)		2 (2.5%)	
Marital status: 3	11 (5.5%)		8 (10%)	
Marital status: 4	35 (17.5%)		9 (11.25%)	
Job status: 0	158 (79.40%)		60 (75%)	
Job status: 1	13 (6.5%)		7 (8.75%)	
Job status: 2	8 (4%)		3 (3.75%)	
Job status: 3	7 (3.5%)		3 (3.75%)	
Job status: 4	13 (6.5%)		7 (8.75%)	
Education 1	24 (13.19%)		8 (11.11%)	
Education 2	7 (3.85%)		4 (5.56%)	
Education 3	151 (82.97%)		60 (83.33%)	
Place of residence 0	21 (10.5%)		7 (8.75%)	
Place of residence 1	12 (6%)		7 (8.75%)	
Place of residence 2	17 (8.5%)		10 (12.5%)	
Place of residence 3	150 (75%)		56 (70%)	

*The data is shown for all N = 80 participants from the Phase II of the experiment. Although not all participants undergone all sessions (check missing data section). *Valid percent is shown in the table and missing data are excluded from the calculations. General information on missing data: job status N = 1 (Phase I), education N = 18 (Phase I) including N = 8 on Phase II, Learning deficits N = 18 (Phase I) including N = 6 on Phase II. Marital status: 0 – married; 1 – partnership; 2 – divorce/separation or during the process; 3 – never married; 4 – single. Job status: 0 – permanent contract; 1 – temporary contract; 2 – unemployment; 3 – retirement/pension; 4 – other. Education: 1 – secondary education; 2 – partial higher education; 3 – higher education. Place of residence: 0 – village; 1 – small-size city (<20 000 residents), 2 – medium-size city (<100 000 residents), 3 – large-size city (>100 000 residents)

Table 7. Health data: descriptive statistics for Phase I and Phase II respectively

	Phase I (N = 200)		**Phase II (N = 80) ***	
Parameter	**Mean ± SD**	**Median**	**Mean ± SD**	**Median**
BMI	26.88 ± 4.69	25.99	27.40 ± 5.05	26.44
AUDIT	3.77 ± 3.28	3.00	4.00 ± 2.80	4.00
	Frequency N (%)		**Frequency N (%)**	
Learning difficulties 0	9 (4.95%)		5 (6.76%)	
Learning difficulties 1	5 (2.75%)		3 (4.05%)	
Learning difficulties 2	2 (1.10%)		1 (1.35%)	
Learning difficulties 3	1 (0.55%)		0	
Learning difficulties 4	167 (91.76%)		66 (89.20%)	
Allergies 0	-		57 (77.03%)	
Allergies 1	-		17 (22.97%)	
Drugs 0	98 (49%)		36 (45%)	
Drugs 1	102 (51%)		44 (55%)	
NSAID 0	52 (26.13%)		21 (26.25%)	
NSAID 1	83 (41.71%)		36 (45%)	
NSAID 2	48 (24.12%)		18 (22.50%)	
NSAID 3	13 (6.5%)		3 (3.75%)	
NSAID 4	3 (1.51%)		2 (2.5%)	
Thyroid 0	177 (88.95%)		72 (91.14%)	
Thyroid 1	12 (6.03%)		3 (3.80%)	
Thyroid 2	2 (1.01%)		1 (1.27%)	
Thyroid 3	8 (4.02%)		3 (3.80%)	
Hypertension 0	153 (76.88%)		60 (75%)	
Hypertension 1	46 (23.12%)		20 (25%)	
Diabetes 0	199 (99.5%)		79 (98.75%)	
Diabetes 1	1 (0.5%)		1 (1.25%)	
Other diseases 0	160 (81.63%)		61 (77.22%)	
Other diseases 1	36 (18.37%)		18 (22.79%)	
Smoking status 0	135 (67.84%)		48 (60.76%)	
Smoking status 1	23 (11.59%)		9 (11.40%)	
Smoking status 2	41 (20.60%)		22 (27.85%)	
Caffeine intake 0	18 (9%)		5 (6.25%)	
Caffeine intake 1	143 (71.5%)		59 (73.75%)	
Caffeine intake 2	38 (19%)		15 (18.75%)	
Caffeine intake 3	1 (0.5%)		1 (1.25%)	
Dementia history 0	134 (67%)		50 (62.5%)	
Dementia history 1	61 (30.5%)		28 (35%)	
Dementia history 2	5 (2.5%)		2 (2.5%)	
Physical activity 0	29 (14.5%)		14 (17.5%)	
Physical activity 1	133 (66.5%)		49 (61.25%)	
Physical activity 2	29 (14.5%)		13 (16.25%)	
Physical activity 3	9 (4.5%)		4 (5%)	
Social activity 0	30 (15%)		12 (15%)	
Social activity 1	118 (59%)		51 (63.75%)	
Social activity 2	52 (26%)		17 (21.25%)	

*The data are shown for all N = 80 participants from the Phase II of the experiment. Although not all participant undergone all sessions (check missing data section). *Valid percent is shown in the table and missing data are excluded from the calculations. General information on missing data: Learning difficulties N = 18 (Phase I) including N = 6 on Phase II; Allergies: N=6 (Phase II); Ibuprofen intake N = 1 (Phase I); Thyroid diseases N = 1 (Phase I/II); Hypertension N = 1 (Phase I); Other diseases N = 4 (Phase I) including N = 1 on Phase II; Smoking status N = 1 (Phase I/II). Participant could choose more than one option in regard to the learning difficulties question. Learning difficulties: 0 – dyslexia, 1 – dysgraphia, 2 – dysortographia, 3 – dyscalculia, 4 – none; 5 – other. Allergies (of any type): 0 – none; 1 – yes. Drugs (information on taking permanent

medication): 0 – none; 1 – yes. NSAID (information on taking non-steroidal anti-inflammatory drugs): 0 – none, 1 – very rarely (several times a year), 2 – rarely (1-4 pills per month), 3 – moderately often (5-11 pills per month), 4 – often (>12 pills per month). Thyroid (having thyroid diseases): 0 – none, 1 – hypothyroidism, 2 – hyperthyroidism, 3 – other. Hypertension: 0 – no, 1 – yes. Diabetes: 0 – no, 1 – yes. Other diseases (having any other chronic diseases/health problems): 0 – no, 1 – yes. Smoking status (including nicotine electronic cigarettes): 0 – no, 1 – yes, 2 – in the past. Caffeine intake: 0 – no, 1 – yes, on a daily basis, 2 – yes, occasionally, 3 – drinking coffee, but only decaffeinated one. Dementia history (family history): 0 – healthy parents, 1 – one demented parent, 2 – both demented parents. Physical activity (subjective level): 0 – basic physical activity (no additional exercises), 1 – light physical activity (exercises at least 1-2 times a week, e.g. walks, 2 – moderately high physical activity (exercises at least 3-4 times a week), 3 – very high physical activity (exercises >4 times a week). Social activity (subjective): 0 – poor (non-socially active person), 1 – high (socially active person), 2 – undecided.

Phase II study groups were homogeneous regarding health and demographic data. No other risks associated with dementia in relation to demographic and general health status differentiate the groups (Table 8).

Table 8. Demographic and health measures: descriptive statistics and group differences (Phase II)

Measure	**N**	**A+P-**	**A+P+**	***p*-value**
Age [years; M±SD]	54.77 ± 2.92	55.70 ± 3.27	55.62 ± 3.31	.47 &
Gender [F/M]	15/16	14/13	10/11	.95 ^
Education: secondary	3 (10.71%)	4 (17.39%)	1 (5%)	.45 ^
Education: partial higher	2 (7.14%)	2 (8.70%)	0 (0%)	
Education: higher	23 (82.14%)	17 (73.91%)	19 (95%)	
Handedness EHI	87.85 ± 20.95	86.67 ± 18.81	90.16 ± 6.75	.67 &
AUDIT scores [M±SD]	3.76 ± 3.52	4.19 ± 2.91	3.87 ± 2.09	.61 &
Smokers [N]	2 (6.45%)	5 (18.52%)	2 (9.52%)	.24 ^
Former smokers [N]	7 (22.58%)	10 (37.04%)	4 (19.05%)	
Caffeine intake [N]	28 (90.32%)	25 (92.59%)	20 (95.24%)	.81 ^
Diabetes [N]	0 (0%)	0 (0%)	1 (4.76%)	.25 ^
Hypertension [N]	6 (19.36%)	9 (33.33%)	5 (23.81%)	.47 ^
Thyroid [N]	2 (6.67%)	3 (11.11%)	2 (9.52%)	.84 ^
Other diseases [N]	7 (23.33%)	6 (22.22%)	5 (23.81%)	.99 ^
Allergies [N]	7 (25.00%)	5 (19.23%)	4 (21.05%)	.87 ^
BMI [M±SD]	26.70 ± 4.35	27.24 ± 5.48	28.58 ± 5.55	.47 &
Drugs [N]	19 (61.29%)	17 (62.96%)	8 (38.10%)	.17 ^
NSAID [N]	7 (22.58%)	11 (40.74%)	5 (23.81%)	.26 ^
Learning difficulties [N]	4 (13.33%)	3 (12.50%)	1 (5.26%)	.65 ^
Family history of dementia [N]	8 (25.81%)	14 (51.85%)	8 (38.10%)	.19 ^
Physical activity [N]	**30 (96.77%)**	**18 (66.67%)**	**17 (80.95%)**	**< .05 ^**
Social activity [N]	19 (61.29%)	20 (74.04%)	11 (52.38%)	.22 ^

M – mean; SD – standard deviation; F – females; M – male. # One-way ANOVA; & Kruskal-Wallis test; ^ Chi-square test. Caffeine intake: the N of participants drinking caffeine (0/3 vs 1/2, see description of Table 7). Thyroid: the N of participants having any thyroid disease. NSAID: the N of participants taking NSAID drugs more than couple of times a year (0/1 vs. 2/3/4, see description of Table 7). Family history of dementia: the N of participants having one/both parents with dementia. Learning difficulties: the N of participants with any learning difficulties. Physical activity: N of participants physically active (0 vs 1/2/3, see description of Table 7). Social activity: N of participants socially active. The bolded font indicate a significant or trend result

However, it is important to note that the measure of physical activity, assessed through a single subjective question, revealed some differences. Specifically, the A+P- group exhibited lower levels of physical activity compared to the N group ($X^2(2) = 9.01$, $p < .05$; post-hoc: A+P- vs N $p < .05$). A+P- and A+P+ groups had more relatives (parents) with

dementia than the N group (51.85% & 38.10% versus 25.81%), but these differences are not statistically significant. Test assumptions for statistical tests were summarized in Appendix (Table 34).

4.1.3 Psychometric assessment

Various psychometric tests were administered to assess intelligence (RAVEN), verbal memory (CVLT), personality traits (NEO-FFI), stress coping strategies (Mini-Cope), depression levels (BDI), and self-esteem (SES).

There was no linear relationship between psychometric measures and age in any group, as assessed by visual inspection of a scatter plot and R^2 values, which were all lower than 0.2. Therefore, age was not considered as a covariate. Only A+P- group had a small linear relationship with age in 5 of the CVLT scales (R^2 = 0.23 to 0.30). Most tests and scales did not meet the assumptions criteria for two-way ANOVA, as indicated in Table 35 in Appendix. The assumption for one-way ANOVA (Table 36) was also assessed. Consequently, all scales were tested using either a one-way ANOVA or Kruskal-Wallis test, without considering sex as a factor.

The psychometric test results indicated minimal differences in scales related to depression/mood and self-esteem (BDI and SES, Table 9), with the A+P- group scoring worse than the N group (BDI: H(2) = 6.37, $p < .05$, post-hoc: A+P- vs. N $p < .05$, SES F(2,76) = 3.17, $p < .05$, post-hoc: A+P- vs. N $p < .05$). Additionally, the A+P- group exhibited elevated neuroticism levels (NEO-NEU: H(2) = 6.04, $p < .05$, post-hoc: A+P- vs. N $p < .05$), and there was a tendency for higher scores on the hopelessness scale in a test assessing stress coping strategies (F(2,74) = 2.72, $p = 0.07$, post-hoc: A+P- vs. N $p = .06$).

Given that a larger number of individuals underwent psychometric testing and provided data on family history of dementia and demographic data (N = 200 group), comparisons for significant findings in the Phase II groups were tested for replication and further insight for the entire N = 200 group, which included the A-P+ group (not present in Phase II of the study). To maintain consistent group structures based on allele assignment, individuals possessing the *APOE*-ε2 allele, not affiliated with any defined group, were excluded from the analysis. Consequently, calculations were conducted on the remaining N = 174 participants. However, this led to unequal group sizes, unlike the groups selected for the second stage of the study, thereby reducing the statistical power of the comparisons (A+P+ group, N = 21; the A+P- group, N = 28; N group, N = 76; and the additional A-P+ group involved N = 49 subjects). No outliers were excluded from the analysis. In this extended comparison, the groups exhibited significant differences in terms of family history of dementia ($X^2(3) = 10.03$, p < .05, N = 174, post-hoc: A+P- vs. N $p < .05$), where A+P- group was characterized by having more first relatives with dementia than subjects from the N group. The differences in physical activity between A+P- and N group were also

identified/confirmed ($X^2(3) = 11.31$, $p < .01$, N = 174, post-hoc: A+P- vs. N $p < .05$). No significant differences were observed for BDI, SES, and the Mini-Cope-2 scale. However, it is noteworthy that the N group (from Phase I cohort, N = 174) encompassed individuals with notably high BDI scores (along with consistently low SES scores), who were not included in the Phase II of the study for this reason. In the Phase II of the study, only 10 individuals across all groups had scores exceeding 14 points (considered high). Regarding neuroticism, differences were again identified, but with $p = 0.05$ ($H(3) = 7.72$, $p = 0.05$). Subsequent post-hoc tests, considering six different comparisons after introducing the A-P+ group, revealed no significant differences considering adjusted for multiple comparisons *p*-values, even though the A+P- group consistently exhibited the highest scores on neuroticism scale and the N group the lowest (A+P-: 20.29±9.42, A-P+: 20.41±8.77, A+P+: 15.62±8.18, N: 17.31±8.48).

Table 9. Psychometric tests assessment: descriptive statistics and group differences (Phase II)

Test	N	A+P-	A+P+	*p*-value
BDI	**4.61 ± 4.90**	**8.70 ± 6.51**	**6.62 ± 6.98**	**& < .05**
SES	**33.19 ± 3.99**	**30.59 ± 4.05**	**32.29 ± 3.76**	**# < .05**
Mini-Cope-1	2.26 ± 0.33	2.06 ± 0.48	2.21 ± 0.49	& .18
Mini-Cope-2	**0.60 ± 0.43**	**0.85 ± 0.40**	**0.74 ± 0.40**	**# .07**
Mini-Cope-3	1.74 ± 0.56	1.60 ± 0.64	1.51 ± 0.71	& .48
Mini-Cope-4	1.02 ± 0.39	1.24 ± 0.33	1.07 ± 0.43	& .11
Mini-Cope-5	0.52 ± 0.82	0.32 ± 0.72	1.26 ± 1.19	# .16
Mini-Cope-6	2.14 ± 0.48	2.09 ± 0.65	2.07 ± 0.73	.93
Mini-Cope-7	0.86 ± 0.63	0.94 ± 0.70	1.10 ± 0.65	& .35
NEO-NEU	**14.23 ± 5.91**	**19.96 ± 9.44**	**15.62 ± 8.18**	**& < .05**
NEO-EXT	27.90 ± 6.65	25.48 ± 7.06	26.05 ± 6.85	# .38
NEO-OPE	30.77 ± 5.31	30.82 ± 6.04	31.43 ± 6.08	# .91
NEO-AGR	33.58 ± 5.83	30.96 ± 6.60	32.81 ± 6.17	# .27
NEO-CON	32.68 ± 6.86	29.33 ± 6.29	30.86 ± 7.65	# .19
RAVEN	53.87 ± 3.19	52.11 ± 6.04	53.05 ± 4.08	& .73
CVLT-1	61.29 ± 8.86	63.63 ± 8.13	59.76 ± 8.89	& .39
CVLT-2	9.39 ± 1.69	9.70 ± 2.02	8.91 ± 1.90	& .41
CVLT-3	8.38 ± 1.91	8.41 ± 2.31	7.81 ± 1.85	& .36
CVLT-4	12.97 ± 2.65	12.74 ± 2.49	12.86 ± 3.10	& .78
CVLT-5	13.42 ± 1.96	13.59 ± 1.65	12.38 ± 2.27	& .99
CVLT-6	13.68 ± 2.36	13.33 ± 2.69	13.24 ± 3.24	& .95
CVLT-7	13.71 ± 2.02	13.67 ± 2.00	13.38 ± 2.96	& .98
CVLT-8	2.94 ± 3.85	4.63 ± 5.51	4.67 ± 4.80	& .18
CVLT-9	1.39 ± 1.94	0.85 ± 1.35	1.14 ± 1.49	& .33
CVLT-10	1.19 ± 1.87	0.78 ± 1.22	1.43 ± 3.08	& .77
CVLT-11	15.32 ± 1.30	15.19 ± 1.24	15.45 ± 0.89	& .63
CVLT-12	0.52 ± 1.09	0.44 ± 1.01	1.05 ± 2.09	& .41

Mini-Cope-1: Active coping subscale; Mini-Cope-2: Hopelessness; Mini-Cope-3: Support seeking; Mini-Cope-4: Avoidance behavior; Mini-Cope-5: Turning to religion; Mini-Cope-6: Acceptance; Mini-Cope-7: Humor; NEO-NEU: neuroticism scale; NEO-EXT: extraversion scale; NEO-OPE: openness scale; NEO-AGR: agreeableness scale; NEO-CON: conscientiousness scale; CVLT-1: List A, task 1-5; CVLT-2: List A, task 1; CVLT-3: List B; CVLT-4: Short-term delay free recall; CVLT-5: Short-term delay cued recall; CVLT-6: Long-term delay free recall; CVLT-7: Long-term delay cued recall; CVLT-8: Perseverations; CVLT-9: Intrusion errors, free recall; CVLT-10: Intrusion errors, cued recall; CVLT-11: Recognition, total hits; CVLT-12: Recognition, false alarms. # One-way ANOVA; & Kruskal-Wallis test; ^ Chi-square test. The bolded font indicate a significant or trend result

4.2 Phase II results

The Phase II of the experiment involved a subset of participants selected based on genetic and psychometric screening, resulting in the formation of three balanced groups distinguished by the severity of Alzheimer's disease risk: control (N), single risk (A+P-), and double risk (A+P+). Blood tests were employed to assess general health, while neuroimaging was utilized to monitor brain function at rest and during cognitively demanding tasks.

4.2.1 Blood counts results

There was no linear relationship between any blood measures and age in any groups, as assessed by visual inspection of a scatter plot and R^2 values, which were lower than 0.2, therefore age was not considered a covariate. Minor linear relationships with age were detected only for A+P- group regarding neutrophils ($R^2 = 0.22$), A+P+ group regarding platelets ($R^2 = 0.23$), and N group regarding the MCHC levels ($R^2 = 0.20$).

A+P- was characterized by higher MCH levels than N and A+P+ groups ($H(2) = 9.27$, $p < .01$; post-hoc: A+P- vs. A+P+ $p < .05$, A+P- vs. N $p < .05$), and MCHC levels ($H(2) = 6.93$, $p < .05$; A+P- vs. A+P+ $p < .05$, A+P- vs. N $p = 0.07$) (Table 10 and Figure 9). There was also a trend for eosinophils ($H(2) = 5.10$, $p = 0.078$, A+P+ vs. N $p < 0.08$) to be higher in A+P+ group than N group, and RDW-CV ($H(2) = 4.99$, $p = 0.08$; A+P+ vs. A+P- $p < .09$) to be higher than in A+P- group (Table 10). There was no interaction between the group and sex factors (Table 42). There was, in fact, a significant difference between females and males in neutrophils ($M > F$; $F(1,70) = 4.57$, $p < .05$), erythrocytes ($M > F$; $F(1,70) = 16.71$, $p < .001$), hemoglobin ($M > F$; $F(1,70) = 25.02$, $p < .001$), hematocrit ($M > F$; $F(1,70) = 17.17$, $p < .001$), monocytes ($M > F$; $F(1,70) = 23.89$, $p < .001$), total cholesterol ($F > M$; $F(1,70) = 16.94$, $p < .001$) and HDL cholesterol ($F > M$; $F(1,70) = 42.09$, $p < .001$) measures (Table 42). These results showed generally known differences in blood counts between males and females and will not be further discussed.

Test assumptions for statistical tests were summarized in Appendix (Table 42 for two-way ANOVA and exact additional exact p-values for moderator sex variable and interaction, Table 43 and for one-way ANOVA where former requirements were not met).

Figure 9 and Figure 10 display blood measurements across groups using boxplots, highlighting significant results. In cases where no significance was observed for the main comparison for each measure, no additional markings were added on the figures (like ns) to ensure readability.

Table 10. Blood measures: descriptive statistics and group differences

Blood tests	Group			*p*-value for Group
	A+P+	**A+P-**	**N**	
Eosinophils [K/µl]	**0.225 ± 0.195**	**0.176 ± 0.094**	**0.141 ± 0.076**	**.078 &~**
Basophils [K/µl]	0.058 ± 0.025	0.043 ± 0.019	0.047 ± 0.024	.12 &
Neutrophils [K/µl]	3.327 ± 1.039	3.482 ± 1.030	3.180 ± 0.952	.47
Leukocytes [K/µl]	6.41 ± 1.74	6.28 ± 1.37	5.95 ± 1.40	.42 &
Erythrocytes [K/µl]	4.89 ± 0.46	4.80 ± 0.41	4.93 ± 0.45	.54
Hemoglobin [K/µl]	14.51 ± 1.21	14.77 ± 1.32	14.67 ± 1.55	.72
Hematocrit [%]	44.05 ± 3.57	44.00 ± 3.15	44.58 ± 3.70	.86
MCV [fl]	90.57 ± 4.32	92.04 ± 3.78	90.55 ± 4.05	.37
MCH [pg]	**29.71 ± 1.42**	**30.88 ± 1.39**	**29.77 ± 1.75**	**< .01 &**
MCHC [g/dl]	**32.82 ± 0.62**	**33.48 ± 0.91**	**32.83 ± 1.30**	**< .05 &**
RDW-CV [%]	**13.33 ± 0.66**	**12.93 ± 0.70**	**13.19 ± 1.26**	**.08 &~**
Platelets [K/µl]	252.14 ± 42.80	257.83 ± 49.95	258.19 ± 58.55	.91 #
PDW [fl]	14.01 ± 2.40	13.68 ± 2.26	13.70 ± 2.39	.81 &
MPV [fl]	11.22 ± 1.06	11.01 ± 0.90	11.04 ± 1.0	.75
P-LCR [%]	35.16 ± 8.75	33.49 ± 7.64	33.74 ± 8.27	.77
Lymphocytes [K/µl]	2.21 ± 0.91	2.00 ± 0.51	2.02 ± 0.60	.75 &
Monocytes [K/µl]	0.57 ± 0.15	0.56 ± 0.14	0.54 ± 0.14	.53
Total cholesterol [mg/dl]	212.49 ± 50.59	209.08 ± 38.11	206.33 ± 41.11	.91
HDL cholesterol [mg/dl]	59.70 ± 18.18	53.86 ± 15.97	57.60 ± 18.02	.28
Non-HDL cholesterol [mg/dl]	152.80 ± 42.17	155.22 ± 35.94	148.73 ± 39.51	.83 &
LDL cholesterol [mg/dl]	126.72 ± 41.08	123.84 ± 32.40	123.31 ± 35.68	.94 &
HSV IgG positive [N]	19 (90.48%)	20 (83.33%)	27 [87.10%]	.78 ^

One-way ANOVA; & Kruskal-Wallis test; ^ Chi-square test. MCV – mean corpuscular volume, MCH – mean corpuscular hemoglobin, MCHC – mean corpuscular hemoglobin concentration, RDW-CV – red blood cell distribution width, PDW – platelet distribution width, MPV – mean platelet volume, P-LCR – platelet-large cell ratio, HSV – herpes simplex virus. The bolded font indicate a significant or trend result

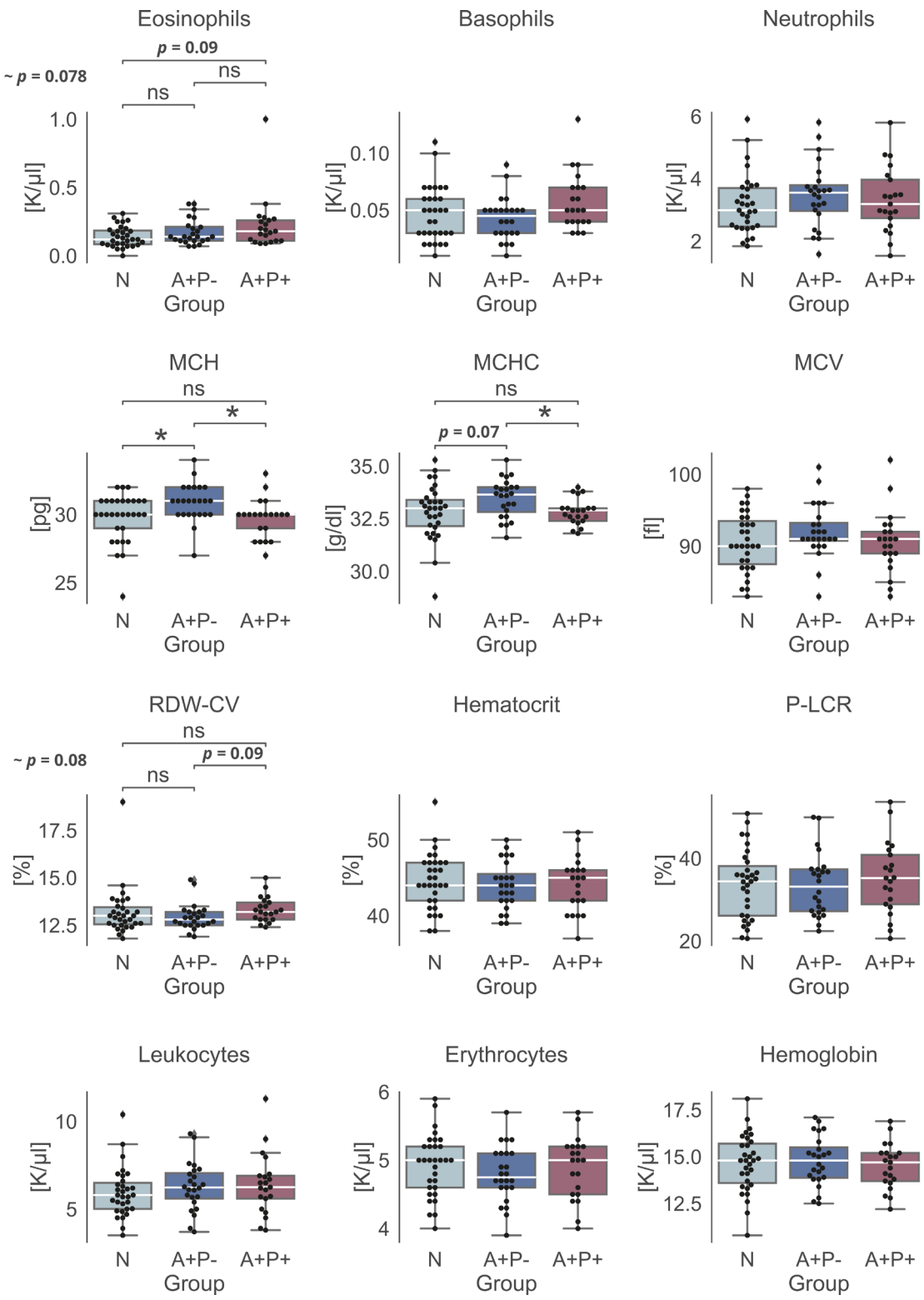

Figure 9. Blood count data: first twelve measurements

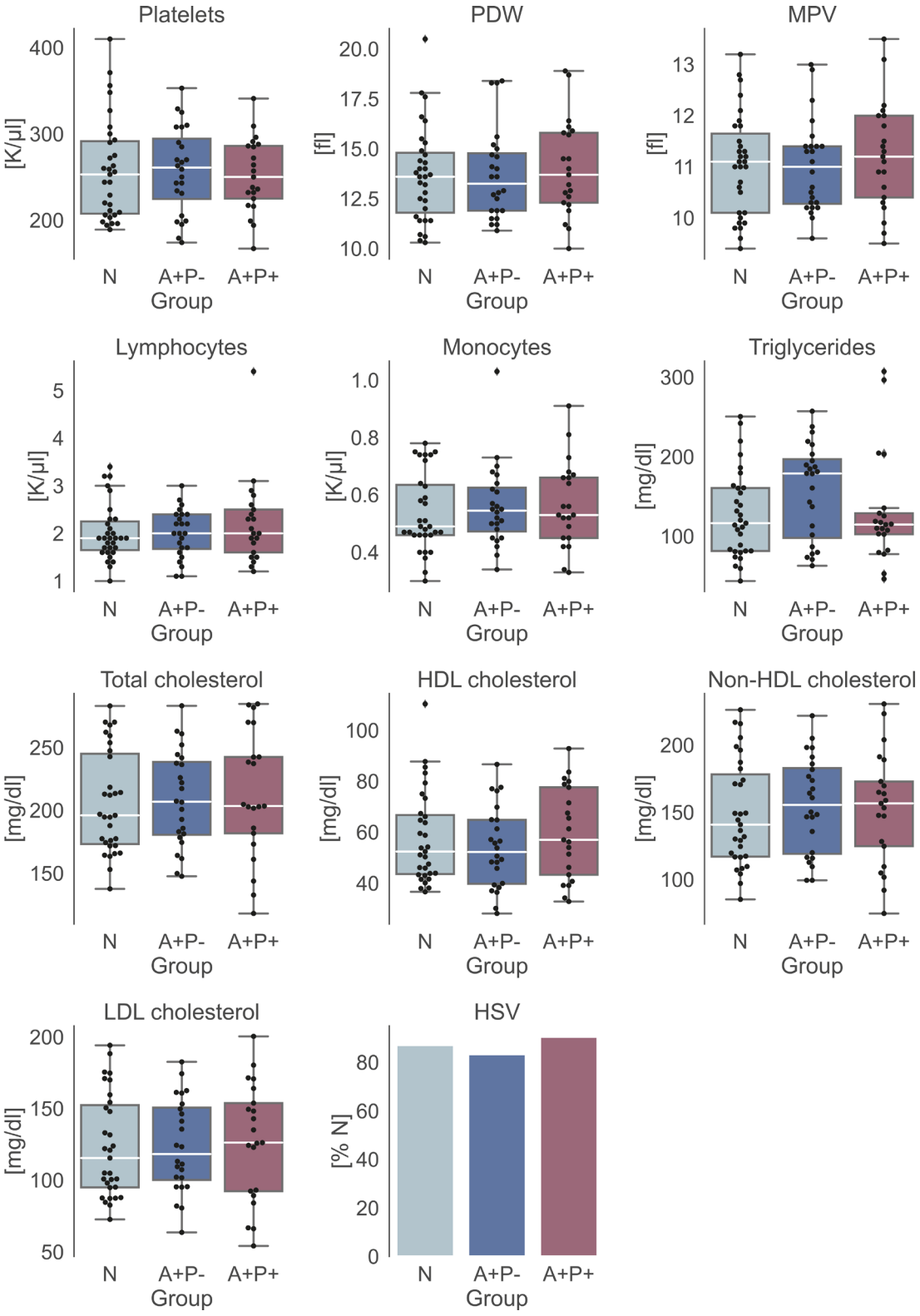

Figure 10. Continuation of blood count data, in addition to lipid profile information and details regarding HSV IgM antibodies (% of individuals having IgM antibodies).

4.2.2 miRNA

Since specific panels of circulating miRNAs were proposed as biomarkers of LOAD, we verified their levels in our cohort. Information about *p*-value for group differences can be found in Table 11. Test assumptions for statistical evaluation are summarized in the Appendix (Table 37 for two-way ANOVA and exact *p*-values for moderator sex variable and interaction, and Table 38 for one-way ANOVA assumptions where the former requirements were not met). Out of 11 miRNAs tested miR-29b-3p was found to have lower level in A+P- group than in N and A+P+ groups ($F(2,70) = 9.66$, $p < 0.001$; post-hoc: A+P- vs. N $p < 0.01$, A+P- vs. A+P+ $p < 0.001$). No other changes within the miRNA panel were detected (Table 11, Figure 11), including no significant changes in relation to sex factor.

Table 11. miRNA: descriptive statistics and exact p-value for difference between the study groups

Parameter [log2 fold change]	**Group**			***p*-value**
	A+P+	**A+P-**	**N**	
miR-29b-3p	**0.139 ± 0.414**	**-0.289 ± 0.218**	**$3.226x10^{-11}$ ± 0.341**	**< .001**
miR-30-5p	-0.104 ± 0.353	-0.113 ± 0.533	$-3226x10^{-11}$ ± 03.14	0.52
miR-34a-5p	0.294 ± 0.694	0.214 ± 1.118	$3.226x10^{-11}$ ± 1.018	0.32 &
miR-125b-5p	0.314 ± 0.469	0.277 ± 0.731	$-3.226x10^{-11}$ ± 0.658	0.17
miR-135a-5p	-0.019 ± 0.835	-0.567 ± 1.349	$-3.333x10^{-11}$ ± 0.978	0.12
miR-142-3p	0.143 ± 0.691	-0.292 ± 0.954	$3.226x10^{-11}$ ± 0.523	0.23 ##
miR-146-5p	-0.119 ± 0.501	0.029 ± 0.534	$-3.226x10^{-11}$ ± 0.68	0.54 &
miR-200a-3p	-0.139 ± 0.944	-0.168 ± 0.730	$-3.226x10^{-11}$ ± 0.68	0.70
miR-483-5p	0.253 ± 0.819	0.426 ± 1.108	$2.256x10^{-18}$ ± 1.042	0.50 &
miR-486-5p	0.006 ± 0.619	0.153 ± 0.726	$6.452x10^{-11}$ ± 0.59	0.72 &
miR-502-3p	-0.005 ± 0.603	-0.250 ± 0.493	$6.452x10^{-11}$ ± 0.545	0.21

One-Way ANOVA with Welch's correction; & Kruskal-Wallis test. The bolded font indicate a significant or trend result. *p*-value for Group factor.

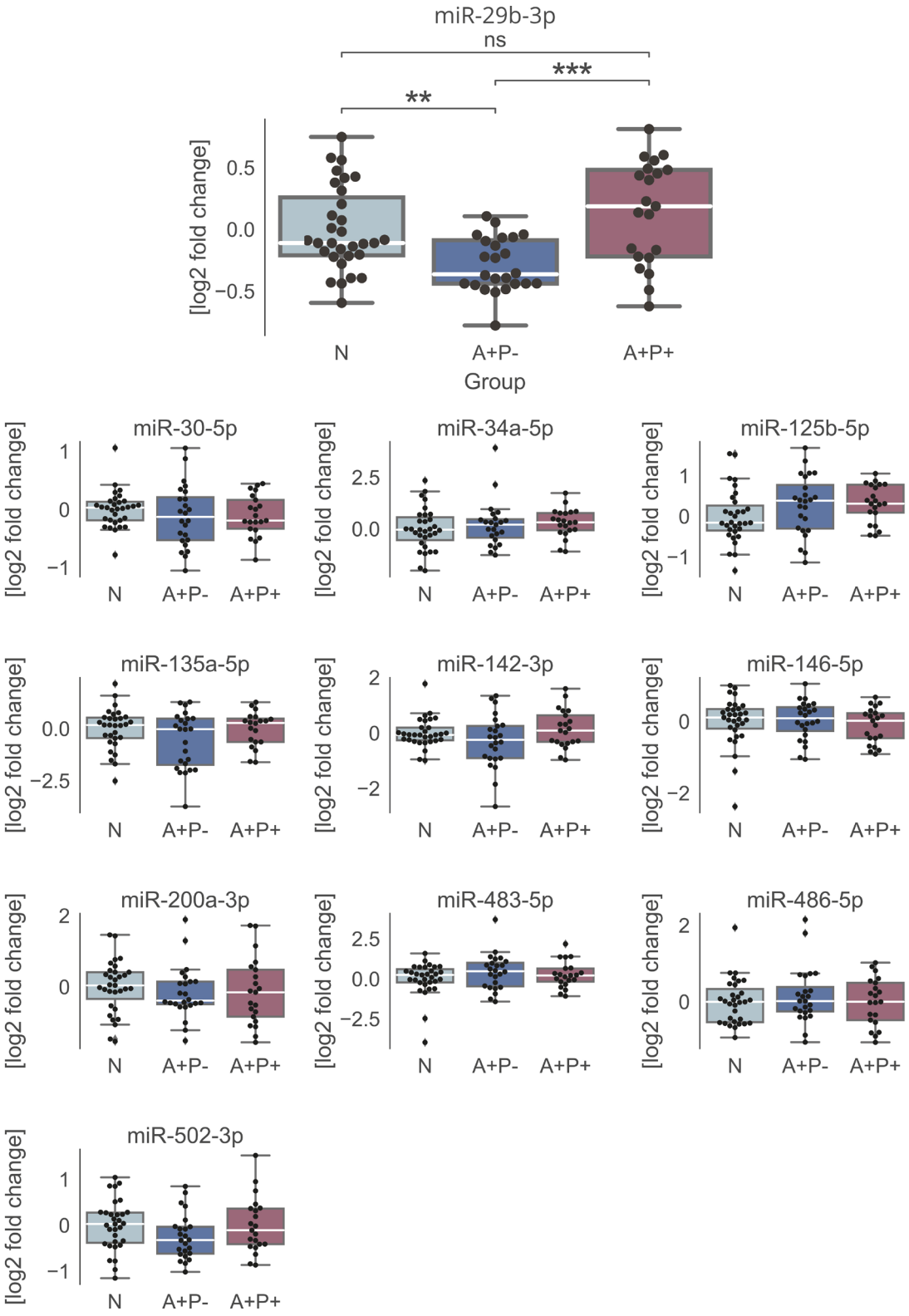

Figure 11. Group differences regarding the tested miRNAs panel.

4.2.3 Behavioral data

Behavioral data were recorded in the Presentation logfiles during both cognitive tasks i.e., MSIT and STM during both EEG and fMRI experiments. Reaction times (RT) and accuracy for the given stimuli were calculated and compared between the study groups.

There was no linear relationship between reaction times and age in any group, as assessed by visual inspection of a scatter plot and R^2 values, which were lower than 0.2, therefore age was not considered a covariate. Test assumptions for statistical evaluation are summarized in Appendix (Table 39 for two-way ANOVA and exact additional exact *p*-values for moderator sex variable and interaction), for both raw and log transformed reaction time data. To ensure normal distribution log transformed reaction time data were used in statistical testing for STM (from EEG and fMRI sessions) and for MSIT task (EEG session). Information about *p*-value for group differences can be found in Table 12 and Table 13 for MSIT/STM data respectively during an EEG experiment, and Table 14/Table 15 for MSIT/STM data respectively during a fMRI experiment. Due to the ceiling effect in accuracy data, which corresponds to the highly not gaussian data distributions, the Kruskal-Wallis test was used to measure differences between the groups (without log transforming the data, which would not be effective in this case).

The groups did not differ in accuracy neither in low nor in high-demanding conditions in both tasks during both EEG and fMRI experiments. There were however significant differences in reaction times in high-demanding conditions, but not low-demanding conditions, including both tasks during an EEG experiment (Table 12 and Table 13, Figure 12). There was a statistically significant main effect of group ($F(2, 72) = 3.80$, $p < .05$) on the reaction time in high-demanding condition in MSIT task, as A+P- group was characterized by longer reaction times than N group (post-hoc: $p < .05$) and same nearly significant result ($F(2,72) = 2.99$, $p = 0.057$) in high-demanding condition of STM task (post-hoc: $p = 0.055$). There was no such difference in the data from fMRI session (Table 14 and Table 15, Figure 13, see *Discussion* for possible explanation of this discrepancy).

Additionally, sex proved to be a significant factor influencing reaction time (males tended to respond quicker than females) in high-demanding condition in MSIT task, both in EEG ($F(1, 72) = 8.86$, $p < .01$) and fMRI ($F(1,61) = 5.76$, $p < .05$), and in low-demanding condition in MSIT task, also both in EEG ($F(1,72) = 5.36$, $p < .05$), as well as in fMRI experiment ($F(1,61) = 4.38$, $p < .05$). No interaction between the sex and group was detected, thought.

Table 12. Reaction time and accuracy data for MSIT task during an EEG experiment

Task	Group			*p-value*
	A+P+	**A+P-**	**N**	
MSIT LD RT	705.54 ± 89.59	730.51 ± 96.26	689.19 ± 90.26	.25
MSIT HD RT	**924.76 ± 90.38**	**997.14 ± 158.18**	**912.44 ± 114.62**	**< .05**
MSIT LD AC	99.54 ± 0.89	99.43 ± 1.30	99.88 ± 0.37	.27 &
MSIT HD AC	93.88 ± 13	94.54 ± 8.02	94.81 ± 6.54	.49 &

& Kruskal-Wallis test. The bolded font indicate a significant or trend result

Table 13. Reaction time and accuracy data for STM task during an EEG experiment

Task	Group			*p-value*
	A+P+	**A+P-**	**N**	
STM LD RT	963.27 ± 130.57	1007.81 ± 170.86	942.03 ± 121.55	.26
STM HD RT	**1089.32 ± 151.07**	**1175.76 ± 198.38**	**1068.69 ± 145.72**	**.057 ~**
STM LD AC	95.28 ± 3.78	95.58 ± 4.27	96.28 ± 3.29	0.67 &
STM HD AC	77.85 ± 9.65	77.93 ± 8.54	76.43 ± 6.39	0.54 &

& Kruskal-Wallis test; ~ trend level. The bolded font indicate a significant or trend result

Table 14. Reaction time and accuracy data for MSIT task during a fMRI experiment

Task	Group			*p-value*
	A+P+	**A+P-**	**N**	
MSIT LD RT	713.48 ± 113.49	727.57 ± 98.68	711.57 ± 93.39	.85
MSIT HD RT	946.09 ± 146.07	1001.70 ± 133.67	944.98 ± 130.42	.27
MSIT LD AC	96.85 ± 3.82	93.88 ± 7.76	95.59 ± 6.04	.55 &
MSIT HD AC	89.67 ± 7.13	90.40 ± 8.57	91.34 ± 7.74	.39 &

& Kruskal-Wallis test

Table 15. Reaction time and accuracy data for STM task during a fMRI experiment

Task	Group			*p-value*
	A+P+	**A+P-**	**N**	
STM LD RT	961.61 ± 172.61	971.07 ± 135.02	948.04 ± 120.90	.88
STM HD RT	1086.67 ± 181.40	1112.88 ± 170.05	1049.48 ± 161.91	.85
STM LD AC	92.05 ± 10.08	91.10 ± 11.51	95.42 ± 2.80	.11 &
STM HD AC	44.69 ± 2.35	45.71 ± 2.00	44.33 ± 2.54	.13 &

& Kruskal-Wallis test

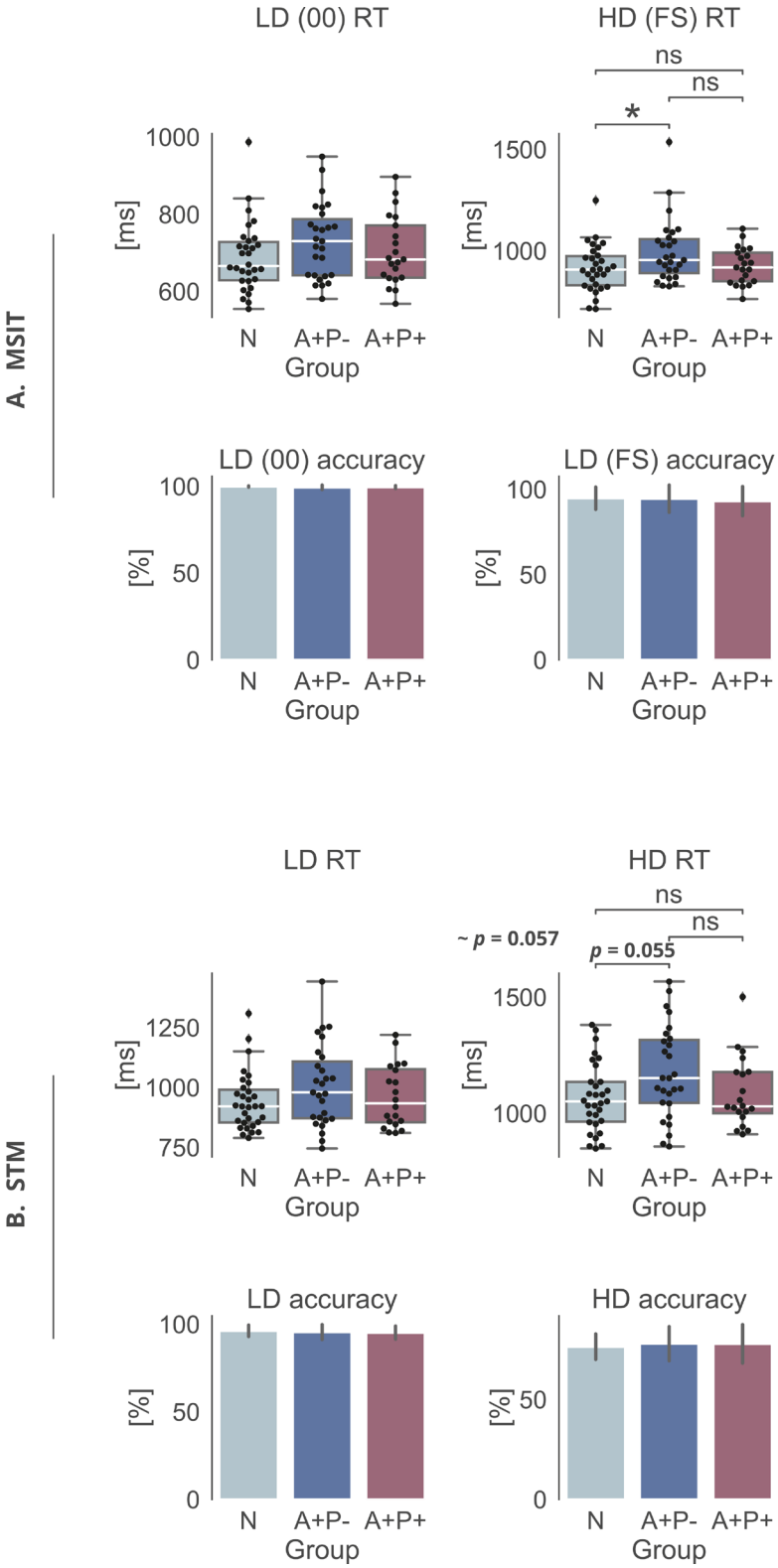

Figure 12. Reaction time and accuracy data for MSIT and STM tasks during an EEG experiment.

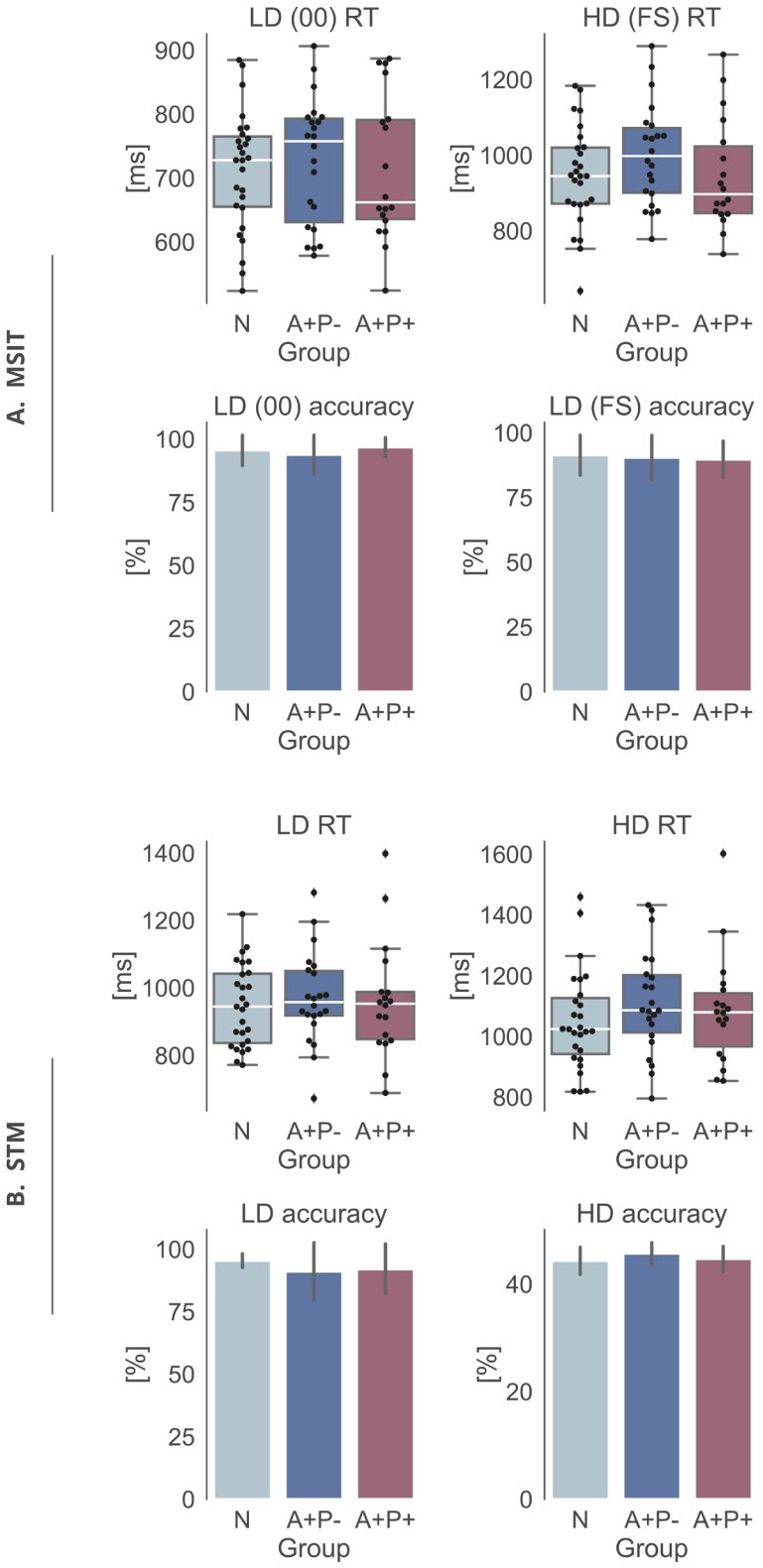

Figure 13. Reaction time and accuracy data for MSIT and STM tasks during a fMRI experiment

4.2.4 Structural neuroimaging: cortical thickness

Since brain atrophy is a hallmark of Alzheimer's disease, we analyzed structural MRI data to estimate cortical thickness. No linear relationship between thickness measures and age was detected in any of the groups, as assessed by visual inspection of a scatter plot and R^2 values, which were lower than 0.2, therefore age was not considered a covariate. There was only weak correlation of age and cortical thickness in inferior temporal gyrus in N group ($R^2 = 0.3$). Test assumptions for statistical evaluation were summarized in Appendix (Table 40 for two-way ANOVA and exact additional exact *p*-values for moderator sex variable and interaction), and Table 41 for one-way ANOVA when two-way ANOVA requirements were not met). Specific information about *p*-value for group differences can be found in Table 16. A+P- group was characterized by thinner cortex in the right temporal pole than N group ($F(2,63) = 3.59$, $p < .05$, post-hoc: $p < .05$; Figure 14, Figure 15). Additionally, females tended to have thicker cortex at left temporal pole than males ($F(1,63) = 8.98$, $p < .01$), and similar strong trend was observable for left supramarginal gyrus ($F(1,63) = 3.47$, $p = .07$).

Table 16. Cortical thickness: descriptive statistics and group differences

Area	Group			*p*-value
	A+P+	A+P-	N	
Parahippocampal gyrus left	2.81 ± 0.25	2.78 ± 0.18	2.78 ± 0.22	.81
Parahippocampal gyrus right	2.88 ± 0.20	2.90 ± 0.16	2.88 ± 0.19	.93
Supramarginal gyrus left	2.56 ± 0.13	2.53 ± 0.11	2.53 ± 0.12	.73
Supramarginal gyrus right	2.57 ± 0.14	2.54 ± 0.10	2.57 ± 0.12	.69
Temporal pole left	3.14 ± 0.24	3.07 ± 0.18	3.13 ± 0.20	.42
Temporal pole right	**3.19 ± 0.24**	**3.07 ± 0.12**	**3.19 ± 0.19**	**< .05**
Superior parietal lobule left	2.56 ± 0.13	2.53 ± 0.11	2.53 ± 0.12	.58 &
Superior parietal lobule right	2.57 ± 0.14	2.54 ± 0.10	2.57 ± 0.12	.64 &
Inferior temporal gyrus left	2.67 ± 0.15	2.67 ± 0.14	2.69 ± 0.15	.91
Inferior temporal gyrus right	2.71 ± 0.20	2.70 ± 0.17	2.70 ± 0.17	.97

& Kruskal-Wallis test. The bolded font indicate a significant or trend result. *p*-value is shown for *Group* factor.

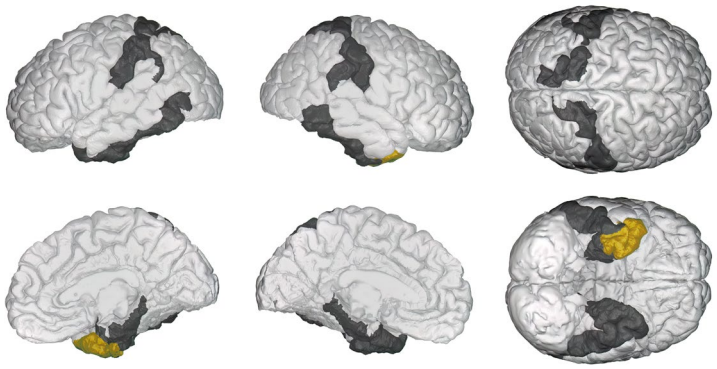

Figure 14. Analyzed ROIs (chosen from Destrieux atlas) marked in black; yellow color marks ROI (right temporal pole) with significantly thinner cortex in A+P- group as compared to N group. Generated using BrainPainter (Marinescu et al., 2019).

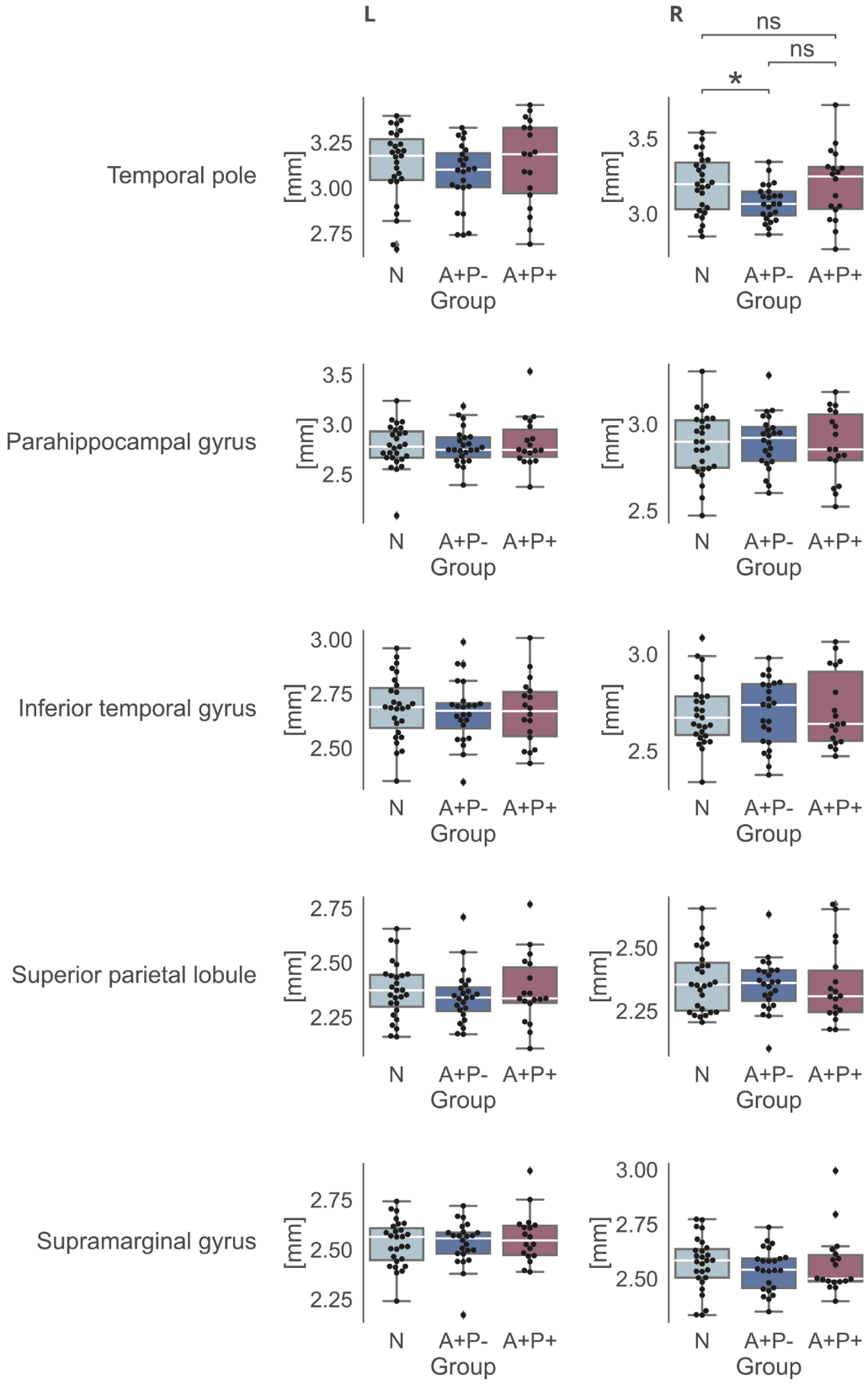

Figure 15. Cortical thickness measurements in chosen ROIs.

4.2.5 Functional neuroimaging: resting-state protocol

4.2.5.1 EEG: signal complexity

EEG signal complexity is assumed to correlate with cognitive abilities and is reduced in AD patients. EEG complexity (estimated with Higuchi Fractal Dimension index, see *Method* section) was compared between study groups of nondemented participants. There was no linear relationship between HFD measures and age in any group, as assessed by visual inspection of a scatter plot and R^2 values, which were lower than 0.2, therefore age was not considered a covariate. Test assumptions for statistical evaluation were summarized in Appendix (Table 44 for two-way ANOVA and exact additional exact *p*-values for moderator sex variable and interaction, and Table 45 for one-way ANOVA assumptions when former requirements were not met). Specific information about *p*-value for group differences can be found in Table 17. The signal complexity analysis and results are shown in Figure 16 where an average global HFD is plotted as a function of the tuning parameter k_{max}. Appropriate k_{max} value to calculate statistics of group difference.

A+P+ group was characterized by significantly lowered signal complexity in comparison to the N group and in some clusters (on a trend level) to the A+P- group both globally ($F(2,72) = 5.23$, $p < 0.01$, post-hoc: A+P+ vs. N $p < .01$, A+P+ vs. A+P- $p = 0.07$) and in some anatomical electrode clusters (see Figure 17, Table 17, Table 18).

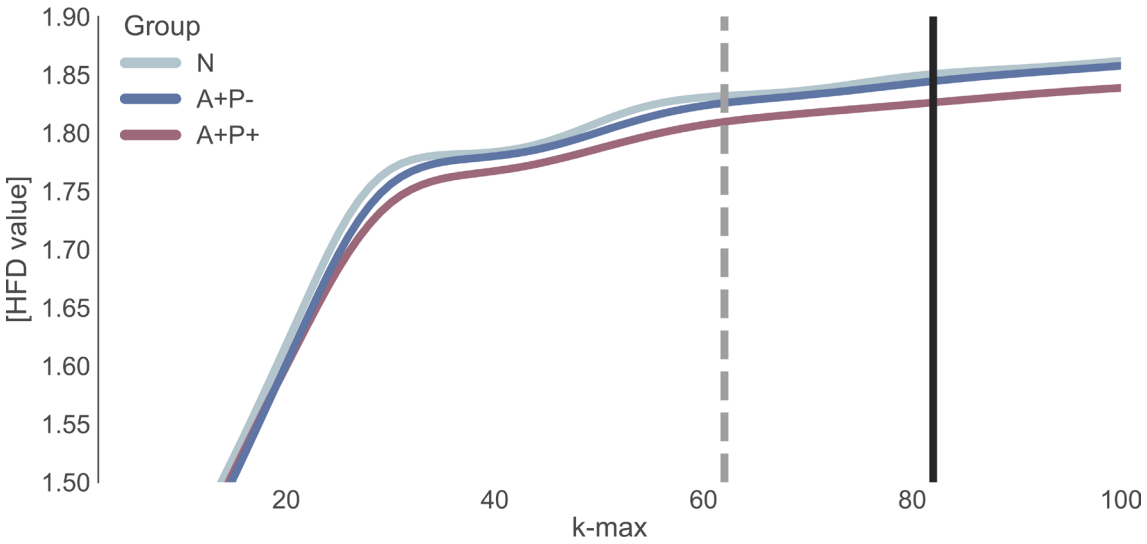

Figure 16. Dependence of Higuchi's Fractal Dimension value on the parameter k_{max}. Whole brain average HFD in dependence on k_{max}. The dotted line represents the start of HFD stability, and the black line represents the k_{max} selected for the between group comparison of HFD measure.

Table 17. HFD values. Descriptive statistics and group differences

Electrode clusters	Group			*p*-value
	A+P+	A+P-	N	
Global	**1.83 ± 0.04**	**1.85 ± 0.03**	**1.85 ± 0.03**	**< .01**
MF, midfrontal	**1.82 ± 0.04**	**1.84 ± 0.03**	**1.84 ± 0.03**	**.08 &**
FL, frontal-left	**1.81 ± 0.05**	**1.83 ± 0.04**	**1.84 ± 0.04**	**< .05**
FR, frontal-right	**1.81 ± 0.05**	**1.84 ± 0.03**	**1.84 ± 0.03**	**< .05**
C, central	**1.82 ± 0.04**	**1.84 ± 0.03**	**1.83 ± 0.03**	**< .05**
CTL, central-left	**1.83 ± 0.04**	**1.85 ± 0.03**	**1.86 ± 0.03**	**< .05**
CTR, central-right	**1.83 ± 0.05**	**1.85 ± 0.03**	**1.86 ± 0.03**	**< .01**
PC, posterior-central	1.82 ± 0.04	1.83 ± 0.03	1.84 ± 0.03	.10
PTL, posterior-left	**1.84 ± 0.04**	**1.86 ± 0.02**	**1.86 ± 0.02**	**< .05**
PTR, posterior-right	**1.84 ± 0.04**	**1.86 ± 0.02**	**1.86 ± 0.02**	**.08 #**
OC, occipital-central	1.83 ± 0.04	1.85 ± 0.03	1.85 ± 0.03	.10
OL, occipital-left	1.85 ± 0.03	1.85 ± 0.03	1.86 ± 0.03	.13
OR, occipital-right	**1.84 ± 0.03**	**1.86 ± 0.03**	**1.86 ± 0.03**	**.09 #**

One-way ANOVA; & Kruskal-Wallis test. The bolded font indicate a significant or trend result. *p*-value is shown for *Group* factor.

Table 18. HFD values. Statistical values and post-hoc tests

Cluster	Statistic	Post-hoc details
FL, frontal-left	4.36 #	A+P+ vs. N ($p < .05$)
FR, frontal-right	4.70 #	A+P+ vs. N ($p < .05$)
C, central	4.44 #	A+P+ vs. N ($p < .05$); A+P+ vs. A+P- ($p = .09$)
CTL, central-left	4.69 #	A+P+ vs. N ($p < .01$)
CTR, central-right	5.13 #	A+P+ vs. N ($p < .01$); A+P+ vs. A+P- ($p < .09$)
PTL, posterior-left	4.70 #	A+P+ vs. N ($p < .01$); A+P+ vs. A+P- ($p < .09$)
Trend level differences		
MF, midfrontal	5.00 &	A+P+ vs. N ($p < .08$)
PTR, posterior-right	3.43 #	A+P+ vs. N ($p = .053$); A+P+ vs. A+P- ($p = .06$)
OR, occipital-right	2.5 #	A+P+ vs. N ($p = .09$)

Anova statistic (F) marked by #; Kruskal-Wallis statistc (W) marked with &.

Additionally, sex was also significantly influencing HFD values, where males were characterized by lowered signal complexity, both globally ($F(1,72) = 4.08$, $p < .05$), and in some electrode clusters (Table 44) (CTR cluster ($F(1,72) = 5.46$, $p < .05$), PTL ($F(1,72) = 6.81$, $p < .05$) and on a trend level in C cluster ($F(1,72) = 3.69$, $p = 0.06$)). Interaction between sex and group factors was detected for clusters summarized in Table 19: FL and FR (Figure 18), and on a trend ($p = .06$) level in CTR cluster and globally. These results covered the same pattern as main results for group factor alone, females/males (depending on the particular comparison) from A+P+ group were characterized by the lowest HFD values, compared to females/males from A+P- group, and N group (with the highest values). This is true also for trend level differences for CTR cluster and globally (which were not illustrated on Figure 18).

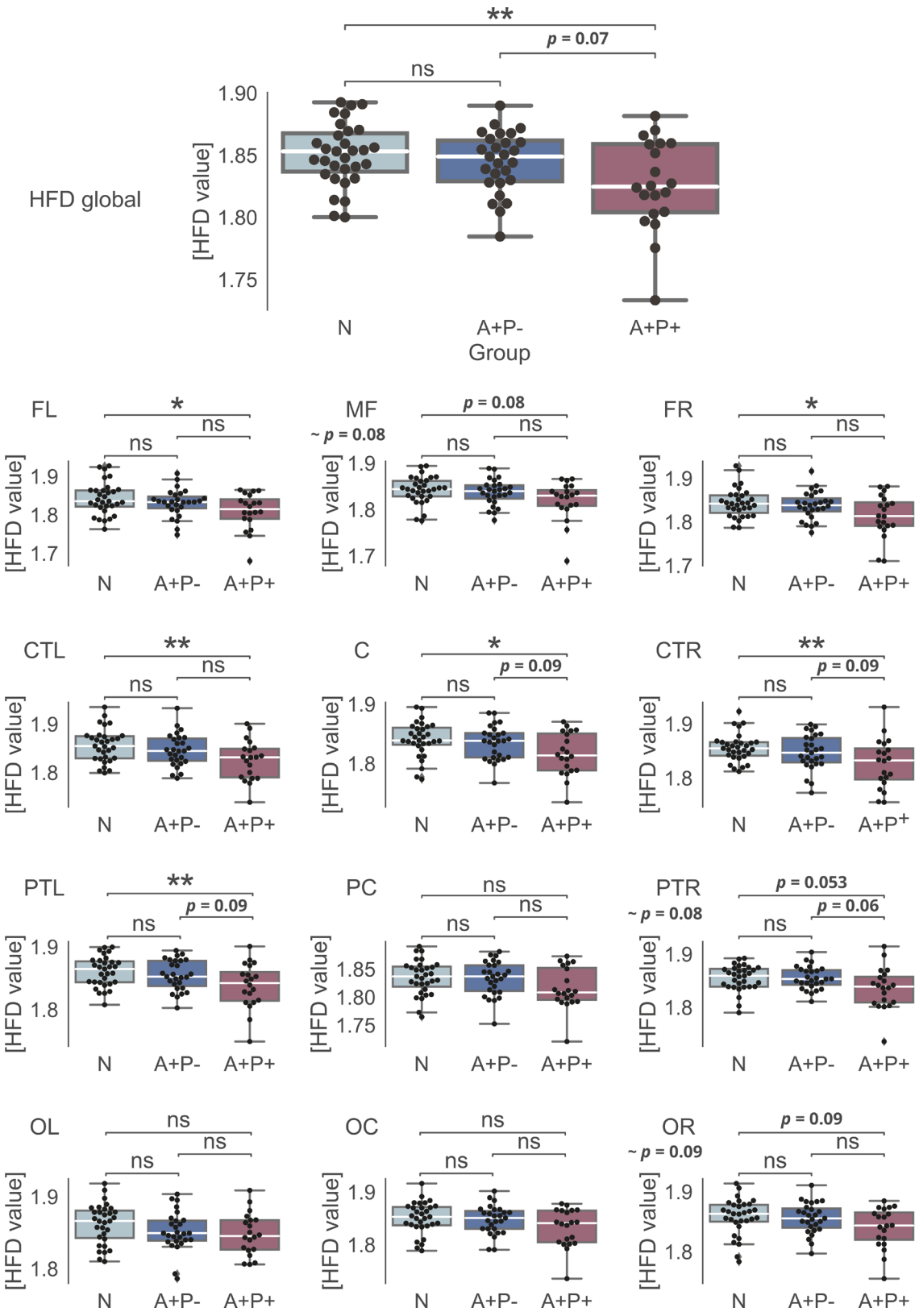

Figure 17. Average Higuchi's Fractal Dimension. Differences between the groups on k_{max} = 82.

Table 19. Statistical values and post-hoc information regarding *sex*group* interaction in HFD analysis (significant or trend-level results).

Electrode cluster	Statistic	Post-hoc details
FL, frontal-left	5.41	M N > M A+P+ ($p < .001$); M A+P+ < M A+P- ($p < .05$); F A+P+ > M A+P+ ($p = .06$); F N > M A+P+ ($p < .05$)
FR, frontal-right	5.03	F N > M A+P+ ($p < .05$); M N > M A+P+ ($p < .001$); F A+P+ > M A+P+ ($p < .05$); M A+P+ < F A+P- ($p < .01$); M A+P+ < M A+P- ($p < .05$)
Trend level differences		
Global	2.92	F N > M A+P+ ($p < .01$); M N > M A+P+ ($p < .01$); F A+P+ > M A+P+ ($p < .05$); M A+P+ < F A+P- ($p < .01$)
CTR, central-right	2.97	F N > M A+P+ ($p < .01$); M N > M A+P+ ($p < .01$); F A+P+ > M A+P+ ($p < .05$); M A+P+ < F A+P- ($p < .01$); M A+P+ < M A+P- ($p = .07$)

The table displays the Anova statistic (F). M = males, F = females.

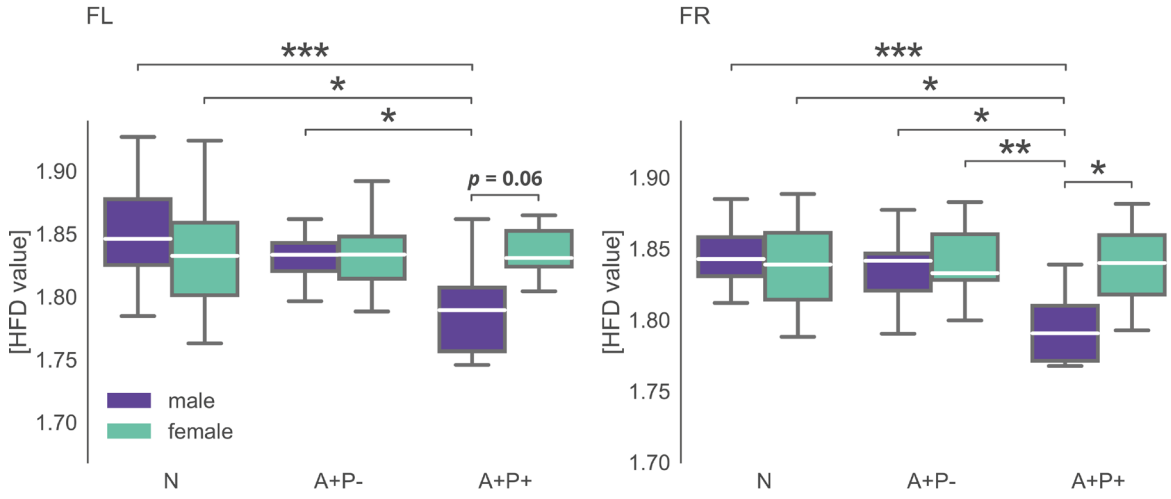

Figure 18. Average Higuchi's Fractal Dimension. A summarize of results described in Table 19 for FL and FR clusters, regarding the interaction of *sex*group* factors.

4.2.5.2 EEG: power spectrum distribution

The conventional approach to analyzing EEG data includes the decomposition of the signal into its spectral components, which are then classified into specific frequency bands. The absolute or relative power within these bands is employed to characterize the EEG with respect to its functional state, providing insights into potential pathological changes.

The power of analyzed frequency bands was not correlated with age in any of the groups, as assessed by visual inspection of a scatter plot and R^2 values, which were lower than 0.2, therefore age was not considered a covariate. Minor linear relationship with age were detected only for A+P+ group in high alpha relative power in PTR ($R^2 = 0.20$) and PC ($R^2 = 0.21$) electrode clusters. Test assumptions for statistical evaluation were summarized in the

Appendix (Table 46, Table 48, Table 49 and Table 51 for two-way ANOVA and exact additional exact *p*-values for moderator sex variable and interaction, and Table 47, Table 50 and, Table 52 for one-way ANOVA where former requirements were not met). Detailed information about *p*-values for risk group differences can be found in Table 20 and main findings on group level are shown on Figure 19.

A+P+ group was characterized by higher delta relative power than N and/or A+P- group globally ($F(2,72) = 4.19$, $p < .05$, post-hoc: A+P- vs. A+P+ $p < .05$, A+P+ vs. N $p < .05$) and in some electrode clusters (see Figure 19, Table 21).

Table 20. Relative power: *p*-values for group differences

Cluster	**Group differences in main EEG frequency bands: *p*-value**			
	Delta	**Theta**	**Alpha-1**	**Alpha-2**
Global	**< .05**	.62	.58	# .13
MF, midfrontal	.31	.81	# .60	# .25
FL, frontal-left	**.07** &	.43	.51	& .36
FR, frontal-right	**.055** &	.57	.27	& .19
C, central	**< .05**	.95	# .68	.20
CTL, central-left	.11 &	.49	.71	.33
CTR, central-right	**< .05**	.65	.81	**.052**
PC, posterior-central	**.09**	.65	.59	**.07**
PTL, posterior-left	**< .05**	.55	.70	.15
PTR, posterior-right	**< .01**	.52	.63	# **<.05**
OC, occipital-central	**.06**	.54	.53	**.055**
OL, occipital-left	.21 &	.60	.55	.12
OR, occipital-right	**< .05**	.58	.62	**.07**

One-way ANOVA; & Kruskal-Wallis test

Table 21. Relative power within delta band: statistical values and post-hoc information regarding group differences that are either significant or show a trend

Cluster	**Statistic**	***p*-value**	**Post-hoc details**
C, central	3.70 #	< .05	A+P- vs. A+P+ ($p < .05$); A+P+ vs. N ($p < .05$)
CTR, central-right	4.79 #	< .05	A+P- vs. A+P+ ($p < .01$); A+P+ vs. N ($p < .05$)
PTL, posterior-left	3.97 #	< .05	A+P+ vs. N ($p < .05$)
PTR, posterior-right	5.43 #	< .01	A+P- vs. A+P+ ($p < .01$); A+P+ vs. N ($p < .05$)
OR, occipital-right	4.80 #	< .05	A+P- vs. A+P+ ($p < .05$); A+P+ vs. N ($p < .05$)
Trend level differences			
FL, frontal-left	5.25 &	.07	A+P- vs. A+P+ ($p = .085$)
FR, frontal-right	5.80 &	.055	A+P- vs. A+P+ ($p = .057$)
PC, posterior-central	2.97 #	.09	A+P- vs. A+P+ ($p = .09$)
OC, occipital-central	2.90 #	.07	A+P- vs. A+P+ ($p = .09$); A+P+ vs. N ($p = .09$)

Anova statistic (F) marked by #; Kruskal-Wallis statistc (W) marked with &. *p*-value: group factor.

Male participants tended to have higher delta power than females in two clusters (trend level effects in PTL ($F(1,72) = 3.67$, $p = .06$ and OR $F(1,72) = 3.19$, $p = .08$). There was an interaction between sex and group in regards to delta relative power (Figure 20), basically showing the same direction of change, where males from A+P+ group were characterized by higher delta power than males or females of N or A+P- groups, both globally ($F(2,72) =$

3.17, $p < .05$, post-hoc: M A+P- vs. M A+P+ ($p < .01$), M A+P+ vs. M N ($p < .05$), M A+P+ vs. F N ($p < .05$), F A+P- M vs. A+P+ ($p = .08$)) and in chosen electrode clusters (Table 22).

Table 22. Relative power within delta band: statistical values and post-hoc information regarding differences for *sex*group* interaction that are either significant or show a trend

Cluster	**Statistic**	***p*-value**	**Post-hoc details**
C, central	3.41	< .05	A+P- M vs. A+P+ M ($p < .01$); A+P+ M vs. N F ($p < .05$); A+P+ M vs. M N ($p = .06$)
PTL, posterior-left	3.52	< .05	F A+P- vs. M A+P+ ($p < .05$); M A+P- vs. M A+P+ ($p < .05$); F A+P+ vs. M A+P+ ($p < .05$); M A+P+ vs. F N ($p < .01$); M A+P+ vs. M N ($p < .05$)
PTR, posterior-right	3.16	< .05	F A+P- vs. M A+P+ ($p < .01$); M A+P- vs. M A+P+ ($p < .01$); M A+P+ vs. F N ($p < .01$); M A+P+ vs. M N ($p < .05$); F A+P+ vs. M A+P+ ($p = .06$)
Trend level differences			
CTR, central-right	2.88	.07	M A+P- vs. M A+P+ ($p < .05$); M A+P+ vs. F N ($p < .01$); M A+P+ vs. M N ($p < .05$); F A+P- vs. M A+P+ ($p = .09$)
OR, occipital-central	3.05	.054	F A+P- vs. M A+P+ ($p < .05$); M A+P- vs. M A+P+ ($p < .01$); M A+P+ vs. F N ($p < .01$); M A+P+ vs. M N ($p = .09$)

The table displays the Anova statistic (F). M = males, F = females. *p*-value: group factor.

There were no significant differences between the groups in theta relative power. Male participants were, once again, characterized by higher theta relative power than females: globally ($F(1,72) = 5.90$, $p < .05$) and in some electrode clusters (Table 23).

Table 23. Relative power within theta band: statistical values and post-hoc information regarding sex factor that are either significant or show a trend

Cluster	**Statistic**	***p*-value**
MF, midfrontal	4.01	< .05
FL, frontal-left	4.73	< .05
FR, frontal-right	4.04	< .05
C, central	5.21	< .05
CTL, central-left	4.13	< .05
CTR, central-right	6.10	< .05
PTL, posterior-left	5.90	< .05
PTR, posterior-right	5.65	< .05
OC, occipital-central	4.99	< .05
OL, occipital-left	10.48	< .01
OR, occipital-right	8.10	< .01
Trend level differences		
PC, posterior-central	3.56	.06

The table displays the Anova statistic (F).

There was a statistically significant interaction (Figure 20) between the group and sex factors on lower alpha relative power, where female participants from A+P+ group were characterized by lower low alpha relative power than males in A+P- group, and males from N group were characterized by lower low alpha relative power in relation to males from A+P- group. Additionally, females from A+P- group were characterized by lower low alpha relative power than males from the same group. The results were significant globally

(F(2,72) = 5.84, $p < .01$, post-hoc: F A+P- vs. M A+P- $p < .05$, M A+P- vs. M N $p < .05$, M A+P- vs. F A+P+ $p = .07$) or in individual electrode clusters (Table 24).

Table 24. Relative power within lower alpha band: statistical values and post-hoc information regarding differences for *sex*group* interaction that are either significant or show a trend

Cluster	Statistic	*p*-value	Post-hoc details
FL, frontal-left	5.76	< .01	F A+P- vs. M A+P- ($p < .05$); M A+P- vs. M N ($p < .05$)
FR, frontal-right	5.65	< .01	F A+P- vs. M A+P- ($p < .05$); M A+P- vs. F A+P+ ($p < .05$); M A+P- vs. M N ($p < .05$)
CTL, central-left	5.75	< .01	F A+P- vs. M A+P- ($p < .05$); M A+P- vs. M N ($p < .05$)
CTR, central-right	5.44	< .01	F A+P- vs. M A+P- ($p < .05$); M A+P- vs. F A+P+ ($p < .05$) M A+P- vs. M N ($p < .05$)
PC, posterior-central	5.93	< .01	F A+P- vs. M A+P- ($p < .05$); M A+P- vs. M N ($p < .05$)
PTL, posterior-left	5.96	< .01	F A+P- vs. M A+P- ($p < .05$); M A+P- vs. M N ($p = .07$)
PTR, posterior-right	5.00	< .01	F A+P- vs. M A+P- ($p < .05$); M A+P- vs. F A+P+ ($p = .09$); M A+P- vs. M N ($p = .08$)
OC, occipital-central	5.29	< .01	F A+P- vs. M A+P- ($p = .07$); M A+P- vs. F A+P+ ($p < .05$); M A+P- vs. M N ($p = .08$)
OL, occipital-left	5.11	< .01	M A+P- vs. F A+P+ ($p = .07$)
OR, occipital-right	5.76	< .01	F A+P- vs. M A+P- ($p = .07$); M A+P- vs. M N ($p < .05$)

The table displays the Anova statistic (F). M = males, F = females. *p*-value: group factor.

A+P+ group was also characterized by lower relative power of high alpha band in some electrode clusters than N group (Table 25).

Table 25. Relative power within higher alpha band: statistical values and post-hoc information regarding group differences that are either significant or show a trend

Cluster	Statistic	*p*-value	Post-hoc details
FL, frontal-left	3.27	< .05	A+P+ vs. N ($p < .05$)
Trend level differences			
CTR, central-right	3.09	.052	A+P+ vs. N ($p < .05$)
PC, posterior-central	3.02	.055	A+P+ vs. N ($p = .053$)
OC, occipital-central	2.70	.07	A+P+ vs. N ($p = .06$)
OR, occipital-right	2.70	.07	A+P+ vs. N ($p = .08$)

The table displays the Anova statistic (F). *p*-value: group factor.

Males were additionally characterized by lower power of high alpha band than females in some electrode clusters (Table 26).

Table 26. Relative power within higher alpha band: statistical values and post-hoc information regarding sex that are either significant or show a trend

Cluster	*Statistic*	*p-value*
CTL, central-left	4.89	< .05
CTR, central-right	4.00	< .05
PTL, posterior-left	4.47	< .05
OC, occipital-central	6.10	< .05
OL, occipital-left	8.45	< .01
OR, occipital-right	8.48	< .01
Trend level differences		
C, central	3.19	.08

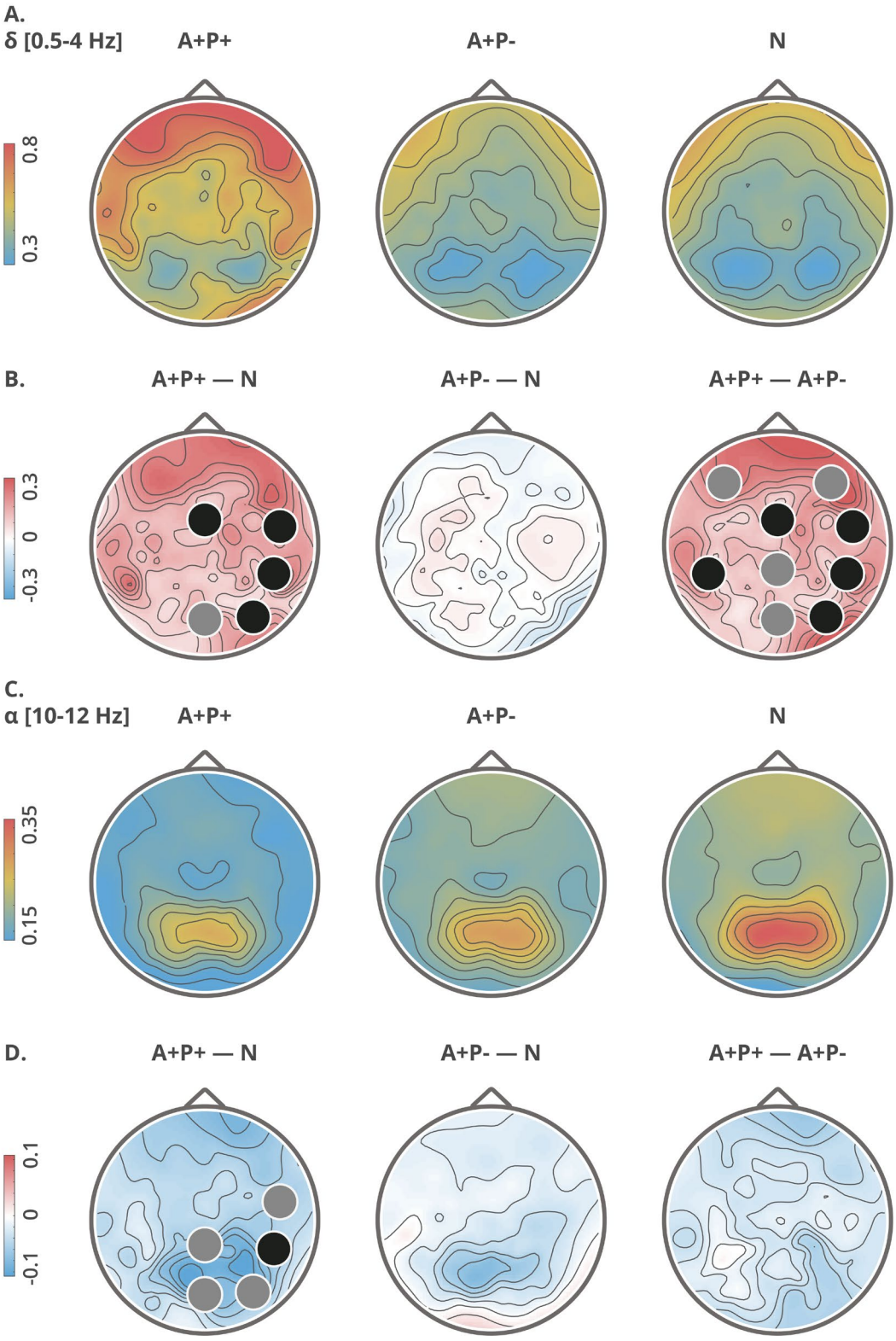

Figure 19. Topographical maps of delta (A., B.) and alpha (C., D.) relative power: group averages (upper rows, A., C.) and group differences (lower rows, B., D.). Clusters with significant ($p < 0.05$) differences between the groups are marked with black circles and trend ($p < 0.09$) differences are marked with gray circles. Topographic maps are calculated from high-density data (all 128 electrodes).

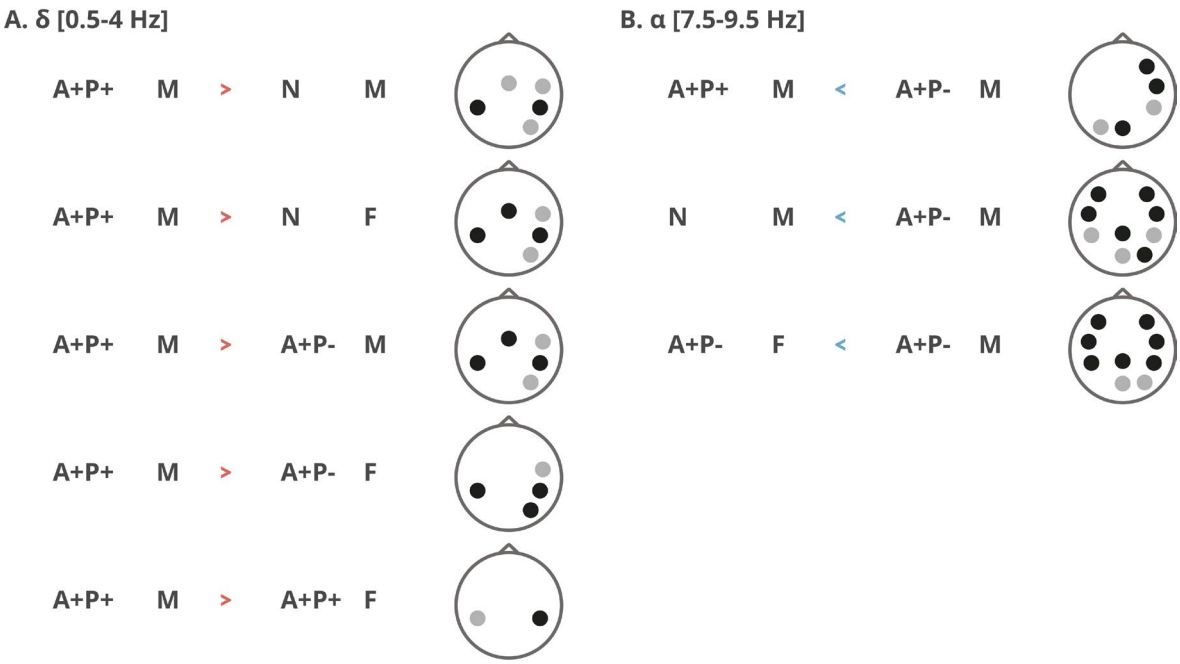

Figure 20. A graphic summary outlining the interaction between the group and sex factors: delta relative power (A.) and low alpha relative power (B.). An upward arrow indicates higher power for the first reported group, and a downward arrow indicates lower power. The topographic maps indicate the location of clusters with significant and near-significance effects. Clusters with significant ($p < 0.05$) are marked with black circles and trend ($p < 0.09$) differences are marked with gray circles.

4.2.5.3 EEG: functional connectivity

The analysis of connectivity, as evaluated by the coherence of EEG frequency components (bands), uncovered subtle patterns indicating some differences between the groups. Within the delta band, the A+P+ group exhibited comparatively greater coherence in comparison to the A+P- and N groups. Moreover, the A+P- group exhibited reduced theta coherence in comparison to the N group. Both the A+P+ (low and high alpha) and A+P- (low alpha) groups showed (mostly) decreased coherence in the alpha band compared to the N group (as illustrated in Figure 21, with uncorrected *p*-values lower than the alpha .05 level). However, it is crucial to highlight that none of these associations retained significance after applying the false discovery rate (FDR) correction. Figure 29 in the Appendix shows coherence results, utilizing a high-density montage with all 128 electrodes. This figure incorporates connectograms and difference matrix representations, offering a more thorough and precise depiction of global connectivity. Frequently, global representations (like on Figure 29) are excluded in result descriptions that concentrate solely on specific electrodes chosen based on a hypothesis-driven approach (Figure 21).

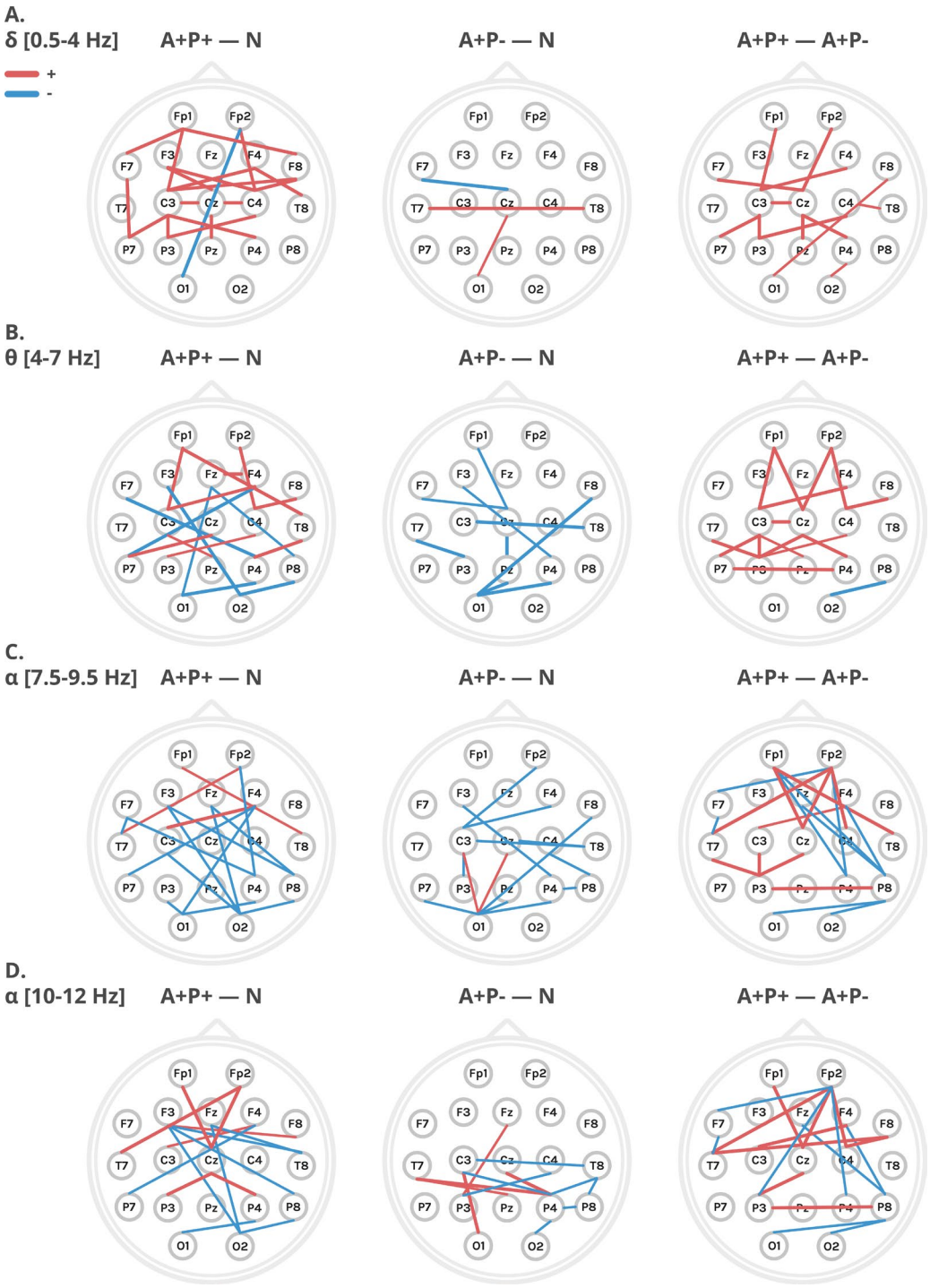

Figure 21. Differences in connectivity, as measured by coherence, were assessed among the 19 electrodes in the classical 10-20 montage for each frequency band. Red lines indicate higher coherence for the first group compared to the second group (e.g., A+P+ – N), while blue lines represent the lower coherence. Only significant t-test results (Fieldtip) between the electrodes are displayed in the image, but none of these remained significant after applying the FDR correction.

4.2.5.4 fMRI: network alterations

Hypothesis-driven approach: alterations in the Default Mode Network

Resting-state independent component analysis (ICA) is a widely employed method in functional magnetic resonance imaging to investigate intrinsic connectivity patterns in the brain. Changes in the default mode network (DMN) have been identified as a characteristic feature of Alzheimer's disease patients. Therefore, we primary focused on this particular network.

Group-level ICA was performed to estimate temporally coherent patterns in combined fMRI data of all subjects. The mapping of 21 estimated components to known networks (i.e., their correlation with the standard network map) is detailed in Table 27 (three components with strongest affiliation are indicated for each network). Three components (IC 5, 11 and 20) matched to the DMN were chosen for further group comparisons. It is important to note that the IC components are not perfectly aligned with the conventional DMN areas (for example, among other areas, they include anterior cingulate cortex (ACC) and anterior insula (IA) which are commonly recognized as key components within the Salience Network). Note: the notation "group #1 – group #2" used in the description of fMRI results (tables/figures) corresponds to the contrast "#1 minus #2".

Table 27. Mapping of the 21 Independent Components to neural networks

Neural network	Independent component No and its correlation coefficient with the given network
Default Mode Network	**11 (r=0.38)**, 5 (r=0.34), 20 (r=0.11)
Sensorimotor Network	**21 (r=0.46)**, 16 (r=0.43), 19 (r=0.24)
Visual Network	**12 (r=0.56)**, 15 (r=0.41), 13 (r=0.25)
Salience Network	**2 (r=0.35)**, 10 (r=0.10), 14 (r=0.08)
Dorsal Attention Network	**19 (r=0.38)**, 10 (r=0.27), 13 (r=0.10)
Fronto-Parietal Network	**6 (r=0.20)**, 17 (r=0.17), 4 (r=0.14)
Language Network	**3 (r=0.39)**, 8 (r=0.21), 10 (r=0.11)
Cerebellar Network	**1 (r=0.37)**, 18 (r=0.34), 17 (r=0.20)

A+P- group had significantly more network strength in several clusters within IC 20, encompassing also parts of DMN (among multiple other areas), like posterior cingulate cortex or precuneus, than the N group. At the same time, A+P- group had also significantly less network strength in the small cluster encompassing right temporooccipital part of middle temporal gyrus (toMTG, IC11, not typically considered a core component of the DMN) compared to the N group. Double risk participants (A+P+) did not show any differences in the DMN as compared to control but exhibited less network strength in comparison to the A+P- group within other areas being a part IC20 (like ACC). All effects were significant on a level of p-FDR < 0.01 or p-FDR < 0.001. The significant findings from this analysis are detailed in Table 28 and visually represented in Figure 22. No significant differences were found in IC 5 among the groups.

Table 28. Spatial clusters (their location, size, and anatomical alignment) belonging to independent components 11 and 20, showing significant differences between the groups.

Group comparison	IC	Cluster (x, y, z)	*k*	*p*-FDR <	Label	% of voxels in the cluster covering % of labeled area
A+P- – N	11	62, -44, 6	141	0.01	toMTG r	98% / 12%
		-12, 18, 34	1160	0.001	ACC	43% / 19%
					PCC	11% / 5%
					SMA r	15% / 24%
					SMA l	4% / 7%
					PaCiG r	4% / 3%
					PaCiG l	5% / 4%
					PreCG r	4% / 1%
		-36, -4, -8	736	0.001	IC l	45% / 25%
					CO l	18% / 14%
					Pu l	5% / 4%
		34, -4, 2	709	0.001	IC r	22% / 12%
					Pu r	16% / 14%
					PreCG r	13% / 2%
					IFG op r	10% / 11%
					CO r	7% / 6%
					FO r	4% / 8%
A+P- – N	20	68, -34, 28	236	0.001	aSMG r	47% / 14%
					pSMG r	40 % / 8%
					PO r	3% / 1%
		34, -4, 42	225	0.001	PreCG r	44 % / 2%
					MidFG r	20% / 9%
		14, -48, 54	211	0.001	SPL r	35% / 5%
					Prec	31% / 1%
					PostCG r	10% / 5%
		-54, -64, -6	166	0.005	iLOC I	67% / 5%
					toMTG l	52% / 31%
		-16, 0, 54	140	0.01	SFG l	16 % / 1%
					SMA l	14 % / 10%
		16, -60, -22	101	0.05	Cer r	100 % / 8%
		-18, -44, 66	88	0.05	PostCG l	43% / 1%
					Prec	42% / 1%
					SPL l	10% / 1%
		26, -48, -30	84	0.05	Cer r	94% / 6%
A+P+ – A+P-	20	-10, 2, 44	281	0.001	ACC	67% / 7%
					PaCiG r	11% / 2%
					PaCiG l	10% / 2%
					SMA l	9% / 4%
		-42, 6, 2	116	0.05	IC l	67% / 6%
					CO l	15% / 2%

r – right; l – left; *k* – cluster size; toMTG – middle temporal gyrus temporooccipital part; SPL – superior parietal lobule; ACC – anterior division cingulate gyrus; SMA – supplementary motor cortex; PCC – posterior cingulate cortex; PaCiG – paracingulate gyrus; PreCG – precentral gyrus; PostCG – postcentral gyrus; IC – insular cortex; CO – central opercular cortex; Pu – putamen; IFG op – inferior frontal gyrus pars opercularis; MidFG – middle frontal gyrus; SFG – superior frontal gyrus; FO – frontal operculum cortex; PO – parietal operculum cortex; aSMG – supramarginal gyrus anterior division; pSMG – supramarginal gyrus posterior division; Prec – precuneus; iLOC – lateral occipital cortex inferior division; Cer – cerebellum.

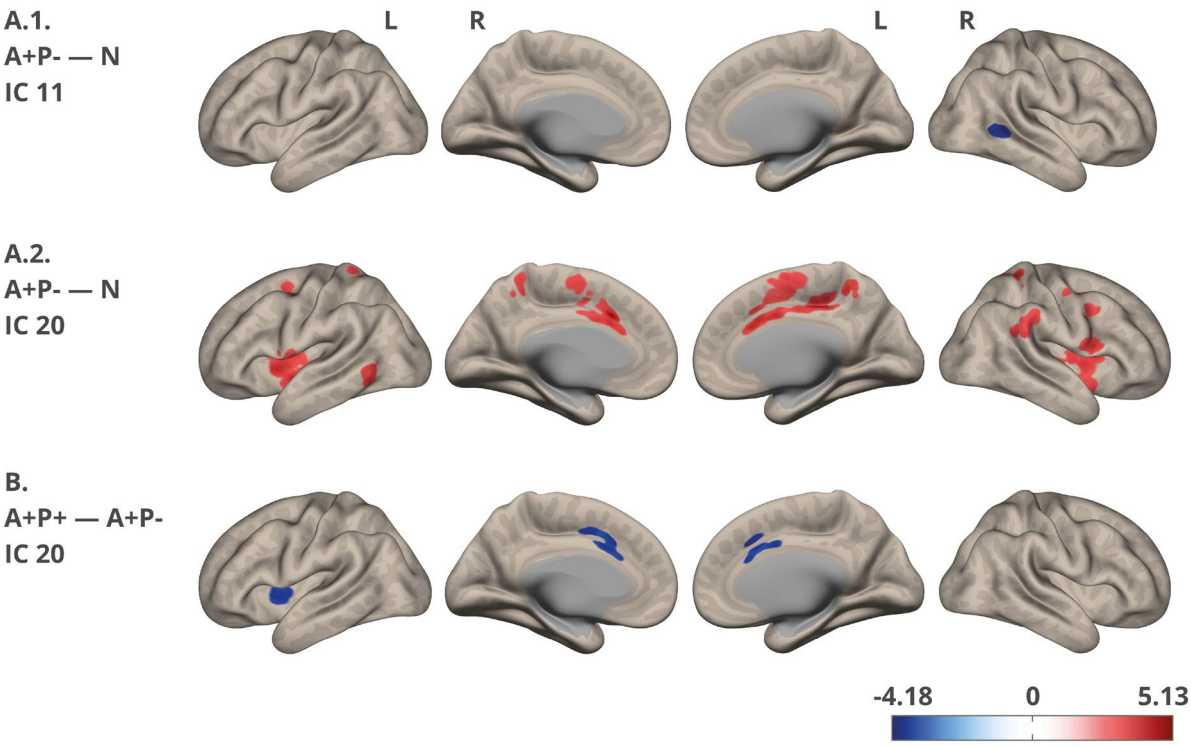

Figure 22. Differences in network strength/connectivity between the groups. Results based on ICA focusing on the components showing the highest correlation with the DMN network. Significantly different areas are marked with color according to the direction of difference and obtained t-values. Significant differences were observed between the A+P- and N groups, with IC 11 (A.1.) and IC 20 (A.2.). Significant differences were also identified between the A+P+ and A+P- groups (B.) within IC 20. The separate images were visualized using the CONN toolbox, with the t-values adjusted to align with the cortical structure on a glass ICBM template brain surface display. Lateral and medial view.

4.2.6 Brain activity during cognitive task

4.2.6.1 Event-related potentials (ERP)

To validate the employed protocol and the quality of acquired EEG data, the basic task effects were analyzed for all participants together. Namely, ERP differences between the low demanding condition and the high demanding condition were examined (Figure 23). The analysis considered only trials with correct responses. Three ERP waves associated with cognitive control, observed during the Multi-Source Interference Task, are the P300 (P3), N200 (N2), and late sustained potential (LSP). Both were clearly present in analyzed data and shown differences (with FDR correction) between low (00) and high (FS) demanding conditions (Figure 23).

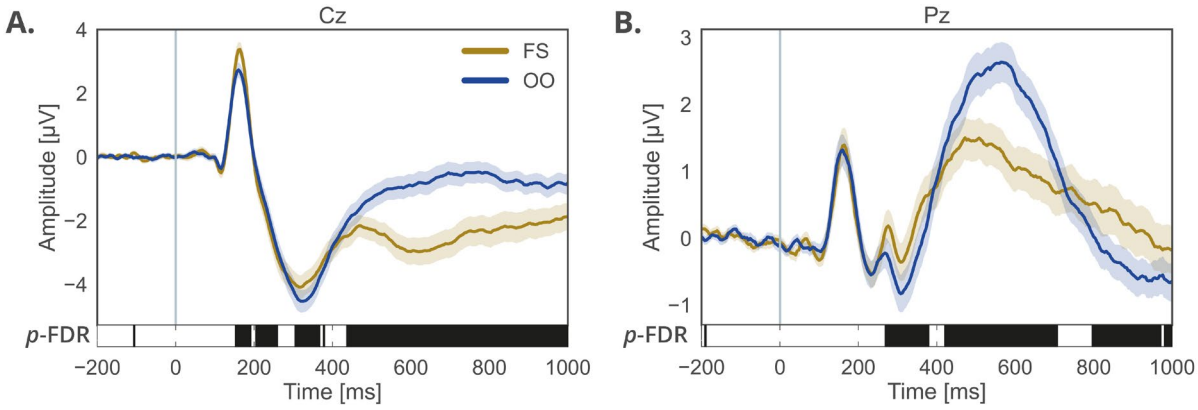

Figure 23. ERPs for low demanding (00) and high-demanding (FS) trials of MSIT task from Cz and Pz electrodes. Beneath ERP images, *p*-value statistics is provided for each point-to-point comparison (FDR-corrected values, calculated withing the EEGLAB toolbox, see *Methods*).

Next, an analysis was conducted to determine if ERP components related to MSIT are influenced by the studied risk genes. In Figure 24 (low demanding 00 condition) and Figure 25 (high demanding FS condition), group differences in event-related potentials for Cz and Pz electrodes are presented, showcasing N2, P3 and LSP potentials. Test assumptions for statistical estimations were summarized in Appendix (Table 53, Table 54). Detailed information about *p*-value for group differences can be found in Table 29 (00 condition) and Table 30 (FS condition).

No substantial differences between the groups were detected in the low-demanding (00) condition neither in peak amplitude not in latency measures of any component. In high-demand (FS) condition two ERP waves differentiated the groups. A significant difference was visible in N2 peak latency between A+P+ and N group, and on a trend level between A+P+ and A+P- groups (Table 30 and Figure 25) ($F(2,76) = 4.84$, $p < .01$; post-hoc: A+P- vs. A+P+ $p = .07$, A+P+ vs. N $p < .01$). There were no evident differences in P3 window, but the LSP wave differentiated A+P- and A+P+ group on a trend level ($H(2) = 5.93$, $p = .052$; post-hoc: A+P- vs. A+P+ $p = .059$).

Table 29. ERP: descriptive statistics and group differences in 00 condition

Measure	**Group**			***p*-value**
	A+P+	**A+P-**	**N**	
N2 peak amplitude: Cz	-5.12 ± 3.24	-5.53 ± 3.10	-6.01 ± 2.82	& .44
N2 peak latency: Cz	344.19 ± 32.39	323.70 ± 43.56	325.81 ± 43.56	# .15
P3 peak amplitude: Pz	3.44 ± 1.46	2.85±2.93	4.21 ± 3.15	& .28
P3 peak latency: Pz	552.00 ± 69.55	547.26 ± 89.16	533.16 ± 67.51	# .64
LSP average amplitude: Pz	0.01 ± 1.41	-0.67 ± 3.47	-0.18 ± 1.10	& .84

One-way ANOVA; & Kruskal-Wallis test. Latencies: milliseconds, amplitudes: microvolts. p-value for group factor.

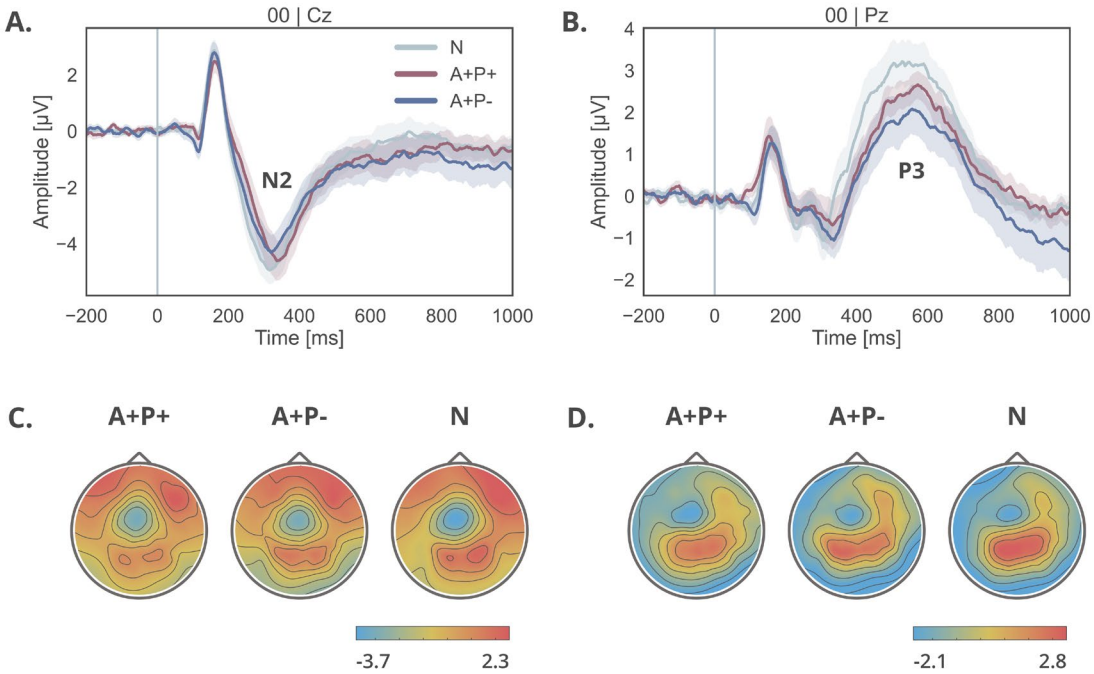

Figure 24. Event-related potentials for 00 condition. ERPs are shown with SE. A. and B. present ERPs for the Cz and Pz electrodes, respectively. C. and D. depict the topography of the N2 (200-400 ms) and P3 (400-700 ms), respectively.

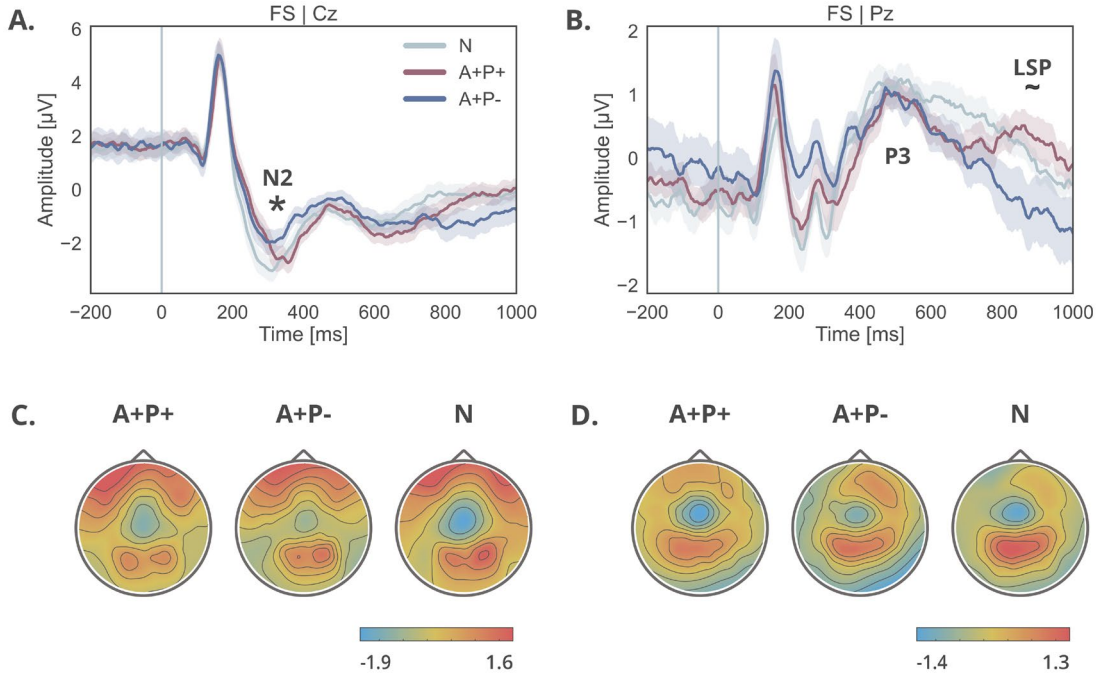

Figure 25. Event-related potentials for FS condition. ERPs are shown with SE. A. and B. present ERPs for the Cz and Pz electrodes, respectively. C. and D. depict the topography of the N2 (200-400 ms) and P3 (400-700 ms), respectively. * mark significant difference in N2 latencies.

Table 30. ERP: descriptive statistics and group differences in FS condition

Measure	Group			*p*-value
	A+P+	A+P-	N	
N2 peak amplitude: Cz	-3.37 ± 1.91	-3.30 ± 1.89	-4.17 ± 1.83	& .16
N2 peak latency: Cz	**344.76 ± 41.12**	**314.67 ± 43.62**	**305.42± 49.97**	**# < .01**
P3 peak amplitude: Pz	1.86 ± 0.99	1.91 ± 1.15	2.27 ± 1.44	& .62
P3 peak latency: Pz	524.95 ± 80.85	540.74 ± 98.17	533.68 ± 97.84	& .88
LSP average amplitude: Pz	**0.41 ± 1.17**	**-0.71 ± 2.47**	**0.20 ± 1.06**	**& .052**

One-way ANOVA; & Kruskal-Wallis test. Latencies: milliseconds, amplitudes: microvolts. The bolded font indicate a significant or trend result. *p*-value for group factor.

4.2.6.2 Brain activation patterns (fMRI)

A whole-brain fMRI analysis was conducted to identify differences in brain activation patterns between study groups during the Multi-Source Interference Task. The differences were assessed in three scenarios: specifically, during subjects' engagement in the low-demanding condition (00), specifically during their involvement in the high-demanding condition (FS), and when comparing the conditions to identify the interference effect (FS vs. 00).

First, the differences between the task conditions (00 and FS) were checked for all participants to assess whether the task was correctly implemented and executed. As can be seen in Figure 26, significant differences were detected between the task conditions in areas that are reported in the literature (as superior parietal lobule, cingulate cortex or superior frontal gyrus) (Bush & Shin, 2006; Bush et al., 2003; Deng et al., 2018; Wojciechowski et al., 2023). Detailed information is provided in Table 31 (only FDR significant clusters above > 500 voxels are shown, solely for the purpose of demonstrating task functionality).

Table 31. Regions exhibiting differences in BOLD activity between the FS and 00 conditions within the Phase II cohort.

Coordinates (x y z)	Cluster size	*p*-FDR	Cluster label (NMM atlas)
-26 -56 46	7246	< 0.001	Superior parietal lobule, Angular gyrus
38 -64 -22	3196	< 0.001	Fusiform gyrus
22 -64 58	1613	< 0.001	Superior parietal lobule
-4 8 52	1093	< 0.001	Supplementary motor area, Midcingulate cortex, Anterior cingulate cortex
34 -4 66	632	< 0.001	Precentral gyrus, Middle frontal gyrus, Superior frontal gyrus

NMM atlas: neuromorphometrics atlas (SPM12)

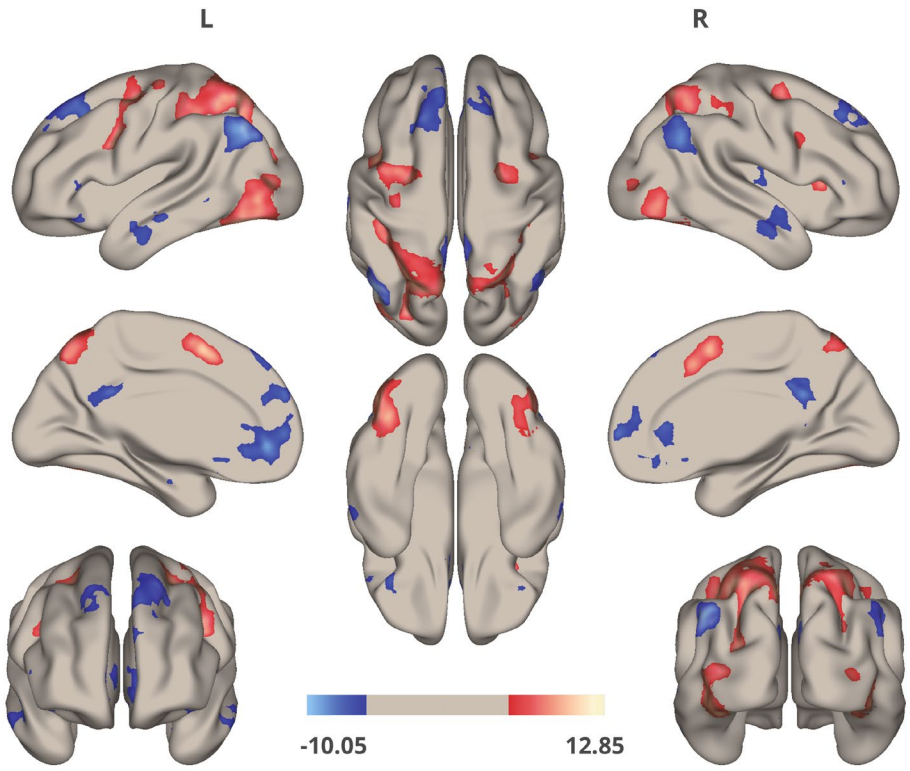

Figure 26. Brain regions involved in solving MSIT task. Contrast between multi-source conflict condition (FS, high-demanding trials) and no-conflict condition (00, low-demanding trials). The brain was visualized with the BrainNet Viewer (Xia et al., 2013).

It is important to acknowledge that accurately and meaningfully representing the information contained in three-dimensional volumetric data into two-dimensional surface representations for visualization is challenging. Here, the *most neighbor voxel* algorithm was used for mapping of group differences and *interpolated* algorithm was used for mapping of condition differences, which was chosen in regard to the size of significant clusters for better visualization (as implemented in BrainNet Viewer (Xia et al., 2013)).

No significant differences (FDR cluster level) were found when comparing the groups during high-demanding (FS) trials. Interestingly, group differences were found in low-demanding condition. A+P- group showed less activity than no-risk group (N) in the left inferior temporal gyrus, and more activity than A+P+ in supramarginal gyrus. Additionally, the interference effect (the contrast between high-demanding (FS) and low-demanding (00) conditions) seemed to be reflected in the lower activation of angular gyrus – stronger in A+P- group than in control participants. Figure 27 and Table 32 shows the results described above.

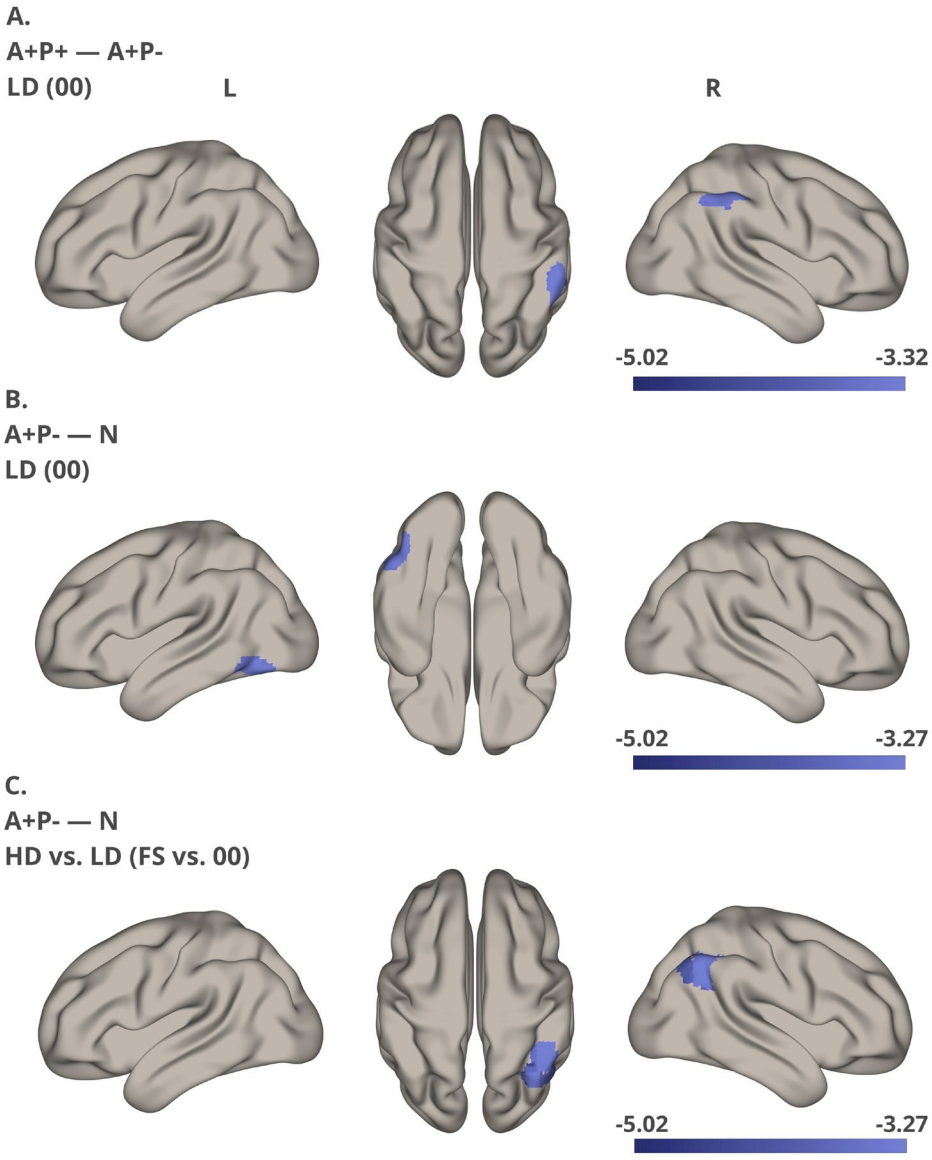

Figure 27. Differences in volumetric analysis among the study groups. The legend displays the obtained t-value. A. Contrast between A+P+ vs. A+P- group in 00 condition, lateral and dorsal views. B. Contrast between A+P- vs. N group in 00 condition, lateral and ventral view. C. Contrast between A+P- vs. N group during an interference effect (FS vs. 00 condition), lateral and dorsal view. The brain was visualized with the BrainNet Viewer (Xia et al., 2013)

Table 32. Spatial clusters (their location, size, and anatomical alignment) showing significant differences between the groups.

Groups comparison	**Condition**	**Coordinates (x y z)**	**Cluster size**	***p*-FDR**	**Cluster label (NMM atlas)**
A+P- – N	00	-50, -64, -14	123	< 0.05	Inferior temporal gyrus left (48.8%)
A+P+ – A+P-	00	56, -38, 52	150	< 0.05	Supramarginal gyrus right (55.4%)
A+P- – N	FS vs. 00	42, -54, 36	252	< 0.05	Angular gyrus right (40%)

NMM atlas: neuromorphometrics atlas (SPM12). The percentage (%) of cluster voxels within each anatomical region is provided.

5 Discussion

The following sections of discussion focus on the findings of each experiment. The results are briefly reminded, interpreted, and compared to studies concerning Alzheimer's disease patients, as well as other studies involving healthy, presymptomatic subjects. An overview of the entire project is presented in the *Summary* section.

5.1 Demographic, health, and psychometric tests

The project focused on a cohort of 200 participants during its initial phase. Following genetic screening, this cohort was sampled to form three groups with different levels of genetic risk (*APOE*/*PICALM*) for Alzheimer's disease (main experiments, Phase II). When selecting participants for Phase II, data gathered during Phase I were considered to allow for clear comparison of genetic influences on both brain activity and cognitive functions among the groups (to balance all other relevant factors as much as possible). As a result, it was anticipated that there would be no differences between the groups in measures related to demography or health, unless a specific characteristic was linked to a genetic trait. However, achieving a perfect balance was challenging due to the limited cohort. Consequently, caution should be exercised when interpreting differences in demographic, health, and psychometric measures. The slight variances identified during Phase II were also confirmed within the entire group to assess whether the subsampling introduced any bias.

The entire cohort consisted of well-functioning individuals, coming from major urban areas, professionally active, with a high level of education. Based on questionnaire scores, all participants generally exhibited good health. Moreover, a significant proportion of individuals showed no heightened risks across nearly all examined factors, e.g. the majority of participants were socially active, well-educated, professionally involved and non-smokers. The same overall characterization is relevant for the groups that were subsampled for the Phase II of the experiments. However, some characteristics revealed slight variations among the experimental groups. Single risk (A+P-) participants reported a slightly lower level of physical activity than control group. The effect was evident in both comparison levels (Phase I cohort and across the Phase II groups), validating the reliability of the

findings. However, it should be remembered that this finding is based on subjective responses to a single question. In Alzheimer's disease research, physical activity is discussed mainly in the context of its positive effects reducing probability of developing dementia in individuals at risk due to the *APOE*-ε4 genotype (de Frutos Lucas et al., 2023). Our result points to a different aspect: middle-aged *APOE*-ε4 carriers, without signs of dementia, were less likely to engage in physical activity. There were no health or body mass factors that could justify the difference. It would rather stem from psychological characteristics of participants who had also worse scores on some psychometric scales (see below). The effect was visible for single risk and not double risk group, pointing to complex interaction of *APOE* and *PICALM* genes.

More participants from A+P- group reported having a family history of dementia (first-degree relatives: parents). This effect achieved statistical significance in the Phase I comparisons within the main cohort. After subsampling participants for Phase II comparison, the difference lost statistical significance however the pattern remained the same. The higher percentage of individuals with a family history of dementia in the risk group is not surprising. Carriers of *APOE*-ε4 likely inherited the allele from their parents, who were also at risk of developing dementia (Alzheimer's Association, 2022). Interestingly, having both the *APOE*-ε4 allele and a family history of dementia poses a greater risk for AD compared to the presence of these factors alone (Huang et al., 2004). This implies the presence of additional genetic factors that, when combined with *APOE*-ε4, further elevate the risk of dementia. The *PICALM* GG variant might be involved, but our findings contradict this (at least for our study cohort). The number of participants who reported having parents with dementia in the double-risk group (A+P+) was equal to the number in the control no-risk group.

Our aim was to investigate the genetic impact on brain activity and cognitive functions in middle-aged, non-demented individuals at risk of AD. The crucial part of the study was to verify that the participants did not actually present any cognitive impairments. They performed exceptionally well on the intelligence test. The California Verbal Learning Test, which assesses verbal learning and memory, showed consistently high and comparable scores. Thus, the conducted tests objectively verified that all participants in the study exhibited a high level of cognitive function. CVLT results were previous reported for healthy, but much older, *APOE* carriers who either did not differ from no-risk groups (Lim et al., 2013) or demonstrated a higher frequency of CVLT recall intrusion errors (Peavy et al., 2007). In the latter case 13% of participants would develop dementia within following 6 years. This means that "healthy" *APOE* group in this research actually included substantial number of early/prodromal AD patients. This might have biased the comparison because individuals with Alzheimer's disease and Mild Cognitive Impairment tend to perform poorly on the CVLT task compared to controls (Greenaway et al., 2006).

Despite the absence of clear cognitive impairment, the subjects displayed group differences in specific psychological characteristics. Participants with a single risk factor (A+P-) in the Phase II comparison, on average, demonstrated poorer psychological well-

being compared to the participants in the no-risk group. They exhibited lower self-esteem, higher scores on BDI scale (related to depression and lowered mood), heightened levels of neuroticism, and a tendency to employ less effective stress coping strategies. It is important to highlight that the A+P+ group did not exhibit any notable differences from the no-risk group (N) in these specific measures. These differences achieved statistical significance when considering all subjects in the study (Phase I) only for neuroticism. It is well established that factors such as depression, lowered mood or neuroticism act as risk factors for Alzheimer's disease and in some cases may interact with *APOE* in provoking disease (Alzheimer's Association, 2022; Armstrong, 2019; Milligan Armstrong et al., 2021; Peavy et al., 2007; Silva et al., 2019). Although, not all studies found an association between the *APOE* and depression or neuroticism (Surtees et al., 2009). All these psychological symptoms can be caused by prolonged stress which by itself also was described as a risk factor (Machado et al., 2014; Milligan Armstrong et al., 2021). Particularly, stress in midlife was reported to be associated with development of dementia in late life (Johansson et al., 2010). While there are studies connecting a specific personality traits to Alzheimer's disease risk (Low et al., 2013; Wang et al., 2009), it remains challenging to provide a biological or genetic explanation for why this particular risk group (A+P-) would exhibit these psychological traits. A more plausible explanation may be associated with the higher reported incidence of a family history of dementia within this specific group. Caring for someone with Alzheimer's disease can be an emotionally and physically demanding role, often leading to significant stress and mental exhaustion for caregivers (Alzheimer's Association, 2022). Individuals responsible for caregiving are at a higher risk of experiencing depression and anxiety when compared to those without such responsibilities, which is supported by findings from meta-analysis studies (Ma et al., 2018). Certain psychological features can induce changes in specific brain activity, thus the described characteristics can serve as crucial factors that influence the neuroimaging results obtained for the A+P- study group in Phase II of the experiment.

5.2 Blood counts and miRNA

Most blood parameters showed no differences between the control and risk groups. No differences were detected in lipid profile, despite the fact that *APOE* functions are primarily associated with lipid transport and metabolism (Huang & Mahley, 2014; Mahley, 1988). On the other hand, variations were observed in the profile of erythrocyte hemoglobin content/concentration and eosinophil levels. The A+P- group exhibited higher levels of mean corpuscular hemoglobin (MCH) and mean corpuscular hemoglobin concentration (MCHC) compared to both other groups, along with a trend toward lower values in red blood cell

distribution width (RDW-CV) in comparison to the A+P+ group. The A+P+ group exhibited a tendency toward elevated eosinophil values in comparison to the N group.[1]

Elevated levels of eosinophils are typically associated with asthma, allergic reactions or parasitic infections (Tao et al., 2022). Individuals diagnosed with these conditions typically exhibit eosinophil levels higher than the normal range. In this study, no excessive health problems that could account for eosinophil differences were identified in any of the studied groups. Moreover, all results regarding the eosinophil levels were within normal laboratory range. Eosinophil production is stimulated by interleukin-3 (IL-3), a cytokine released in the brain – just like *APOE* – by astrocytes (Tao et al., 2022), and its level is elevated in Alzheimer's disease patients carrying *APOE* related risk (Soares et al., 2012). Analysis of the Chinese Alzheimer's Biomarker and Lifestyle (CABLE) database indicated that peripheral eosinophil were elevated in elderly individuals who were defined as positive for CSF AD biomarkers (Aβ42 and p-tau) (Zhang et al., 2022). Notably, eosinophil count demonstrated an upward trend with increasing burden of these biomarkers, but there was no interaction between any of the peripheral immune cells with *APOE*-ε4 (Zhang et al., 2022). Interestingly, symptomatic AD patients seems to have lower levels of eosinophils (Chen et al., 2017; Järemo et al., 2013). This may suggest the emergence of a mild subclinical low-grade systemic inflammation process (Holmes et al., 2009; Xie et al., 2021) in individuals with higher disease risks. A conclusive answer may emerge through the longitudinal observation of our cohort.

Due to the brain's substantial oxygen requirements, accounting for nearly 20% of the body's oxygen supply, multiple studies have focused on cellular respiration processes and oxidative stress as potential mechanisms underlying neurodegeneration. The erythrocytes play a crucial role in tissue oxygenation and they are linked to Alzheimer's pathology (Wojsiat et al., 2017). Research on erythrocyte hemoglobin content in Alzheimer's patients has yielded conflicting results, with some studies suggesting a decrease (Faux et al., 2014) and others proposing an increase (Chen et al., 2017). However, no studies have explored the correlation between erythrocyte features and Alzheimer's risk genes in the general healthy population. In our risk group (A+P-), we observed a slight elevation in MCH/MCHC, both falling within normal laboratory norms. These findings may indicate a mild dysregulation in hematopoiesis, possibly linked to vitamin deficiency. It is plausible that individuals in the A+P- group exhibiting worse psychological health may also have an unhealthy diet. Unfortunately, we did not collect dietary information or conduct objective assessments of vitamins, micro, and macronutrients through blood tests.

Changes in the levels of microRNAs in the blood have been demonstrated to effectively distinguish individuals with Alzheimer's disease from control subjects (Nagaraj et al., 2017, 2019). As a result, we examined the levels of circulating miRNAs associated with AD, as

[1] The analysis and discussion of the blood count findings from this project have already been published, with a particular emphasis on the comparisons between *APOE* carriers and non-carriers (Dzianok & Kublik, 2023)

identified in previous studies (Nagaraj et al., 2017, 2019). Our findings revealed a downregulation of miR-29b-3p in the A+P- group compared to both control (N) and double-risk (A+P+) groups. Importantly, the results for the A+P+ group were indistinguishable from those of the N group. The miR-29 family potentially plays a role in neuroprotection and neuroinflammation (Li et al., 2023). No alterations were observed in the other selected miRNAs within the panel. Evidence consistently indicates the downregulation of miR-29b-3p in the blood of Alzheimer's disease patients across various studies (Leidinger et al., 2013; Nagaraj et al., 2019; Satoh et al., 2015). Research has also demonstrated an association between levels of miR-29b-3p and cognitive performance, specifically in the domains of visual processing and sustained attention, among the healthy population, particularly in young individuals, irrespective of genotype (Marttila et al., 2021). Notably, this effect was primarily observed in the rapid visual information processing (RVP) test, which involves executive attention and working memory, two cognitive domains known to be impaired in AD (Marttila et al., 2021). Our project is in fact the first to present comparable results in healthy middle-aged subjects.

5.3 Cognitive tasks (neuroimaging and behavior)

A diagnosis of cognitive functions in clinical settings is based on standardized questionnaires of which we used two adequate for non-demented population: RPM and CVLT. The participants achieved high scores in both. We also asked participants to perform more challenging, computer based cognitive tests aimed at measuring subtle nuances of memory (STM) and conflict-related/attentional task (MSIT). Neuroimaging data collected during the tests and the results of behavioral assessments were analyzed to identify any noticeable differences between genetic groups. Performance was consistently high in both tasks, with no differences detected between risk carriers and non-carriers in response accuracy. However, a slight yet consistent difference was found in reaction times. The A+P- group displayed a subtle prolongation of reaction times, particularly during challenging conditions in both tasks (STM on a trend level). Task performance is negatively affected by aging (Gorus et al., 2008; Hardwick et al., 2022; Porciatti et al., 1999), in a continuous process over the lifetime (Fozard et al., 1994). However, if the observed changes were solely related to age, they should affect all participants, not just those who were assigned to A+P- group. This phenomenon, thus, might be a non-pathological characteristic, representing a stable trait associated with the *APOE*-ε4 variant, which was modulated by the *PICALM* risks. Previous studies suggested that among older individuals without dementia, the ε4 variant adversely affects cognitive performance, specifically impacting episodic memory and executive functioning (Gharbi-Meliani et al., 2021; Small et al., 2004; Wilson et al., 2002). The effects are more pronounced and, in some studies, only observable in individuals who are homozygous carriers of the ε4 variant (Engel et al., 2020). Here, it is important to remind the resource modulation and the pleiotropic hypotheses (described in the *Introduction*). Therefore, studies demonstrating improved cognitive performance in young carriers of

APOE-ε4 do not contradict later cognitive decline (Jochemsen et al., 2012; Mondadori et al., 2006; Rusted & Carare, 2015). In the case of AD patients, their reaction times are notably prolonged when compared to healthy individuals (Gordon & Carson, 1990; Gorus et al., 2008; Medina et al., 2021). Some studies have also identified trend-level worsening of performance associated with the *PICALM* GG genotype in patients with Mild Cognitive Impairment (the same study did not observe any effect of *APOE* risk alleles) (Cruz-Sanabria et al., 2021). The subtle increase in reaction time, evident only in challenging and attentionally demanding conditions, carries potential diagnostic implications. While this phenomenon may go unnoticed in everyday activities, our findings demonstrate that it can differentiate the risk groups in controlled laboratory tests. The reaction times of the MSIT task successfully differentiated individuals at risk from those not at risk, despite the facts that the groups exhibited similar performance on the RPM/CVLT tests. Using multiple tasks or tests in the study of non-demented populations has been demonstrated to be more effective than relying on a single test for predicting the subsequent development of Mild Cognitive Impairment (Gustavson et al., 2020). It is crucial to start using diagnostic paradigms that concentrate not only on the content of memory but also on the dynamics of cognitive processing. It was shown that performance in tasks involving cognitive challenges can be regarded as a preclinical marker in AD (Gorus et al., 2008; Medina et al., 2021).

Comparable accuracy levels were observed for all groups, despite the increase in response times and visible differences in the brain activity (such as EEG slowing, slight network disruption, and ERP results). This suggests that individuals at risk possess a cognitive reserve significant enough to enable them to perform the task at a level similar to those without the risk. Despite (or perhaps because) of a double genetic risk, the reserve appears to be more effective in A+P+ participants, as they exhibited no decline in response speed.

Comments on the stability of RT results in EEG and fMRI sessions are necessary. Longer response times in A+P- participants showed significance for challenging tasks during EEG sessions but not for tasks performed in fMRI. We attribute this difference to the specificity of experimental settings. EEG recordings were conducted in a seated position and participants used standard keyboard, providing a comfortable and ergonomic environment. During fMRI session, participants lied down and used an unfamiliar fMRI-dedicated response pad, which they did not see as their hands were positioned on the abdomen. This less comfortable environment contributes to a general rise in reaction times in fMRI (Foucher et al., 2008) as opposed to EEG. The differences between study groups became smaller in a scanner and significance was not reached. However, the observed pattern of RT mirrored that of the EEG results.

Event-related potentials are electrical brain responses that occur in the EEG following the presentation of a stimulus. These responses can be time-locked to the onset of a specific event, and they reflect the brain's electrical activity associated with the processing of that event. Similarly, as for the response time results, no differenced in ERPs were noted among

the groups in the easy (low-demanding) condition. However, significant differences were found in the FS (high-demanding) condition of the MSIT task. There was an increase in N2 latency in the A+P+ group when compared to the N and A+P- groups. Additionally, the late sustained potential (LSP) component distinguished between the groups (A+P+ and A+P-), with the A+P+ group exhibiting the highest amplitude and the A+P- group displaying the lowest amplitude out of all three groups. Both, reduction of N2 amplitude and its delayed latency were described in individuals with Mild Cognitive Impairment (Cid-Fernández et al., 2014) and in AD patients (O'Mahony et al., 1996). Healthy adults carrying the *APOE*-e4 allele have been previously demonstrated to have prolonged N2 latencies, and these alterations were predictive of subsequent decline in verbal learning abilities (Espeseth et al., 2009). N2 is believed to reflect conflict monitoring processes (Folstein & Van Petten, 2008; Heidlmayr et al., 2020), and LSP can follow N2 in cognitive control/conflict tasks and reflect the conflict resolution processes and response selection (Heidlmayr et al., 2020). The prolonged N2 component could potentially delay response selection and reaction time. However, this is not observed in our results. Participants with a double risk exhibited delayed N2, yet their reaction times were identical to those in the control group. The results from our ERP analysis, coupled with RTs, reveal intriguing patterns in the cognitive processes involved in conflict resolution among middle-aged individuals with *APOE*/*PICALM* risks. In A+P+ participants, a compensatory mechanism is triggered, maintaining a normal level of speed responses without sacrificing accuracy. Single risk participants employ a distinct mechanism. In this group, diminished attentional control during late task monitoring is counterbalanced by prolonged response selection and execution.

Regarding the fMRI during the execution of the MSIT task, our first step was to confirm the accurate programming of the task and to determine if there were significant differences between the easy and difficult conditions. To accomplish this, we initially compared task conditions (00 vs. FS) (for the entire cohort). We obtained the same results as those documented in the literature for this specific task, confirming the task reliability (Bush & Shin, 2006; Bush et al., 2003; Deng et al., 2018; Wojciechowski et al., 2023).

Surprising outcomes were revealed when comparing studied groups, indicating group differences in the 00 (low-demanding) rather than the FS (high-demanding) condition. The A+P- group exhibited lowered activation in the left inferior temporal gyrus compared to the no-risk (N) group, while A+P+ group had decreased activation in the right supramarginal gyrus compared to the A+P- group, during execution of low-demanding MSIT condition. Additionally, the interference effect (FS vs. 00) is related with decreased activation of the angular gyrus, and this effect is more pronounced in A+P- participants compared to the control group. Angular gyrus is a part of DMN and its deactivation during tasks resolution is consistent across different studies (Seghier, 2013). Here, stronger deactivation in high-demanding condition (assessed through FS vs. 00 comparison) was more pronounced in A+P- group, probably reflecting a compensatory brain mechanisms. These effects could be associated with a larger brain/cognitive reserve, as indicated by the consistent maintenance of accuracy levels in the 00 condition across all groups, which is observed despite distinct

brain activation patterns in the at-risk group when compared to the N group. Interestingly, the three regions we have identified as influenced by genetic risk – the angular gyrus, inferior temporal gyrus, and supramarginal gyrus – are integral components of the cortical signature associated with Alzheimer's disease (Dickerson et al., 2009). This alignment emphasizes the strength of our findings and their significance in relation to possible early detection of AD predictive features.

These results are also connected to our hypothesis (which is based on the literature on AD), suggesting alterations in the default mode network (DMN) among at-risk groups. The DMN involves multiple brain regions, and the activation of specific areas may vary across different studies – however, the activation of angular gyrus is consistently reported. Moreover, the functions of the angular gyrus are associated with perception, attention, and spatial cognition (Seghier, 2013).

5.4 Cortical thickness

Gray matter atrophy constitutes a fundamental symptom of Alzheimer's disease. The cortical signature of AD encompasses nine regions, five of which (parahippocampal gyrus, supramarginal gyrus, temporal pole, superior parietal lobule, and inferior temporal gyrus) are typically also affected in patients with Mild Cognitive Impairment (MCI) (Bakkour et al., 2009; Dickerson et al., 2009; Verfaillie et al., 2016).

We assessed cortical thickness in these five regions listed above (in both hemispheres). The A+P- group exhibited reduced thickness in comparison to the N group in one specific region – the right temporal pole. On average, this difference was about 0.12 mm, constituting half of the typical difference (~0.25 mm) observed between individuals with Alzheimer's disease and healthy individuals (Dickerson et al., 2009). Alterations in the temporal pole were observed also in patients with MCI (Iannopollo et al., 2021) and asymptomatic individuals with amyloid positivity (Dickerson et al., 2009). The temporal pole, along with the inferior temporal gyrus, inferior parietal areas (supramarginal and angular gyri), posterior cingulate, and precuneus, are among the regions that are early affected in the course of Alzheimer's disease (Arnold et al., 1991; Van Hoesen et al., 1986). Moreover, certain studies have specifically concentrated on characterizing the temporal pole as one of the most adversely affected regions in Alzheimer's disease (Arnold et al., 1994). Patients with AD exhibit notable atrophy in this area, with primary neuronal loss observed in layers III and V and neurofibrillary tangles identified in layers II, III, V, and VI (Arnold et al., 1994). Individuals with Alzheimer ' s disease and Mild Cognitive Impairment who carry the *APOE*-ε4 allele often show reduced volume in various brain areas and reduced cortical thickness, e.g. in amygdala, hippocampus, or entorhinal cortex (Liu et al., 2010; Mattsson et al., 2018; Zhang et al., 2020). In a study investigating the interaction of *APOE* and *PICALM* genotypes in individuals with AD, alterations in prefrontal cortex volume and worse cognitive

performance were observed in group having double risk (*APOE*-ε4 and *PICALM* GG) (Morgen et al., 2014).

The literature has previously explored changes in cortical thickness or volumes of specific brain areas in healthy *APOE* carriers; however, the findings are not consistently conclusive and present conflicting results. Some studies show that elderly *APOE*-ε4 carriers have reduced cortical thickness or reduce brain volumes in selected areas in comparison to non-carriers (Fan et al., 2010; Régy et al., 2022) while other studies show no such differences (Bunce et al., 2012), see Fouquet et al., 2014 for extensive review). On the other hand, another study showed that *PICALM* A carriers (healthy controls, MCI and AD patients) exhibited a decreased cortical thickness in selected areas compared to those carrying the risky G allele (Wu et al., 2022). These findings align closely with ours, as the reduced thickness was only observed in the A+P- group (comprising *APOE*-ε4 carriers with a neutral *PICALM* A allele), and not in the double-risk group (A+P+).

5.5 Brain activity at rest

The EEG reflects the collective neural activity of the entire brain, with primary input of the postsynaptic potentials of cortical pyramidal neurons, with significant contributions from various other cell types and populations, including those in subcortical regions (Buzsaki, 2006). Accurate interpretations of the origin of EEG signal are challenging without the source analyses. Our findings were analyzed at the sensor level, thus the discussion will center on the dynamics of EEG signal.

We identified two EEG features believed to be prominent and sensitive EEG markers associated with AD. Double risk carriers (A+P+ group) compared to N and A+P- groups showed the “slowing of the EEG” (higher delta and lower alpha relative power) and a decreased signal complexity. Given the documented correlation between the slowing of EEG and reduced complexity (Dauwels et al., 2011), our discussion encompasses both of these findings together. The reduction in signal complexity was proposed to be linked to factors such as neuronal loss and decreased levels of acetylcholine (Jeong, 2004). The “EEG slowing” is also believed to be associated with neuronal loss, axonal pathology, and cholinergic deficits, all of which impact functional connections in the cortex (Jeong, 2004). The hypothesis is further supported by evidence that cholinergic drugs have a tendency to reverse “EEG slowing” (Agnoli et al., 1983; Jeong, 2004). Conversely, anticholinergic drugs, such as scopolamine, which block post-synaptic receptor stimulation, induce “EEG slowing” (Agnoli et al., 1983; Ebert et al., 2001; Jeong, 2004). This provides additional support for the link between cholinergic function and EEG dynamics. The administration of acetylcholinesterase inhibitors has been associated with a reduced deterioration of EEG changes in (some, but not all) AD patients (Babiloni et al., 2006; Rodriguez et al., 2002).

Furthermore, AD patients who are *APOE*-ε4 carriers exhibit more severe cholinergic deficits compared to those with a neutral *APOE* genotype (Soininen et al., 1995).

Higher complexity in brain signals is typically linked to a greater capacity for information processing in contrast to less complex and more predictable signals. In Alzheimer's disease, reduction in complexity is clearly visible and it affects the temporal-occipital regions (Smits et al., 2016). Power perturbations within the temporal and parietal areas have been identified as particularly sensitive for distinguishing Alzheimer's disease patients from healthy controls (Durongbhan et al., 2019). Furthermore, the neuronal loss in AD firstly manifests in the temporal and parietal areas. Upper alpha power (10-13 Hz) has been previously demonstrated to be reduced in other neurodegenerative diseases, such as Parkinson's disease (Benz et al., 2014). Additionally, upper alpha power, but not lower alpha, distinguish between AD patients and controls (Moretti et al., 2004). The occurrence of "EEG slowing" in individuals with AD is modulated by the *APOE* genotype, yielding varied findings. Some studies indicate that *APOE*-ε4 carriers exhibit more pronounced effects (Lehtovirta et al., 2000), while others suggest the opposite trend (de Waal et al., 2013). These conflicting results underscore the complexity of the relationship between *APOE* genotype and "EEG slowing" in AD patients. Regarding the *PICALM* genotype, one study identified an impact on EEG relative power and entropy in patients with Alzheimer's disease, but not in healthy individuals (Maturana-Candelas et al., 2021). Nevertheless, the decline in complexity is also visible during aging and typically begins around the age of 60, with a notable impact on central-parietal areas, predominantly on right-shifted clusters (Smits et al., 2016).

5.5.1 Brain connectivity

Coherence is one of several methods used to evaluate functional connectivity within the EEG signal. It quantifies the consistency of phase relationships among EEG signals within specific frequency bands. The groups did not show significant differences in connectivity, as assessed by EEG coherence at the FDR-corrected level. The subtle trends observed in uncorrected differences between the groups are minor, with the maximum difference being 0.18 on a coherence scale ranging from 0 to 1. Since there are no FDR-corrected differences, it is not possible to draw definitive conclusions about changes in connectivity at this level. It remains unclear whether the absence of an evident effect is due to the study's low statistical power, considering the potential low effect size given the slight differences in coherence, or if there are indeed no changes at the level of EEG connectivity.

The uncorrected findings suggested a more pronounced decrease in alpha coherence for both the A+P+ and A+P- groups in comparison to the N group. Additionally, there was an increased delta coherence (for most connections) in the A+P+ group compared to both the A+P- and N groups. Despite acknowledging the limitations associated with the weak statistical power of these effects, we find these results noteworthy as they align with patterns

frequently observed in Alzheimer's disease research. A recent systematic review (Fischer et al., 2023) revealed that, among 34 studies comparing patients with Alzheimer's disease to healthy controls, 24 studies found a significant decrease in coherence within the alpha band. The reduction in coherence within the alpha band is also apparent in the early stages of Alzheimer's disease when combined with the *APOE* risk factor (Canuet et al., 2012). Similar effect was observable for *PICALM* genotype, where *PICALM* GG carriers exhibited lower widespread connectivity of alpha sources compared to AA/AG carriers (Ponomareva et al., 2020). However, the consistency of results in coherence within lower frequencies (< 7 Hz) was less pronounced, with fewer changes reaching statistical significance (Fischer et al., 2023). Generally, delta and theta coherences show a trend to increase in AD patients when compared to matched controls (Meghdadi et al., 2021).

However, when examining the fMRI signal and employing a connectivity analysis (ICA based approach), certain alterations were observed among the study groups. In this analysis, our primary focus was on the independent components partially linked to the default mode network, as this network is frequently demonstrated to be impaired in Alzheimer's disease patients (Damoiseaux, 2012; Vemuri et al., 2012). The A+P- group demonstrated notably higher network strength in various clusters, including areas of the DMN, such as the posterior cingulate cortex and precuneus, compared to the N group. Concurrently, the A+P- group exhibited also significantly lower strength of a smaller cluster encompassing the right temporooccipital part of the middle temporal gyrus (not considered as a core component of the DMN), in contrast to the N group. Participants at double risk (A+P+) did not exhibit any differences in the DMN compared to the control group but showed reduced network strength compared to the A+P- group in other areas, such as the anterior cingulate cortex (ACC), within independent components functionally linked with DMN. Thus, the A+P+ and A+P- genotypes seems to independently affect functional brain networks. Disruptions within ACC are interesting, as this area is linked to higher-level cognitive processes and plays a crucial role in executive functions that are disrupted in LOAD. Research has consistently indicated decreased connectivity within the posterior DMN in AD patients, individuals with MCI, and older adults with amyloid burden, and recently – an increased connectivity within the frontal parts of DMN (Damoiseaux, 2012; Vemuri et al., 2012). Regarding research on healthy *APOE* carriers, certain studies have revealed decreased connectivity within the posterior DMN in older (70-89 years old) *APOE*-ε4 carriers when compared to non-carriers (Machulda et al., 2011), no effect in middle-aged adults (Dowell et al., 2016), and opposite effects in younger healthy adults (Dowell et al., 2016; Filippini et al., 2009). These seemingly contradictory findings align with the resource-modulation and antagonistic pleiotropy hypotheses and indicate an age-related pattern, with greater disruptions observed in older age and enhanced brain function in younger individuals. Our middle-aged groups falls in the middle of this axis, so depending on the impact of various factors, they may show either still increased connection strength (as in young people) or already worse connection strength (as observed in older individuals). Our study also partially corroborates the findings of Cacciaglia et al., who found that the *APOE*-ε4 allele was related to “higher structural covariance” in a network encompassing similar areas to those shown in our results

(Cacciaglia et al., 2020). Additionally, ACC has been shown to have greater connectivity in the salience network in *APOE*-ε4 healthy, older carriers compared to non-carriers (Machulda et al., 2011).

It is crucial to remember that functional connectivity does not imply direct anatomical connections between brain regions; rather, it reflects the statistical associations or synchronization of their activities. Further research is needed to gain a comprehensive understanding of the mechanisms underlying genotype-related alterations in functional connectivity.

5.6 Overview of the potential *APOE* & *PICALM* interaction

The observed pattern of differences between the groups in our study not only demonstrated that risk genes impact the functioning of middle-aged carriers but also suggested that *PICALM* influences or modifies the effects associated with the *APOE*-ε4 genotype in a non-obvious manner. Our original hypothesis assumed that observed effects would scale up proportionally with the risk burden. Most (but not all) of our results show the opposite – participants with double risk (*APOE*-ε4 and *PICALM*-*GG*) were less different from no-risk group than single *APOE*-ε4 risk carriers.

The genetic interaction between the *APOE* and *PICALM* genes have been confirmed in GWAS studies (Jun et al., 2010). However, the functional impact of both genes has not been earlier evaluated in healthy adults. The only one study also examining the polymorphisms of *APOE* and *PICALM*, but in a cohort of Alzheimer's disease patients, revealed that the combination of *PICALM* GG and *APOE*-ε4 had an adverse impact on the volume of prefrontal areas and decreased performance in tasks associated with processing speed and working memory (Morgen et al., 2014). Some other studies investigating the role of the *PICALM* gene reveal unfavorable outcomes for individuals carrying the A allele, compared to carriers of GG allele, such as reduced cortical thickness in specific regions (Wu et al., 2022). Similar observation, with the preserved function in individuals with A+P+ (carrying *PICALM* GG alleles), as opposed to those with A+P- (carrying *PICALM* A alleles), was repeated several times in our study, regarding prolonged reaction times, miRNA down-regulation, reduced thickness or altered brain activation during mental effort.

This phenomenon might be partially explained by the concept of greater brain resilience, attributed to either cognitive or brain reserves (as outlined in the *Introduction* section). It is plausible that the brain adapts to challenges induced by carrying risk alleles over the course of life, making it easier for participants at this stage to handle complex cognitive tasks. Their (A+P+) neuronal circuits may have already shifted to compensate for some (already, in middle-aged population) long-lasting disruptions. Research has demonstrated that individuals with higher cognitive reserve may exhibit more severe neuropathology and greater disruption within brain integrity (Soldan et al., 2020). It is noteworthy that all proxies

for cognitive reserve, such as IQ, education, or occupation status (Opdebeeck et al., 2016; Song et al., 2022), were examined in this study, and they did not differentiate the groups. However, physical activity can enhance cognitive reserve (Song et al., 2022). In this context, only the A+P- group (and not A+P+) was characterized by subjectively lower physical activity than the no-risk group, although this measure relied on only one subjective question. Generally, the cognitive reserve in this cohort must be above average, with participants predominantly having higher education, being professionally active, and coming from large cities. In fact, the better results (for some, but not all, measures) observed in the A+P+ group compared to the A+P- group ("better" simply as compared to patterns similar to those seen in AD patients), might be attributable to the compensatory mechanism recruitment hypothesis (Han & Bondi, 2008). According to this hypothesis, healthy *APOE*-ε4 carriers engage additional brain resources to address initial cognitive decline. Moreover, ε4 carriers can predominantly recruit right brain regions, primarily frontal areas, as a compensatory strategy to sustain cognitive performance (Han & Bondi, 2008). We have shown that this may be modified by the *PICALM* risk.

It is well-established that both *APOE* and *PICALM* contribute to the Aβ pathology (described in *Introduction*). Some of the effects of these genetic factors on brain function and structure may be then partially dependent on Aβ deposition. However, we did not measure Aβ or phosphorylated tau in our cohort. Therefore, it is unclear which observed patterns may be partially linked to these pathological hallmarks. It is also established that *APOE* influences the brain and health over the lifespan in ways independent of Aβ deposition, demonstrating its effects even in young individuals (Fernandez et al., 2019; Jochemsen et al., 2012; Mondadori et al., 2006; Rusted & Carare, 2015). Different gene-gene interactions, as studied within our cohort (*APOE-PICALM*), and gene-environment interactions are likely modulating the effects of genetic variations on health, brain structure, and function.

In summary, this study not only emphasizes the influence of *APOE* and *PICALM* on cognitive function and health but also underscores the intricate and dynamic interplay between these genetic factors, a complexity challenging to interpret.

6 Summary and conclusion

The project aimed to investigate whether middle-aged individuals with a genetic predisposition for late-onset Alzheimer's disease exhibit any alterations in health, brain function, and cognitive abilities when compared to control group without such genetic risk. An extensive study was conducted with blood tests, multiple psychological and cognitive questionnaires, EEG and MRI neuroimaging at rest and during cognitive tasks. Some differences were identified between individuals with various alleles of *APOE* and *PICALM* genes in brain related measures, psychological and cognitive aspects and in blood tests results. Most of our experiments replicated some of the findings described in literature as characteristic for individuals with Alzheimer's disease (Figure 28). The results indicated that the functioning of the organism, including the brain, is influenced by the *APOE* and *PICALM* genes in middle-aged individuals who may be predisposed to developing dementia. Figure 28 provides a simplified summary of the studied measures and indicates which of them were impacted in the single (A+P-) and double (A+P+) risk group. Table 33 lists two additional measures, that cannot be easily summarized on a AD-risk axis.

To sum up the results and the discussion:

— Examining the functions of Alzheimer's disease risk genes in healthy populations can enhance our understanding of the disease (including its origin and progression), facilitate early detection and diagnosis through risk assessment, accelerate and improve prevention and early therapeutic strategies, potentially accelerate the drug discovery by comprehending the roles of genetic variants, and influencing public health by prompting changes in policies and strategies, as well as the design of screening programs.

— There is still much to uncover regarding the risks related to *APOE* and other genes. It is essential to gain a clear understanding of the interactions between risk genes, especially the simultaneous influence of *APOE* and *PICALM* on both health and brain function. Further research is required to fully comprehend why certain effects are modulated by the *PICALM* gene in *APOE* carriers.

— In practical terms, in the future, a comprehensive model integrating *APOE* and *PICALM* genetic information, cognitive performance, neurobiological measures (including neuroimaging), and blood-based biomarkers, could demonstrate superior predictive accuracy in identifying individuals at an increased risk of progressing to clinical stages of Alzheimer's disease compared to models based on individual factors alone. In fact, it was shown that machine/deep learning algorithms utilizing EEG resting-state features have demonstrated a remarkable ability to classify Alzheimer's disease patients versus controls, achieving high accuracies such as 99% (Durongbhan et al., 2019). The transition of these advancements from basic science to practical applications in real-world scenarios, particularly in public health, poses a substantial challenge that must be addressed for widespread implementation.

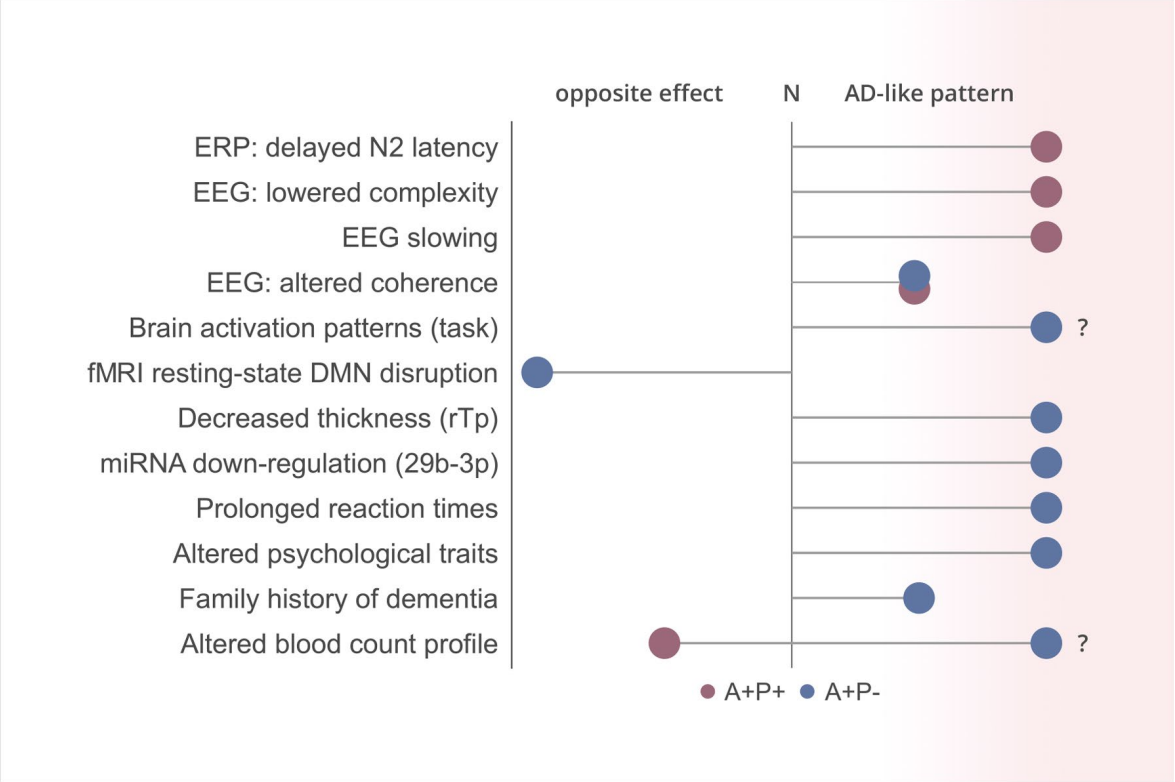

Figure 28. Results summary, listing the effects observed in single (A+P-) and double (A+P+) risk groups that are either in line with AD-like patterns (as indicated by the literature), or are opposite. Differences at the trend level are denoted with half-lines. A question mark near a specific feature (?) indicates inconsistency (or lack) of results in the literature regarding AD patients. rTp – right temporal pole.

Table 33. Results summary: additional weaker effects observable in the study

Experimental measures	**Observed effect**	
Low physical activity	A+P- < N	--
Altered LSP amplitude	A+P+ > A+P-	~

~ – trend-level difference. -- – based on one subjective question.

6.1 Limitations and future perspectives

There are certain limitations of the described study that should be addressed when planning next research, including:

a. Comparing the obtained results to additional A-P+ group, which was not tested during this research in the Phase II of the experiments.

b. Increase the number of enrolled participants in the study to obtain larger statistical power, and therefore more robust results (which requires ensuring adequate funding).

c. Use the multivariate statistics approach of testing the genetic influence on stated markers and study the genes interactions (which would be possible only when points a. and b. will be fulfilled). Study groups were predefined during the study design stage. As for the fact that we have choose three groups to study (N, A+P+, A+P-), the variables of single gene-factors (A+/A- and P+/P-) are a linear combination of each other and such in-depth analysis with use of multivariate design was not possible

d. Another limitation (which, however, can be considered as strength), lies in the methodology's focus solely on two selected risk genes rather than encompassing the broader spectrum of genetic changes associated with Alzheimer's disease (as this is a polygenic diseases). However, this approach allowed the comparison of the studied traits mainly in terms of the selected two genes (this enabled direct comparisons, without the impact of other factors), which are among the strongest genetic risk factors for Alzheimer's disease, and still their functions and effects on brain function are not well understood. A recent trend in studies, including GWAS (Mukherjee et al., 2020), is to categorize affected individuals into biologically cohesive groups with shared characteristics (which was employed in this study). This approach aligns with the concept of personalized medicine and is particularly recommended for research on neurodegenerative diseases (Cholerton et al., 2016; Girard & Rouleau, 2014).

e. The results represent group level data, often indicating statistical trends, but they do not convey information about the specific risk for each individual participant. There was significant variability in results across all measures, with instances of overlap between individuals from at-risk and no-risk groups. Currently, we lack knowledge regarding which subjects from the study will eventually develop MCI or dementia due to AD. To address this uncertainty, future longitudinal studies are essential.

References

1. Agnoli, A., Martucci, N., Manna, V., Conti, L., & Fioravanti, M. (1983). Effect of cholinergic and anticholinergic drugs on short-term memory in Alzheimer's dementia: a neuropsychological and computerized electroencephalographic study. *Clinical Neuropharmacology*, *6*(4), 311–323.
2. Al-Nuaimi, A. H. H., Husseen Al-Nuaimi, A. H., Jammeh, E., Sun, L., & Ifeachor, E. (2018). Complexity Measures for Quantifying Changes in Electroencephalogram in Alzheimer's Disease. In *Complexity* (Vol. 2018, pp. 1–12). https://doi.org/10.1155/2018/8915079
3. Altman, N., & Krzywinski, M. (2016). Analyzing outliers: influential or nuisance? *Nature Methods*, *13*(4), 281–282.
4. Alzheimer's Association. (2022). 2022 Alzheimer's Disease Facts and Figures. *Alzheimer's & Dementia*, *18*(4), 700–789.
5. Ando, K., Nagaraj, S., Küçükali, F., de Fisenne, M.-A., Kosa, A.-C., Doeraene, E., Lopez Gutierrez, L., Brion, J.-P., & Leroy, K. (2022). PICALM and Alzheimer's Disease: An Update and Perspectives. *Cells* , *11*(24). https://doi.org/10.3390/cells11243994
6. Andrew, M. K., & Tierney, M. C. (2018). The puzzle of sex, gender and Alzheimer's disease: Why are women more often affected than men? *Women's Health* , *14*, 1745506518817995.
7. Armstrong, R. (2019). Risk factors for Alzheimer's disease. *Folia Neuropathologica / Association of Polish Neuropathologists and Medical Research Centre, Polish Academy of Sciences*, *57*(2), 87–105.
8. Arnold, S. E., Hyman, B. T., Flory, J., Damasio, A. R., & Van Hoesen, G. W. (1991). The topographical and neuroanatomical distribution of neurofibrillary tangles and neuritic plaques in the cerebral cortex of patients with Alzheimer's disease. *Cerebral Cortex* , *1*(1), 103–116.
9. Arnold, S. E., Hyman, B. T., & Van Hoesen, G. W. (1994). Neuropathologic changes of the temporal pole in Alzheimer's disease and Pick's disease. *Archives of Neurology*, *51*(2), 145–150.
10. Aupperle, P. M. (2006). Navigating patients and caregivers through the course of Alzheimer's disease. *The Journal of Clinical Psychiatry*, *67 Suppl 3*, 8–14; quiz 23.
11. Babić Leko, M., Krbot Skorić, M., Klepac, N., Borovečki, F., Langer Horvat, L., Vogrinc, Ž., Sonicki, Z., Hof, P. R., & Šimić, G. (2018). Event-related Potentials Improve the Efficiency of Cerebrospinal Fluid Biomarkers for Differential Diagnosis of Alzheimer's Disease. *Current Alzheimer Research*, *15*(13), 1244–1260.
12. Babiloni, C., Cassetta, E., Dal Forno, G., Del Percio, C., Ferreri, F., Ferri, R., Lanuzza, B., Miniussi, C., Moretti, D. V., Nobili, F., Pascual-Marqui, R. D., Rodriguez, G., Luca Romani, G., Salinari, S., Zanetti, O., & Rossini, P. M. (2006). Donepezil effects on sources of cortical rhythms in mild Alzheimer's disease: Responders vs. Non-Responders. *NeuroImage*, *31*(4), 1650–1665.
13. Baek, M. S., Cho, H., Lee, H. S., Lee, J. H., Ryu, Y. H., & Lyoo, C. H. (2020). Effect of APOE ε4 genotype on amyloid-β and tau accumulation in Alzheimer's disease. *Alzheimer's Research & Therapy*, *12*(1), 140.
14. Bakkour, A., Morris, J. C., & Dickerson, B. C. (2009). The cortical signature of prodromal AD: regional thinning predicts mild AD dementia. *Neurology*, *72*(12), 1048–1055.
15. Balsis, S., Carpenter, B. D., & Storandt, M. (2005). Personality change precedes clinical diagnosis of dementia of the Alzheimer type. *The Journals of Gerontology. Series B, Psychological Sciences and Social Sciences*, *60*(2), P98–P101.
16. Barber, R. C. (2012). The Genetics of Alzheimer's Disease. *Scientifica*, *2012*(ID 246210), 14.
17. Barnard, N. D., Bush, A. I., Ceccarelli, A., Cooper, J., de Jager, C. A., Erickson, K. I., Fraser, G., Kesler, S., Levin, S. M., Lucey, B., Morris, M. C., & Squitti, R. (2014). Dietary and lifestyle guidelines for the prevention of Alzheimer's disease. *Neurobiology of Aging*, *35 Suppl 2*, S74-8.
18. Barthel, H., Gertz, H.-J., Dresel, S., Peters, O., Bartenstein, P., Buerger, K., Hiemeyer, F., Wittemer-Rump, S. M., Seibyl, J., Reininger, C., & Sabri, O. (2011). Cerebral amyloid-β PET with florbetaben (18F) in patients with Alzheimer's disease and healthy controls: a multicentre phase 2 diagnostic study. *Lancet Neurology*, *10*(5), 424–435.

19. Barulli, D., & Stern, Y. (2013). Efficiency, capacity, compensation, maintenance, plasticity: emerging concepts in cognitive reserve. *Trends in Cognitive Sciences*, *17*(10), 502–509.
20. Beck, A. T., Steer, R. A., & Brown, G. (1996). Beck Depression Inventory–II (BDI-II). *Psychological Assessment*. https://doi.org/10.1037/t00742-000
21. Beck, A. T., Steer, R. A., & Brown, G. K. (2019). *BDI-II. Inwentarz depresji Becka. Podręcznik*. Pracownia Testów Psychologicznych Polskiego Towarzystwa Psychologicznego.
22. Bellenguez, C., Küçükali, F., Jansen, I. E., Kleineidam, L., Moreno-Grau, S., Amin, N., Naj, A. C., Campos-Martin, R., Grenier-Boley, B., Andrade, V., Holmans, P. A., Boland, A., Damotte, V., van der Lee, S. J., Costa, M. R., Kuulasmaa, T., Yang, Q., de Rojas, I., Bis, J. C., … Lambert, J.-C. (2022). New insights into the genetic etiology of Alzheimer's disease and related dementias. *Nature Genetics*, *54*(4), 412–436.
23. Benjamini, Y., & Hochberg, Y. (1995). Controlling the false discovery rate: A practical and powerful approach to multiple testing. *Journal of the Royal Statistical Society*, *57*(1), 289–300.
24. Benz, N., Hatz, F., Bousleiman, H., Ehrensperger, M. M., Gschwandtner, U., Hardmeier, M., Ruegg, S., Schindler, C., Zimmermann, R., Monsch, A. U., & Fuhr, P. (2014). Slowing of EEG background activity in Parkinson's and Alzheimer's disease with early cognitive dysfunction. *Frontiers in Aging Neuroscience*, *6*, 314.
25. Berteau-Pavy, F., Park, B., & Raber, J. (2007). Effects of sex and APOE epsilon4 on object recognition and spatial navigation in the elderly. *Neuroscience*, *147*(1), 6–17.
26. Bigos, K. L., Hariri, A. R., & Weinberger, D. R. (2016). *Neuroimaging Genetics: Principles and Practices*. Oxford University Press.
27. Biswal, B., Yetkin, F. Z., Haughton, V. M., & Hyde, J. S. (1995). Functional connectivity in the motor cortex of resting human brain using echo-planar MRI. *Magnetic Resonance in Medicine: Official Journal of the Society of Magnetic Resonance in Medicine / Society of Magnetic Resonance in Medicine*, *34*(4), 537–541.
28. Blanca Mena, M. J., Alarcón Postigo, R., Arnau Gras, J., Bono Cabré, R., & Bendayan, R. (2017). Non-normal data: Is ANOVA still a valid option? *Psicothema, 2017, Vol. 29, Num. 4, p. 552-557*. https://diposit.ub.edu/dspace/handle/2445/122126
29. Block, M. L., & Calderón-Garcidueñas, L. (2009). Air pollution: mechanisms of neuroinflammation and CNS disease. *Trends in Neurosciences*, *32*(9), 506–516.
30. Blumenthal, J. A., Smith, P. J., Mabe, S., Hinderliter, A., Lin, P.-H., Liao, L., Welsh-Bohmer, K. A., Browndyke, J. N., Kraus, W. E., Doraiswamy, P. M., Burke, J. R., & Sherwood, A. (2019). Lifestyle and neurocognition in older adults with cognitive impairments: A randomized trial. *Neurology*, *92*(3), e212–e223.
31. Bondi, M. W., Salmon, D. P., Monsch, A. U., Galasko, D., Butters, N., Klauber, M. R., Thal, L. J., & Saitoh, T. (1995). Episodic memory changes are associated with the APOE-epsilon 4 allele in nondemented older adults. *Neurology*, *45*(12), 2203–2206.
32. Braem, S., Bugg, J. M., Schmidt, J. R., Crump, M. J. C., Weissman, D. H., Notebaert, W., & Egner, T. (2019). Measuring Adaptive Control in Conflict Tasks. *Trends in Cognitive Sciences*, *23*(9), 769–783.
33. Britschgi, M., & Wyss-Coray, T. (2007). Systemic and acquired immune responses in Alzheimer's disease. *International Review of Neurobiology*, *82*, 205–233.
34. Bunce, D., Anstey, K. J., Cherbuin, N., Gautam, P., Sachdev, P., & Easteal, S. (2012). APOE genotype and entorhinal cortex volume in non-demented community-dwelling adults in midlife and early old age. *Journal of Alzheimer's Disease: JAD*, *30*(4), 935–942.
35. Bush, G., Spencer, T. J., Holmes, J., Shin, L. M., Valera, E. M., Seidman, L. J., Makris, N., Surman, C., Aleardi, M., Mick, E., & Biederman, J. (2008). Functional magnetic resonance imaging of methylphenidate and placebo in attention-deficit/hyperactivity disorder during the multi-source interference task. *Archives of General Psychiatry*, *65*(1), 102–114.
36. Bush, & Shin, L. M. (2006). The Multi-Source Interference Task: an fMRI task that reliably activates the cingulo-frontal-parietal cognitive/attention network. *Nature Protocols*, *1*(1), 308–313.
37. Bush, Shin, L. M., Holmes, J., Rosen, B. R., & Vogt, B. A. (2003). The Multi-Source Interference Task: validation study with fMRI in individual subjects. *Molecular Psychiatry*, *8*(1), 60–70.
38. Buzsaki, G. (2006). *Rhythms of the Brain*. Oxford University Press.
39. Cacciaglia, R., Molinuevo, J. L., Falcón, C., Arenaza-Urquijo, E. M., Sánchez-Benavides, G., Brugulat-Serrat, A., Blennow, K., Zetterberg, H., Gispert, J. D., & ALFA study. (2020). APOE-ε4 Shapes the Cerebral Organization in Cognitively Intact Individuals as Reflected by Structural Gray Matter Networks. *Cerebral Cortex* , *30*(7), 4110–4120.
40. Canuet, L., Tellado, I., Couceiro, V., Fraile, C., Fernandez-Novoa, L., Ishii, R., Takeda, M., & Cacabelos, R. (2012). Resting-state network disruption and APOE genotype in Alzheimer's disease: a lagged functional connectivity study. *PloS One*, *7*(9), e46289.
41. Carver, C. S. (1997). You want to measure coping but your protocol's too long: consider the brief COPE. *International Journal of Behavioral Medicine*, *4*(1), 92–100.
42. Cecchetti, G., Agosta, F., Basaia, S., Cividini, C., Cursi, M., Santangelo, R., Caso, F., Minicucci, F., Magnani, G., & Filippi, M. (2021). Resting-state electroencephalographic biomarkers of Alzheimer's disease. *NeuroImage: Clinical*, *31*, 102711.
43. Chang, Y.-S., Chen, H.-L., Hsu, C.-Y., Tang, S.-H., & Liu, C.-K. (2014). Parallel improvement of cognitive functions and P300 latency following donepezil treatment in patients with Alzheimer's disease: a case-control

study. *Journal of Clinical Neurophysiology: Official Publication of the American Electroencephalographic Society*, *31*(1), 81–85.

44. Chen, S.-H., Bu, X.-L., Jin, W.-S., Shen, L.-L., Wang, J., Zhuang, Z.-Q., Zhang, T., Zeng, F., Yao, X.-Q., Zhou, H.-D., & Wang, Y.-J. (2017). Altered peripheral profile of blood cells in Alzheimer disease: A hospital-based case-control study. *Medicine*, *96*(21), e6843.
45. Chêne, G., Beiser, A., Au, R., Preis, S. R., Wolf, P. A., Dufouil, C., & Seshadri, S. (2015). Gender and incidence of dementia in the Framingham Heart Study from mid-adult life. *Alzheimer's & Dementia: The Journal of the Alzheimer's Association*, *11*(3), 310–320.
46. Cholerton, B., Larson, E. B., Quinn, J. F., Zabetian, C. P., Mata, I. F., Keene, C. D., Flanagan, M., Crane, P. K., Grabowski, T. J., Montine, K. S., & Montine, T. J. (2016). Precision Medicine: Clarity for the Complexity of Dementia. *The American Journal of Pathology*, *186*(3), 500–506.
47. Chumbley, J., Worsley, K., Flandin, G., & Friston, K. (2010). Topological FDR for neuroimaging. *NeuroImage*, *49*(4), 3057–3064.
48. Cid-Fernández, S., Lindín, M., & Díaz, F. (2014). Effects of amnestic mild cognitive impairment on N2 and P3 Go/NoGo ERP components. *Journal of Alzheimer's Disease: JAD*, *38*(2), 295–306.
49. Colom-Cadena, M., Spires-Jones, T., Zetterberg, H., Blennow, K., Caggiano, A., DeKosky, S. T., Fillit, H., Harrison, J. E., Schneider, L. S., Scheltens, P., de Haan, W., Grundman, M., van Dyck, C. H., Izzo, N. J., Catalano, S. M., & Synaptic Health Endpoints Working Group. (2020). The clinical promise of biomarkers of synapse damage or loss in Alzheimer's disease. *Alzheimer's Research & Therapy*, *12*(1), 21.
50. Corder, E. H., Saunders, A. M., Risch, N. J., Strittmatter, W. J., Schmechel, D. E., Gaskell, P. C., Jr, Rimmler, J. B., Locke, P. A., Conneally, P. M., & Schmader, K. E. (1994). Protective effect of apolipoprotein E type 2 allele for late onset Alzheimer disease. *Nature Genetics*, *7*(2), 180–184.
51. Corder, E. H., Saunders, A. M., Strittmatter, W. J., Schmechel, D. E., Gaskell, P. C., Small, G. W., Roses, A. D., Haines, J. L., & Pericak-Vance, M. A. (1993). Gene dose of apolipoprotein E type 4 allele and the risk of Alzheimer's disease in late onset families. *Science*, *261*(5123), 921–923.
52. Costa, P. T., & McCrae, R. R. (1985). *The NEO-Personality Inventory manual*. Psychological Assessment Resources.
53. Costa, P. T., & McCrae, R. R. (1989). *The NEO-PI/FFI Manual Supplement*. Psychological Assessment Resources.
54. Crean, S., Ward, A., Mercaldi, C. J., Collins, J. M., Cook, M. N., Baker, N. L., & Arrighi, H. M. (2011). Apolipoprotein E ε4 prevalence in Alzheimer's disease patients varies across global populations: a systematic literature review and meta-analysis. *Dementia and Geriatric Cognitive Disorders*, *31*(1), 20–30.
55. Cruz-Sanabria, F., Bonilla-Vargas, K., Estrada, K., Mancera, O., Vega, E., Guerrero, E., Ortega-Rojas, J., Mahecha María, F., Romero, A., Montañés, P., Celeita, V., Arboleda, H., & Pardo, R. (2021). Analysis of cognitive performance and polymorphisms of SORL1, PVRL2, CR1, TOMM40, APOE, PICALM, GWAS_14q, CLU, and BIN1 in patients with mild cognitive impairment and cognitively healthy controls. *Neurologia* , *36*(9), 681–691.
56. Dahnke, R., Yotter, R. A., & Gaser, C. (2013). Cortical thickness and central surface estimation. *NeuroImage*, *65*, 336–348.
57. Damoiseaux, J. S. (2012). Resting-state fMRI as a biomarker for Alzheimer's disease? *Alzheimer's Research & Therapy*, *4*(2), 8.
58. Dauwels, J., Srinivasan, K., Ramasubba Reddy, M., Musha, T., Vialatte, F.-B., Latchoumane, C., Jeong, J., & Cichocki, A. (2011). Slowing and Loss of Complexity in Alzheimer's EEG: Two Sides of the Same Coin? *International Journal of Alzheimer's Disease*, *2011*, 539621.
59. Davies, P., & Maloney, A. J. (1976). Selective loss of central cholinergic neurons in Alzheimer's disease. *The Lancet*, *2*(8000), 1403.
60. de Frutos Lucas, J., Sewell, K. R., García-Colomo, A., Markovic, S., Erickson, K. I., & Brown, B. M. (2023). How does apolipoprotein E genotype influence the relationship between physical activity and Alzheimer's disease risk? A novel integrative model. *Alzheimer's Research & Therapy*, *15*(1), 22.
61. de Waal, H., Stam, C. J., de Haan, W., van Straaten, E. C. W., Blankenstein, M. A., Scheltens, P., & van der Flier, W. M. (2013). Alzheimer's disease patients not carrying the apolipoprotein E ε4 allele show more severe slowing of oscillatory brain activity. *Neurobiology of Aging*, *34*(9), 2158–2163.
62. Delis, D. C., Freeland, J., Kramer, J. H., & Kaplan, E. (1988). Integrating clinical assessment with cognitive neuroscience: construct validation of the California Verbal Learning Test. *Journal of Consulting and Clinical Psychology*, *56*(1), 123–130.
63. Delorme, A., & Makeig, S. (2004). EEGLAB: an open source toolbox for analysis of single-trial EEG dynamics including independent component analysis. *Journal of Neuroscience Methods*, *134*(1), 9–21.
64. Deng, Y., Wang, X., Wang, Y., & Zhou, C. (2018). Neural correlates of interference resolution in the multi-source interference task: a meta-analysis of functional neuroimaging studies. *Behavioral and Brain Functions: BBF*, *14*(1), 8.
65. Destrieux, C., Fischl, B., Dale, A., & Halgren, E. (2010). Automatic parcellation of human cortical gyri and sulci using standard anatomical nomenclature. *NeuroImage*, *53*(1), 1–15.
66. DeTure, M. A., & Dickson, D. W. (2019). The neuropathological diagnosis of Alzheimer's disease. *Molecular Neurodegeneration*, *14*(1), 32.

67. Di Battista, A. M., Heinsinger, N. M., & Rebeck, G. W. (2016). Alzheimer's Disease Genetic Risk Factor APOE-ε4 Also Affects Normal Brain Function. *Current Alzheimer Research*, *13*(11), 1200–1207.
68. Dickerson, B. C., Bakkour, A., Salat, D. H., Feczko, E., Pacheco, J., Greve, D. N., Grodstein, F., Wright, C. I., Blacker, D., Rosas, H. D., Sperling, R. A., Atri, A., Growdon, J. H., Hyman, B. T., Morris, J. C., Fischl, B., & Buckner, R. L. (2009). The Cortical Signature of Alzheimer's Disease: Regionally Specific Cortical Thinning Relates to Symptom Severity in Very Mild to Mild AD Dementia and is Detectable in Asymptomatic Amyloid-Positive Individuals. *Cerebral Cortex* , *19*(3), 497–510.
69. Dickson, D. W. (1997). The pathogenesis of senile plaques. *Journal of Neuropathology and Experimental Neurology*, *56*(4), 321–339.
70. DiLoreto, R., & Murphy, C. T. (2015). The cell biology of aging. *Molecular Biology of the Cell*, *26*(25), 4524–4531.
71. Dincer, A., Chen, C. D., McKay, N. S., Koenig, L. N., McCullough, A., Flores, S., Keefe, S. J., Schultz, S. A., Feldman, R. L., Joseph-Mathurin, N., Hornbeck, R. C., Cruchaga, C., Schindler, S. E., Holtzman, D. M., Morris, J. C., Fagan, A. M., Benzinger, T. L. S., & Gordon, B. A. (2022). APOE ε4 genotype, amyloid-β, and sex interact to predict tau in regions of high APOE mRNA expression. *Science Translational Medicine*, *14*(671), eabl7646.
72. Dobson, C. B., & Itzhaki, R. F. (1999). Herpes simplex virus type 1 and Alzheimer's disease. *Neurobiology of Aging*, *20*(4), 457–465.
73. Dowell, N. G., Evans, S. L., Tofts, P. S., King, S. L., Tabet, N., & Rusted, J. M. (2016). Structural and resting-state MRI detects regional brain differences in young and mid-age healthy APOE-e4 carriers compared with non-APOE-e4 carriers. *NMR in Biomedicine*, *29*(5), 614–624.
74. Dubois, B., Hampel, H., Feldman, H. H., Scheltens, P., Aisen, P., Andrieu, S., Bakardjian, H., Benali, H., Bertram, L., Blennow, K., Broich, K., Cavedo, E., Crutch, S., Dartigues, J.-F., Duyckaerts, C., Epelbaum, S., Frisoni, G. B., Gauthier, S., Genthon, R., … Proceedings of the Meeting of the International Working Group (IWG) and the American Alzheimer's Association on "The Preclinical State of AD"; July 23, 2015; Washington DC, USA. (2016). Preclinical Alzheimer's disease: Definition, natural history, and diagnostic criteria. *Alzheimer's & Dementia: The Journal of the Alzheimer's Association*, *12*(3), 292–323.
75. Durongbhan, P., Zhao, Y., Chen, L., Zis, P., De Marco, M., Unwin, Z. C., Venneri, A., He, X., Li, S., Zhao, Y., Blackburn, D. J., & Sarrigiannis, P. G. (2019). A Dementia Classification Framework Using Frequency and Time-Frequency Features Based on EEG Signals. In *IEEE Transactions on Neural Systems and Rehabilitation Engineering* (Vol. 27, Issue 5, pp. 826–835). https://doi.org/10.1109/tnsre.2019.2909100
76. Dzianok, P., & Kublik, E. (2023). Altered granulocyte count and erythrocyte measures in middle-aged, healthy carriers of APOE and PICALM risk genes for Alzheimer's disease. *Acta Neurobiologiae Experimentalis*, *83*(2), 127–139.
77. Dzwonkowska, I., Lachowicz-Tabaczek, K., & Łaguna, M. (2008). *SES. Samoocena i jej pomiar. Polska adaptacja skali SES M. Rosenberga. Podręcznik* (D. Fecenec, Ed.). Pracownia Testów Psychologicznych.
78. Ebert, U., Grossmann, M., Oertel, R., Gramatté, T., & Kirch, W. (2001). Pharmacokinetic-pharmacodynamic modeling of the electroencephalogram effects of scopolamine in healthy volunteers. *Journal of Clinical Pharmacology*, *41*(1), 51–60.
79. Egensperger, R., Kösel, S., von Eitzen, U., & Graeber, M. B. (1998). Microglial activation in Alzheimer disease: Association with APOE genotype. *Brain Pathology* , *8*(3), 439–447.
80. Engel, S., Graetz, C., Salmen, A., Muthuraman, M., Toenges, G., Ambrosius, B., Bayas, A., Berthele, A., Heesen, C., Klotz, L., Kümpfel, T., Linker, R. A., Meuth, S. G., Paul, F., Stangel, M., Tackenberg, B., Then Bergh, F., Tumani, H., Weber, F., … German Competence Network of Multiple Sclerosis. (2020). Is APOE ε4 associated with cognitive performance in early MS? *Neurology(R) Neuroimmunology & Neuroinflammation*, *7*(4). https://doi.org/10.1212/NXI.0000000000000728
81. Ertekin-Taner, N. (2007). Genetics of Alzheimer's disease: a centennial review. *Neurologic Clinics*, *25*(3), 611–667, v.
82. Eskelinen, M. H., Ngandu, T., Tuomilehto, J., Soininen, H., & Kivipelto, M. (2009). Midlife coffee and tea drinking and the risk of late-life dementia: a population-based CAIDE study. *Journal of Alzheimer's Disease: JAD*, *16*(1), 85–91.
83. Espeseth, T., Rootwelt, H., & Reinvang, I. (2009). Apolipoprotein E modulates auditory event-related potentials in healthy aging. *Neuroscience Letters*, *459*(2), 91–95.
84. Esteller, R., Vachtsevanos, G., Echauz, J., & Lilt, B. (1999). A comparison of fractal dimension algorithms using synthetic and experimental data. *1999 IEEE International Symposium on Circuits and Systems (ISCAS)*, *3*, 199–202 vol.3.
85. Esteller, R., Vachtsevanos, G., Echauz, J., & Litt, B. (2001). A comparison of waveform fractal dimension algorithms. *IEEE Transactions on Circuits and Systems I: Fundamental Theory and Applications*, *48*(2), 177–183.
86. Evans, Dowell, N. G., Prowse, F., Tabet, N., King, S. L., & Rusted, J. M. (2020). Mid age APOE ε4 carriers show memory-related functional differences and disrupted structure-function relationships in hippocampal regions. *Scientific Reports*, *10*(1), 3110.
87. Evans, S., Clarke, D., Dowell, N. G., Tabet, N., King, S. L., Hutton, S. B., & Rusted, J. M. (2018). Using event-related fMRI to examine sustained attention processes and effects of APOE ε4 in young adults. *PloS One*, *13*(6), e0198312.

88. Eyler, L. T., Elman, J. A., Hatton, S. N., Gough, S., Mischel, A. K., Hagler, D. J., Franz, C. E., Docherty, A., Fennema-Notestine, C., Gillespie, N., Gustavson, D., Lyons, M. J., Neale, M. C., Panizzon, M. S., Dale, A. M., & Kremen, W. S. (2019). Resting State Abnormalities of the Default Mode Network in Mild Cognitive Impairment: A Systematic Review and Meta-Analysis. *Journal of Alzheimer's Disease: JAD*, *70*(1), 107–120.
89. Fan, M., Liu, B., Zhou, Y., Zhen, X., Xu, C., Jiang, T., & Alzheimer's Disease Neuroimaging Initiative. (2010). Cortical thickness is associated with different apolipoprotein E genotypes in healthy elderly adults. *Neuroscience Letters*, *479*(3), 332–336.
90. Farias, S. T., Mungas, D., Reed, B., Carmichael, O., Beckett, L., Harvey, D., Olichney, J., Simmons, A., & Decarli, C. (2012). Maximal brain size remains an important predictor of cognition in old age, independent of current brain pathology. *Neurobiology of Aging*, *33*(8), 1758–1768.
91. Farrer, L. A., Adrienne Cupples, L., Haines, J. L., Hyman, B., Kukull, W. A., Mayeux, R., Myers, R. H., Pericak-Vance, M. A., Risch, N., & van Duijn, C. M. (1997). Effects of Age, Sex, and Ethnicity on the Association Between Apolipoprotein E Genotype and Alzheimer Disease: A Meta-analysis. *JAMA: The Journal of the American Medical Association*, *278*(16), 1349–1356.
92. Faul, F., Erdfelder, E., Lang, A.-G., & Buchner, A. (2007). G*Power 3: a flexible statistical power analysis program for the social, behavioral, and biomedical sciences. *Behavior Research Methods*, *39*(2), 175–191.
93. Faux, N. G., Rembach, A., Wiley, J., Ellis, K. A., Ames, D., Fowler, C. J., Martins, R. N., Pertile, K. K., Rumble, R. L., Trounson, B., Masters, C. L., AIBL Research Group, & Bush, A. I. (2014). An anemia of Alzheimer's disease. *Molecular Psychiatry*, *19*(11), 1227–1234.
94. Fernandez, C. G., Hamby, M. E., McReynolds, M. L., & Ray, W. J. (2019). The Role of APOE4 in Disrupting the Homeostatic Functions of Astrocytes and Microglia in Aging and Alzheimer's Disease. *Frontiers in Aging Neuroscience*, *11*, 14.
95. Ferreira-Vieira, T., M. Guimaraes, I., R. Silva, F., & M. Ribeiro, F. (2016). Alzheimer's disease: Targeting the Cholinergic System. *Current Neuropharmacology*, *14*(1), 101–115.
96. Ficiarà, E., Crespi, V., Gadewar, S. P., Thomopoulos, S. I., Boyd, J., Thompson, P. M., Jahanshad, N., Pizzagalli, F., & Alzheimer's Disease Neuroimaging Initiative. (2021). Predicting Progression from Mild Cognitive Impairment to Alzheimer's Disease using MRI-based Cortical Features and a Two-State Markov Model. *Proceedings / IEEE International Symposium on Biomedical Imaging: From Nano to Macro. IEEE International Symposium on Biomedical Imaging*, *2021*, 1145–1149.
97. Filippini, N., MacIntosh, B. J., Hough, M. G., Goodwin, G. M., Frisoni, G. B., Smith, S. M., Matthews, P. M., Beckmann, C. F., & Mackay, C. E. (2009). Distinct patterns of brain activity in young carriers of the APOE-epsilon4 allele. *Proceedings of the National Academy of Sciences of the United States of America*, *106*(17), 7209–7214.
98. Fischer, M. H. F., Zibrandtsen, I. C., Høgh, P., & Musaeus, C. S. (2023). Systematic Review of EEG Coherence in Alzheimer's Disease. In *Journal of Alzheimer's Disease* (pp. 1–12). https://doi.org/10.3233/jad-220508
99. Folstein, J. R., & Van Petten, C. (2008). Influence of cognitive control and mismatch on the N2 component of the ERP: a review. *Psychophysiology*, *45*(1), 152–170.
100. Foo, H., Mather, K. A., Jiang, J., Thalamuthu, A., Wen, W., & Sachdev, P. S. (2020). Genetic influence on ageing-related changes in resting-state brain functional networks in healthy adults: A systematic review. *Neuroscience and Biobehavioral Reviews*, *113*, 98–110.
101. Foucher, J., Gounot, D., Pham, B.-T., Marrer, C., & Dufour, A. (2008). 'Magnetized' brains are slower: The cognitive effects of fMRI. *Nature Precedings*, 1–1.
102. Fouquet, M., Besson, F. L., Gonneaud, J., La Joie, R., & Chételat, G. (2014). Imaging brain effects of APOE4 in cognitively normal individuals across the lifespan. *Neuropsychology Review*, *24*(3), 290–299.
103. Fozard, J. L., Vercryssen, M., Reynolds, S. L., Hancock, P. A., & Quilter, R. E. (1994). Age differences and changes in reaction time: the Baltimore Longitudinal Study of Aging. *Journal of Gerontology*, *49*(4), P179-89.
104. Frost, B., Jacks, R. L., & Diamond, M. I. (2009). Propagation of tau misfolding from the outside to the inside of a cell. *The Journal of Biological Chemistry*. https://www.jbc.org/article/S0021-9258(20)58284-7/abstract
105. García-Ayllón, M.-S., Small, D. H., Avila, J., & Sáez-Valero, J. (2011). Revisiting the Role of Acetylcholinesterase in Alzheimer's Disease: Cross-Talk with P-tau and β-Amyloid. *Frontiers in Molecular Neuroscience*, *4*, 22.
106. Gaser, C., Dahnke, R., Thompson, P. M., Kurth, F., Luders, E., & Alzheimer's Disease Neuroimaging Initiative. (2022). CAT – A Computational Anatomy Toolbox for the Analysis of Structural MRI Data. In *bioRxiv* (p. 2022.06.11.495736). https://doi.org/10.1101/2022.06.11.495736
107. Gasser, T., Bächer, P., & Möcks, J. (1982). Transformations towards the normal distribution of broad band spectral parameters of the EEG. *Electroencephalography and Clinical Neurophysiology*, *53*(1), 119–124.
108. Gaubert, S., Raimondo, F., Houot, M., Corsi, M.-C., Naccache, L., Sitt, J. D., Hermann, B., Oudiette, D., Gagliardi, G. P., Habert, M.-O., Dubois, B., Fallani, F. D. V., Bakardjian, H., Epelbaum, S., & the Alzheimer's Disease Neuroimaging Initiative, the MEMENTO study group and the INSIGHT-preAD study group. (2020). EEG: A valuable tool to screen for neurodegeneration in preclinical Alzheimer's disease. *Alzheimer's & Dementia: The Journal of the Alzheimer's Association*, *16*(S5). https://doi.org/10.1002/alz.039696
109. GBD 2019 Dementia Forecasting Collaborators. (2022). Estimation of the global prevalence of dementia in 2019 and forecasted prevalence in 2050: an analysis for the Global Burden of Disease Study 2019. *The Lancet. Public Health*, *7*(2), e105–e125.

110. Ge, T., & Yuan, Y. (2022). Herpes Simplex Virus Infection Increases Beta-Amyloid Production and Induces the Development of Alzheimer's Disease. *BioMed Research International*, *2022*, 8804925.
111. Gharbi-Meliani, A., Dugravot, A., Sabia, S., Regy, M., Fayosse, A., Schnitzler, A., Kivimäki, M., Singh-Manoux, A., & Dumurgier, J. (2021). The association of APOE ε4 with cognitive function over the adult life course and incidence of dementia: 20 years follow-up of the Whitehall II study. *Alzheimer's Research & Therapy*, *13*(1), 5.
112. Girard, S. L., & Rouleau, G. A. (2014). Genome-wide association study in FTD: divide to conquer [Review of *Genome-wide association study in FTD: divide to conquer*]. *Lancet Neurology*, *13*(7), 643–644.
113. Glantz, S. A., Slinker, B. K., & Neilands, T. B. (2016). *Primer of applied regression & analysis of variance 3e* (3rd ed.). McGraw-Hill Education/Medical. http://mhe-assets-asia.s3.amazonaws.com/professional/newtitles/Professional_New_Titles-Feb2016.pdf
114. Gomolka, R. S., Kampusch, S., Kaniusas, E., Thürk, F., Széles, J. C., & Klonowski, W. (2018). Higuchi Fractal Dimension of Heart Rate Variability During Percutaneous Auricular Vagus Nerve Stimulation in Healthy and Diabetic Subjects. *Frontiers in Physiology*, *9*, 1162.
115. Gordon, B., & Carson, K. (1990). The basis for choice reaction time slowing in Alzheimer's disease. *Brain and Cognition*, *13*(2), 148–166.
116. Gorus, E., De Raedt, R., Lambert, M., Lemper, J.-C., & Mets, T. (2008). Reaction times and performance variability in normal aging, mild cognitive impairment, and Alzheimer's disease. *Journal of Geriatric Psychiatry and Neurology*, *21*(3), 204–218.
117. Gramfort, A., Luessi, M., Larson, E., Engemann, D. A., Strohmeier, D., Brodbeck, C., Parkkonen, L., & Hämäläinen, M. S. (2014). MNE software for processing MEG and EEG data. *NeuroImage*, *86*, 446–460.
118. Green, A. E., Gray, J. R., Deyoung, C. G., Mhyre, T. R., Padilla, R., Dibattista, A. M., & William Rebeck, G. (2014). A combined effect of two Alzheimer's risk genes on medial temporal activity during executive attention in young adults. *Neuropsychologia*, *56*, 1–8.
119. Greenaway, M. C., Lacritz, L. H., Binegar, D., Weiner, M. F., Lipton, A., & Munro Cullum, C. (2006). Patterns of verbal memory performance in mild cognitive impairment, Alzheimer disease, and normal aging. *Cognitive and Behavioral Neurology: Official Journal of the Society for Behavioral and Cognitive Neurology*, *19*(2), 79–84.
120. Greicius, M. D., Srivastava, G., Reiss, A. L., & Menon, V. (2004). Default-mode network activity distinguishes Alzheimer's disease from healthy aging: evidence from functional MRI. *Proceedings of the National Academy of Sciences of the United States of America*, *101*(13), 4637–4642.
121. Groppe, D. (2015). *Benjamini & Hochberg/Yekutieli false discovery rate control procedure for a set of statistical tests* (2.3.0.0) [Computer software]. https://www.mathworks.com/matlabcentral/fileexchange/27418-fdr_bh
122. Gu, L., & Guo, Z. (2013). Alzheimer's Aβ42 and Aβ40 peptides form interlaced amyloid fibrils. *Journal of Neurochemistry*, *126*(3), 305–311.
123. Gunes, S., Aizawa, Y., Sugashi, T., Sugimoto, M., & Rodrigues, P. P. (2022). Biomarkers for Alzheimer's Disease in the Current State: A Narrative Review. *International Journal of Molecular Sciences*, *23*(9). https://doi.org/10.3390/ijms23094962
124. Gureje, O., Ogunniyi, A., Baiyewu, O., Price, B., Unverzagt, F. W., Evans, R. M., Smith-Gamble, V., Lane, K. A., Gao, S., Hall, K. S., Hendrie, H. C., & Murrell, J. R. (2006). APOE epsilon4 is not associated with Alzheimer's disease in elderly Nigerians. *Annals of Neurology*, *59*(1), 182–185.
125. Gustavson, D. E., Elman, J. A., Sanderson-Cimino, M., Franz, C. E., Panizzon, M. S., Jak, A. J., Reynolds, C. A., Neale, M. C., Lyons, M. J., & Kremen, W. S. (2020). Extensive memory testing improves prediction of progression to MCI in late middle age. *Alzheimer's & Dementia: The Journal of the Alzheimer's Association*, *12*(1), e12004.
126. Han, S. D., & Bondi, M. W. (2008). Revision of the apolipoprotein E compensatory mechanism recruitment hypothesis. *Alzheimer's & Dementia: The Journal of the Alzheimer's Association*, *4*(4), 251–254.
127. Hardwick, R. M., Forrence, A. D., Costello, M. G., Zackowski, K., & Haith, A. M. (2022). Age-related increases in reaction time result from slower preparation, not delayed initiation. *Journal of Neurophysiology*, *128*(3), 582–592.
128. Hardy, J., & Allsop, D. (1991). Amyloid deposition as the central event in the aetiology of Alzheimer's disease. *Trends in Pharmacological Sciences*, *12*(10), 383–388.
129. Hariri, A. R., & Weinberger, D. R. (2003). Imaging genomics. *British Medical Bulletin*, *65*, 259–270.
130. Harold, D., Abraham, R., Hollingworth, P., Sims, R., Gerrish, A., Hamshere, M. L., Pahwa, J. S., Moskvina, V., Dowzell, K., Williams, A., Jones, N., Thomas, C., Stretton, A., Morgan, A. R., Lovestone, S., Powell, J., Proitsi, P., Lupton, M. K., Brayne, C., … Williams, J. (2009). Genome-wide association study identifies variants at CLU and PICALM associated with Alzheimer's disease. *Nature Genetics*, *41*(10), 1088–1093.
131. Heidlmayr, K., Kihlstedt, M., & Isel, F. (2020). A review on the electroencephalography markers of Stroop executive control processes. *Brain and Cognition*, *146*, 105637.
132. Heise, V., Filippini, N., Trachtenberg, A. J., Suri, S., Ebmeier, K. P., & Mackay, C. E. (2014). Apolipoprotein E genotype, gender and age modulate connectivity of the hippocampus in healthy adults. *NeuroImage*, *98*, 23–30.
133. Higuchi, T. (1988). Approach to an irregular time series on the basis of the fractal theory. *Physica D. Nonlinear Phenomena*, *31*(2), 277–283.

134. Hippius, H., & Neundörfer, G. (2003). The discovery of Alzheimer's disease. *Dialogues in Clinical Neuroscience*, *5*(1), 101–108.
135. Holmes, C., Cunningham, C., Zotova, E., Woolford, J., Dean, C., Kerr, S., Culliford, D., & Perry, V. H. (2009). Systemic inflammation and disease progression in Alzheimer disease. *Neurology*, *73*(10), 768–774.
136. Horvath, A., Szucs, A., Csukly, G., Sakovics, A., Stefanics, G., & Kamondi, A. (2018). EEG and ERP biomarkers of Alzheimer's disease: a critical review. *Frontiers in Bioscience* , *23*, 183–220.
137. Huang, & Mahley. (2014). Apolipoprotein E: Structure and function in lipid metabolism, neurobiology, and Alzheimer's diseases. *Neurobiology of Disease*, *72*, 3–12.
138. Huang, Qiu, C., von Strauss, E., Winblad, B., & Fratiglioni, L. (2004). APOE genotype, family history of dementia, and Alzheimer disease risk: a 6-year follow-up study. *Archives of Neurology*, *61*(12), 1930–1934.
139. Hubbard, B. M., Fenton, G. W., & Anderson, J. M. (1990). A quantitative histological study of early clinical and preclinical Alzheimer's disease. *Neuropathology and Applied Neurobiology*, *16*(2), 111–121.
140. Hunter, J. D. (2007). Matplotlib: A 2D Graphics Environment. *Computing in Science & Engineering*, *9*(3), 90–95.
141. Iannopollo, E., Garcia, K., & Alzheimer' Disease Neuroimaging Initiative. (2021). Enhanced detection of cortical atrophy in Alzheimer's disease using structural MRI with anatomically constrained longitudinal registration. *Human Brain Mapping*, *42*(11), 3576–3592.
142. Itzhaki. (2021). Overwhelming Evidence for a Major Role for Herpes Simplex Virus Type 1 (HSV1) in Alzheimer's Disease (AD); Underwhelming Evidence against. *Vaccines*, *9*(6). https://doi.org/10.3390/vaccines9060679
143. Itzhaki, R. F., Lin, W. R., Shang, D., Wilcock, G. K., & Faragher, B. (1997). Herpes simplex virus type 1 in brain and risk of Alzheimer's disease. *The Lancet*. https://www.sciencedirect.com/science/article/pii/S0140673696101495?casa_token=APwCecyZNEIAAAAA:w8SFyPJOVVep8IRWcLnAxnQS5BJpjrP18Dl8FJMPoG0M3UZVVSXitYnEsFbjPoweQEp9ybFZ0eI
144. Jackson, C. E., & Snyder, P. J. (2008). Electroencephalography and event-related potentials as biomarkers of mild cognitive impairment and mild Alzheimer's disease. *Alzheimer's & Dementia: The Journal of the Alzheimer's Association*, *4*(1 Suppl 1), S137-43.
145. Järemo, P., Milovanovic, M., Buller, C., Nilsson, S., & Winblad, B. (2013). Alzheimer's disease and granulocyte density diversity. *European Journal of Clinical Investigation*, *43*(6), 545–548.
146. Jaworowska, A., & Szustrowa, T. (2010). *TMS. Test Matryc Ravena w wersji Standard. Formy: Klasyczna, Równoległa, Plus. Polskie Standaryzacje* (A. Matczak, Ed.; Vol. 2). Pracownia Testów Psychologicznych Polskiego Towarzystwa Psychologicznego.
147. Jelic, V., Julin, P., Shigeta, M., & Nordberg, A. (1997). Apolipoprotein E ε4 allele decreases functional connectivity in Alzheimer's disease as measured by EEG coherence. *Journal of Neurology*. https://jnnp.bmj.com/content/63/1/59.short
148. Jelic, V., Shigeta, M., Julin, P., Almkvist, O., Winblad, B., & Wahlund, L. O. (1996). Quantitative electroencephalography power and coherence in Alzheimer's disease and mild cognitive impairment. *Dementia* , *7*(6), 314–323.
149. Jeong, J. (2004). EEG dynamics in patients with Alzheimer's disease. *Clinical Neurophysiology: Official Journal of the International Federation of Clinical Neurophysiology*, *115*(7), 1490–1505.
150. Jochemsen, H. M., Muller, M., van der Graaf, Y., & Geerlings, M. I. (2012). APOE ε4 differentially influences change in memory performance depending on age. The SMART-MR study. *Neurobiology of Aging*, *33*(4), 832.e15-22.
151. Johansson, L., Guo, X., Waern, M., Ostling, S., Gustafson, D., Bengtsson, C., & Skoog, I. (2010). Midlife psychological stress and risk of dementia: a 35-year longitudinal population study. *Brain: A Journal of Neurology*, *133*(Pt 8), 2217–2224.
152. Juczyński, Z., & Ogińska-Bulik, N. (2012). *NPSR. Narzędzia Pomiaru Stresu i Radzenia Sobie ze Stresem. Podręcznik* (A. Matczak, Ed.). Pracownia Testów Psychologicznych Polskiego Towarzystwa Psychologicznego.
153. Jun, G., Naj, A. C., Beecham, G. W., Wang, L.-S., Buros, J., Gallins, P. J., Buxbaum, J. D., Ertekin-Taner, N., Fallin, M. D., Friedland, R., Inzelberg, R., Kramer, P., Rogaeva, E., St George-Hyslop, P., Alzheimer's Disease Genetics Consortium, Cantwell, L. B., Dombroski, B. A., Saykin, A. J., Reiman, E. M., … Schellenberg, G. D. (2010). Meta-analysis confirms CR1, CLU, and PICALM as alzheimer disease risk loci and reveals interactions with APOE genotypes. *Archives of Neurology*, *67*(12), 1473–1484.
154. Karch. (2023). Outliers may not be automatically removed. *Journal of Experimental Psychology. General*, *152*(6), 1735–1753.
155. Karch, & Goate. (2015). Alzheimer's disease risk genes and mechanisms of disease pathogenesis. *Biological Psychiatry*, *77*(1), 43–51.
156. Kassambara, A. (2023a). *ggpubr: 'ggplot2' Based Publication Ready Plots* (R package version 0.6.0) [Computer software]. https://CRAN.R-project.org/package=ggpubr
157. Kassambara, A. (2023b). *rstatix: Pipe-Friendly Framework for Basic Statistical Tests* (R package version 0.7.2) [Computer software]. https://CRAN.R-project.org/package=rstatix
158. Katzman, R. (1993). Education and the prevalence of dementia and Alzheimer's disease. *Neurology*, *43*(1), 13–20.

159. Katzman, R., Terry, R., DeTeresa, R., Brown, T., Davies, P., Fuld, P., Renbing, X., & Peck, A. (1988). Clinical, pathological, and neurochemical changes in dementia: a subgroup with preserved mental status and numerous neocortical plaques. *Annals of Neurology*, *23*(2), 138–144.
160. Kinney, J. W., Bemiller, S. M., Murtishaw, A. S., Leisgang, A. M., Salazar, A. M., & Lamb, B. T. (2018). Inflammation as a central mechanism in Alzheimer's disease. *Alzheimer's & Dementia: The Journal of the Alzheimer's Association*, *4*, 575–590.
161. Kong, D., Giovanello, K. S., Wang, Y., Lin, W., Lee, E., Fan, Y., Murali Doraiswamy, P., & Zhu, H. (2015). Predicting Alzheimer's Disease Using Combined Imaging-Whole Genome SNP Data. *Journal of Alzheimer's Disease: JAD*, *46*(3), 695–702.
162. Kovacs, G. G. (2017). Tauopathies. *Handbook of Clinical Neurology*, *145*, 355–368.
163. Kövari, E., Gold, G., Herrmann, F. R., Canuto, A., Hof, P. R., Michel, J.-P., Bouras, C., & Giannakopoulos, P. (2004). Cortical microinfarcts and demyelination significantly affect cognition in brain aging. *Stroke; a Journal of Cerebral Circulation*, *35*(2), 410–414.
164. Kucikova, L., Goerdten, J., Dounavi, M.-E., Mak, E., Su, L., Waldman, A. D., Danso, S., Muniz-Terrera, G., & Ritchie, C. W. (2021). Resting-state brain connectivity in healthy young and middle-aged adults at risk of progressive Alzheimer's disease. In *Neuroscience & Biobehavioral Reviews* (Vol. 129, pp. 142–153). https://doi.org/10.1016/j.neubiorev.2021.07.024
165. Kwan, H., Scarapicchia, V., Halliday, D., MacDonald, S., & Gawryluk, J. R. (2022). Functional near infrared spectroscopy activation during an executive function task differs between healthy older and younger adults. *Aging Brain*, *2*, 100029.
166. Laakkonen, M.-L., Raivio, M. M., Eloniemi-Sulkava, U., Saarenheimo, M., Pietilä, M., Tilvis, R. S., & Pitkälä, K. H. (2008). How do elderly spouse care givers of people with Alzheimer disease experience the disclosure of dementia diagnosis and subsequent care? *Journal of Medical Ethics*, *34*(6), 427–430.
167. Lehtovirta, M., Partanen, J., Könönen, M., Hiltunen, J., Helisalmi, S., Hartikainen, P., Riekkinen, P., Sr, & Soininen, H. (2000). A longitudinal quantitative EEG study of Alzheimer's disease: relation to apolipoprotein E polymorphism. *Dementia and Geriatric Cognitive Disorders*, *11*(1), 29–35.
168. Leidinger, P., Backes, C., Deutscher, S., Schmitt, K., Mueller, S. C., Frese, K., Haas, J., Ruprecht, K., Paul, F., Stähler, C., Lang, C. J. G., Meder, B., Bartfai, T., Meese, E., & Keller, A. (2013). A blood based 12-miRNA signature of Alzheimer disease patients. *Genome Biology*, *14*(7), R78.
169. Letemendia, F., & Pampiglione, G. (1958). Clinical and electroencephalographic observations in Alzheimer's Disease. In *Journal of Neurology, Neurosurgery & Psychiatry* (Vol. 21, Issue 3, pp. 167–172). https://doi.org/10.1136/jnnp.21.3.167
170. Li, Lei, Z., & Sun, T. (2023). The role of microRNAs in neurodegenerative diseases: a review. *Cell Biology and Toxicology*, *39*(1), 53–83.
171. Li, T., Pappas, C., Le, S. T., Wang, Q., Klinedinst, B. S., Larsen, B. A., Pollpeter, A., Lee, L. Y., Lutz, M. W., Gottschalk, W. K., Swerdlow, R. H., Nho, K., & Willette, A. A. (2022). APOE, TOMM40, and sex interactions on neural network connectivity. *Neurobiology of Aging*, *109*, 158–165.
172. Lim, Y. Y., Ellis, K. A., Ames, D., Darby, D., Harrington, K., Martins, R. N., Masters, C. L., Rowe, C., Savage, G., Szoeke, C., Villemagne, V. L., Maruff, P., & AIBL Research Group. (2013). Aβ amyloid, cognition, and APOE genotype in healthy older adults. *Alzheimer's & Dementia: The Journal of the Alzheimer's Association*, *9*(5), 538–545.
173. Lindenberger, U., Nagel, I. E., Chicherio, C., Li, S.-C., Heekeren, H. R., & Bäckman, L. (2008). Age-related decline in brain resources modulates genetic effects on cognitive functioning. *Frontiers in Neuroscience*, *2*(2), 234–244.
174. Liu, Dai, X., Zhang, J., Li, X., Chen, Y., Ma, C., Chen, K., Peng, D., & Zhang, Z. (2018). The Interactive Effects of Age and PICALM rs541458 Polymorphism on Cognitive Performance, Brain Structure, and Function in Non-demented Elderly. *Molecular Neurobiology*, *55*(2), 1271–1283.
175. Liu, Paajanen, T., Westman, E., Wahlund, L.-O., Simmons, A., Tunnard, C., Sobow, T., Proitsi, P., Powell, J., Mecocci, P., Tsolaki, M., Vellas, B., Muehlboeck, S., Evans, A., Spenger, C., Lovestone, S., Soininen, H., & AddNeuroMed Consortium. (2010). Effect of APOE ε4 allele on cortical thicknesses and volumes: the AddNeuroMed study. *Journal of Alzheimer's Disease: JAD*, *21*(3), 947–966.
176. Liu, Xie, Y., Meng, X.-Y., & Kang, J.-S. (2019). History and progress of hypotheses and clinical trials for Alzheimer's disease. *Signal Transduction and Targeted Therapy*, *4*, 29.
177. Lizio, R., Vecchio, F., Frisoni, G. B., Ferri, R., Rodriguez, G., & Babiloni, C. (2011). Electroencephalographic rhythms in Alzheimer's disease. *International Journal of Alzheimer's Disease*, *2011*, 927573.
178. Locatelli, T., Cursi, M., Liberati, D., Franceschi, M., & Comi, G. (1998). EEG coherence in Alzheimer's disease. *Electroencephalography and Clinical Neurophysiology*, *106*(3), 229–237.
179. Łojek, E., & Stańczak, J. (2010). *CVLT. Podręcznik do Kalifornijskiego Testu Uczenia się Językowego Deana C. Delisa, Joela H. Kramera, Edith Kaplan i Beth A. Ober. Polska normalizacja* (A. Matczak, Ed.). Pracownia Testów Psychologicznych Polskiego Towarzystwa Psychologicznego.
180. Lott, I. T., & Head, E. (2019). Dementia in Down syndrome: unique insights for Alzheimer disease research. *Nature Reviews. Neurology*, *15*(3), 135–147.
181. Low, L.-F., Harrison, F., & Lackersteen, S. M. (2013). Does personality affect risk for dementia? A systematic review and meta-analysis. *The American Journal of Geriatric Psychiatry: Official Journal of the American Association for Geriatric Psychiatry*, *21*(8), 713–728.

182. Luck, T., Then, F. S., Luppa, M., Schroeter, M. L., Arélin, K., Burkhardt, R., Thiery, J., Löffler, M., Villringer, A., & Riedel-Heller, S. G. (2015). Association of the apolipoprotein E genotype with memory performance and executive functioning in cognitively intact elderly. *Neuropsychology*, *29*(3), 382–387.
183. Lumley, T., Diehr, P., Emerson, S., & Chen, L. (2002). The importance of the normality assumption in large public health data sets. *Annual Review of Public Health*, *23*, 151–169.
184. Lunnon, K., Ibrahim, Z., Proitsi, P., Lourdusamy, A., Newhouse, S., Sattlecker, M., Furney, S., Saleem, M., Soininen, H., Kłoszewska, I., Mecocci, P., Tsolaki, M., Vellas, B., Coppola, G., Geschwind, D., Simmons, A., Lovestone, S., Dobson, R., Hodges, A., & AddNeuroMed Consortium. (2012). Mitochondrial dysfunction and immune activation are detectable in early Alzheimer's disease blood. *Journal of Alzheimer's Disease: JAD*, *30*(3), 685–710.
185. Ma, M., Dorstyn, D., Ward, L., & Prentice, S. (2018). Alzheimers' disease and caregiving: a meta-analytic review comparing the mental health of primary carers to controls. *Aging & Mental Health*, *22*(11), 1395–1405.
186. Machado, A., Herrera, A. J., de Pablos, R. M., Espinosa-Oliva, A. M., Sarmiento, M., Ayala, A., Venero, J. L., Santiago, M., Villarán, R. F., Delgado-Cortés, M. J., Argüelles, S., & Cano, J. (2014). Chronic stress as a risk factor for Alzheimer's disease. *Reviews in the Neurosciences*, *25*(6), 785–804.
187. Machulda, M. M., Jones, D. T., Vemuri, P., McDade, E., Avula, R., Przybelski, S., Boeve, B. F., Knopman, D. S., Petersen, R. C., & Jack, C. R., Jr. (2011). Effect of APOE ε4 status on intrinsic network connectivity in cognitively normal elderly subjects. *Archives of Neurology*, *68*(9), 1131–1136.
188. Mahley. (1988). Apolipoprotein E: cholesterol transport protein with expanding role in cell biology. *Science*, *240*(4852), 622–630.
189. Mahley. (2016). Apolipoprotein E: from cardiovascular disease to neurodegenerative disorders. *Journal of Molecular Medicine* , *94*(7), 739–746.
190. Mao, C. P., Zhang, Q. L., Bao, F. X., Liao, X., Yang, X. L., & Zhang, M. (2014). Decreased activation of cingulo-frontal-parietal cognitive/attention network during an attention-demanding task in patients with chronic low back pain. *Neuroradiology*, *56*(10), 903–912.
191. Marinescu, R. V., Eshaghi, A., Alexander, D. C., & Golland, P. (2019). BrainPainter: A software for the visualisation of brain structures, biomarkers and associated pathological processes. *Multimodal Brain Image Analysis and Mathematical Foundations of Computational Anatomy : 4th International Workshop, MBIA 2019, and 7th International Workshop, MFCA 2019, Held in Conjunction with MICCAI 2019, Shenzhen, China, October 17,...*, *11846*, 112–120.
192. Marttila, S., Rovio, S., Mishra, P. P., Seppälä, I., Lyytikäinen, L.-P., Juonala, M., Waldenberger, M., Oksala, N., Ala-Korpela, M., Harville, E., Hutri-Kähönen, N., Kähönen, M., Raitakari, O., Lehtimäki, T., & Raitoharju, E. (2021). Adulthood blood levels of hsa-miR-29b-3p associate with preterm birth and adult metabolic and cognitive health. *Scientific Reports*, *11*(1), 9203.
193. Mattsson, N., Ossenkoppele, R., Smith, R., Strandberg, O., Ohlsson, T., Jögi, J., Palmqvist, S., Stomrud, E., & Hansson, O. (2018). Greater tau load and reduced cortical thickness in APOE ε4-negative Alzheimer's disease: a cohort study. *Alzheimer's Research & Therapy*, *10*(1), 77.
194. Maturana-Candelas, A., Gómez, C., Poza, J., Rodríguez-González, V., Pablo, V. G., Lopes, A. M., Pinto, N., & Hornero, R. (2021). Influence of PICALM and CLU risk variants on beta EEG activity in Alzheimer's disease patients. *Scientific Reports*, *11*(1), 20465.
195. Medina, L. D., Woo, E., Rodriguez-Agudelo, Y., Chaparro Maldonado, H., Yi, D., Coppola, G., Zhou, Y., Chui, H. C., & Ringman, J. M. (2021). Reaction time and response inhibition in autosomal dominant Alzheimer's disease. *Brain and Cognition*, *147*, 105656.
196. Meghdadi, A. H., Stevanović Karić, M., McConnell, M., Rupp, G., Richard, C., Hamilton, J., Salat, D., & Berka, C. (2021). Resting state EEG biomarkers of cognitive decline associated with Alzheimer's disease and mild cognitive impairment. *PloS One*, *16*(2), e0244180.
197. Mengel-From, J., Christensen, K., McGue, M., & Christiansen, L. (2011). Genetic variations in the CLU and PICALM genes are associated with cognitive function in the oldest old. *Neurobiology of Aging*, *32*(3), 554.e7-554.e11.
198. Mentink, L. J., Guimarães, J. P. O. F. T., Faber, M., Sprooten, E., Olde Rikkert, M. G. M., Haak, K. V., & Beckmann, C. F. (2021). Functional co-activation of the default mode network in APOE ε4-carriers: A replication study. *NeuroImage*, *240*, 118304.
199. Michaelson, D. M. (2014). APOE ε4: the most prevalent yet understudied risk factor for Alzheimer's disease. *Alzheimer's & Dementia: The Journal of the Alzheimer's Association*, *10*(6), 861–868.
200. Milligan Armstrong, A., Porter, T., Quek, H., White, A., Haynes, J., Jackaman, C., Villemagne, V., Munyard, K., Laws, S. M., Verdile, G., & Groth, D. (2021). Chronic stress and Alzheimer's disease: the interplay between the hypothalamic-pituitary-adrenal axis, genetics and microglia. *Biological Reviews of the Cambridge Philosophical Society*, *96*(5), 2209–2228.
201. Mondadori, C. R. A., de Quervain, D. J.-F., Buchmann, A., Mustovic, H., Wollmer, M. A., Schmidt, C. F., Boesiger, P., Hock, C., Nitsch, R. M., Papassotiropoulos, A., & Henke, K. (2006). Better Memory and Neural Efficiency in Young Apolipoprotein E ε4 Carriers. *Cerebral Cortex* , *17*(8), 1934–1947.
202. Monge-Álvarez, J. (2015). *Higuchi and Katz fractal dimension measures* (1.1.0.0). https://www.mathworks.com/matlabcentral/fileexchange/50290-higuchi-and-katz-fractal-dimension-measures
203. Montagne, A., Nation, D. A., Sagare, A. P., Barisano, G., Sweeney, M. D., Chakhoyan, A., Pachicano, M., Joe, E., Nelson, A. R., D'Orazio, L. M., Buennagel, D. P., Harrington, M. G., Benzinger, T. L. S., Fagan, A. M.,

Ringman, J. M., Schneider, L. S., Morris, J. C., Reiman, E. M., Caselli, R. J., … Zlokovic, B. V. (2020). APOE4 leads to blood-brain barrier dysfunction predicting cognitive decline. *Nature*, *581*(7806), 71–76.

204. Moretti, D. V., Babiloni, C., Binetti, G., Cassetta, E., Dal Forno, G., Ferreric, F., Ferri, R., Lanuzza, B., Miniussi, C., Nobili, F., Rodriguez, G., Salinari, S., & Rossini, P. M. (2004). Individual analysis of EEG frequency and band power in mild Alzheimer's disease. *Clinical Neurophysiology: Official Journal of the International Federation of Clinical Neurophysiology*, *115*(2), 299–308.
205. Morgen, K., Ramirez, A., Frölich, L., Tost, H., Plichta, M. M., Kölsch, H., Rakebrandt, F., Rienhoff, O., Jessen, F., Peters, O., Jahn, H., Luckhaus, C., Hüll, M., Gertz, H.-J., Schröder, J., Hampel, H., Teipel, S. J., Pantel, J., Heuser, I., … Meyer-Lindenberg, A. (2014). Genetic interaction of PICALM and APOE is associated with brain atrophy and cognitive impairment in Alzheimer's disease. *Alzheimer's & Dementia: The Journal of the Alzheimer's Association*, *10*(5 Suppl), S269-76.
206. Mukherjee, S., Mez, J., Trittschuh, E. H., Saykin, A. J., Gibbons, L. E., Fardo, D. W., Wessels, M., Bauman, J., Moore, M., Choi, S.-E., Gross, A. L., Rich, J., Louden, D. K. N., Sanders, R. E., Grabowski, T. J., Bird, T. D., McCurry, S. M., Snitz, B. E., Kamboh, M. I., … Crane, P. K. (2020). Genetic data and cognitively defined late-onset Alzheimer's disease subgroups. *Molecular Psychiatry*, *25*(11), 2942–2951.
207. Mumford, J. A., Poline, J.-B., & Poldrack, R. A. (2015). Orthogonalization of regressors in FMRI models. *PloS One*, *10*(4), e0126255.
208. Nagaraj, S., Laskowska-Kaszub, K., Dębski, K. J., Wojsiat, J., Dąbrowski, M., Gabryelewicz, T., Kuźnicki, J., & Wojda, U. (2017). Profile of 6 microRNA in blood plasma distinguish early stage Alzheimer's disease patients from non-demented subjects. *Oncotarget*, *8*(10), 16122–16143.
209. Nagaraj, S., Zoltowska, K. M., Laskowska-Kaszub, K., & Wojda, U. (2019). microRNA diagnostic panel for Alzheimer's disease and epigenetic trade-off between neurodegeneration and cancer. *Ageing Research Reviews*, *49*, 125–143.
210. Namba, Y., Tomonaga, M., Kawasaki, H., Otomo, E., & Ikeda, K. (1991). Apolipoprotein E immunoreactivity in cerebral amyloid deposits and neurofibrillary tangles in Alzheimer's disease and kuru plaque amyloid in Creutzfeldt-Jakob disease. *Brain Research*, *541*(1), 163–166.
211. Nation, D. A., Sweeney, M. D., Montagne, A., Sagare, A. P., D'Orazio, L. M., Pachicano, M., Sepehrband, F., Nelson, A. R., Buennagel, D. P., Harrington, M. G., Benzinger, T. L. S., Fagan, A. M., Ringman, J. M., Schneider, L. S., Morris, J. C., Chui, H. C., Law, M., Toga, A. W., & Zlokovic, B. V. (2019). Blood-brain barrier breakdown is an early biomarker of human cognitive dysfunction. *Nature Medicine*, *25*(2), 270–276.
212. Neu, S. C., Pa, J., Kukull, W., Beekly, D., Kuzma, A., Gangadharan, P., Wang, L.-S., Romero, K., Arneric, S. P., Redolfi, A., Orlandi, D., Frisoni, G. B., Au, R., Devine, S., Auerbach, S., Espinosa, A., Boada, M., Ruiz, A., Johnson, S. C., … Toga, A. W. (2017). Apolipoprotein E Genotype and Sex Risk Factors for Alzheimer Disease: A Meta-analysis. *JAMA Neurology*, *74*(10), 1178–1189.
213. Neurobehavioral Systems, Inc. Berkeley, CA. (n.d.). *Presentation® software* (20.0) [Computer software]. www.neurobs.com
214. Nieto-Castanon, A. (2020). *Handbook of functional connectivity Magnetic Resonance Imaging methods in CONN*. Hilbert Press.
215. O'Donoghue, M. C., Murphy, S. E., Zamboni, G., Nobre, A. C., & Mackay, C. E. (2018). APOE genotype and cognition in healthy individuals at risk of Alzheimer's disease: A review. *Cortex; a Journal Devoted to the Study of the Nervous System and Behavior*, *104*, 103–123.
216. Oldfield, R. C. (1971). The assessment and analysis of handedness: the Edinburgh inventory. *Neuropsychologia*, *9*(1), 97–113.
217. O'Mahony, D., Coffey, J., Murphy, J., O'Hare, N., Hamilton, D., Rowan, M., Freyne, P., Walsh, J. B., & Coakley, D. (1996). Event-related potential prolongation in Alzheimer's disease signifies frontal lobe impairment: evidence from SPECT imaging. *The Journals of Gerontology. Series A, Biological Sciences and Medical Sciences*, *51*(3), M102-7.
218. Oostenveld, R., Fries, P., Maris, E., & Schoffelen, J.-M. (2011). FieldTrip: Open source software for advanced analysis of MEG, EEG, and invasive electrophysiological data. *Computational Intelligence and Neuroscience*, *2011*, 156869.
219. Opdebeeck, C., Martyr, A., & Clare, L. (2016). Cognitive reserve and cognitive function in healthy older people: a meta-analysis. *Neuropsychology, Development, and Cognition. Section B, Aging, Neuropsychology and Cognition*, *23*(1), 40–60.
220. Osuntokun, B. O., Sahota, A., Ogunniyi, A. O., Gureje, O., Baiyewu, O., Adeyinka, A., Oluwole, S. O., Komolafe, O., Hall, K. S., & Unverzagt, F. W. (1995). Lack of an association between apolipoprotein E epsilon 4 and Alzheimer's disease in elderly Nigerians. *Annals of Neurology*, *38*(3), 463–465.
221. Ouanes, S., & Popp, J. (2019). High Cortisol and the Risk of Dementia and Alzheimer's Disease: A Review of the Literature. *Frontiers in Aging Neuroscience*, *11*, 43.
222. Paitel, E. R., & Nielson, K. A. (2023). Cerebellar EEG source localization reveals age-related compensatory activity moderated by genetic risk for Alzheimer's disease. *Psychophysiology*, *60*(12), e14395.
223. Pastor, P., Roe, C. M., Villegas, A., Bedoya, G., Chakraverty, S., García, G., Tirado, V., Norton, J., Ríos, S., Martínez, M., Kosik, K. S., Lopera, F., & Goate, A. M. (2003). Apolipoprotein Eε4 modifies Alzheimer's disease onset in an E280A PS1 kindred. In *Annals of Neurology* (Vol. 54, Issue 2, pp. 163–169). https://doi.org/10.1002/ana.10636

224. Peavy, G. M., Lange, K. L., Salmon, D. P., Patterson, T. L., Goldman, S., Gamst, A. C., Mills, P. J., Khandrika, S., & Galasko, D. (2007). The effects of prolonged stress and APOE genotype on memory and cortisol in older adults. *Biological Psychiatry*, *62*(5), 472–478.
225. Penny, W. D., Friston, K. J., Ashburner, J. T., Kiebel, S. J., & Nichols, T. E. (2011). *Statistical Parametric Mapping: The Analysis of Functional Brain Images*. Elsevier.
226. Peters, R. (2006). Ageing and the brain. *Postgraduate Medical Journal*, *82*(964), 84–88.
227. Phillips, C. (2017). Lifestyle Modulators of Neuroplasticity: How Physical Activity, Mental Engagement, and Diet Promote Cognitive Health during Aging. *Neural Plasticity*, *2017*, 3589271.
228. Polich, J., & Corey-Bloom, J. (2005). Alzheimer's disease and P300: review and evaluation of task and modality. *Current Alzheimer Research*, *2*(5), 515–525.
229. Polich, Ladish, C., & Bloom, F. E. (1990). P300 assessment of early Alzheimer's disease. *Electroencephalography and Clinical Neurophysiology*, *77*(3), 179–189.
230. Poline, J., Kherif, F., Pallier, C., & Penny, W. (2007). Contrasts and classical inference. In *Statistical Parametric Mapping* (pp. 126–139). Elsevier.
231. Ponomareva, N., Andreeva, T., Protasova, M., Konovalov, R., Krotenkova, M., Malina, D., Mitrofanov, A., Fokin, V., Illarioshkin, S., & Rogaev, E. (2020). Genetic Association Between Alzheimer's Disease Risk Variant of the PICALM Gene and EEG Functional Connectivity in Non-demented Adults. *Frontiers in Neuroscience*, *14*, 324.
232. Porciatti, V., Fiorentini, A., Morrone, M. C., & Burr, D. C. (1999). The effects of ageing on reaction times to motion onset. *Vision Research*, *39*(12), 2157–2164.
233. Posit team. (2023). *RStudio: Integrated Development Environment for R* (2023.6.0.421) [Computer software]. Posit Software, PBC. http://www.posit.co
234. R Core Team. (2023). *R: A Language and Environment for Statistical Computing* (4.3.1) [Computer software]. https://www.R-project.org
235. Raghavendra, B. S., & Narayana Dutt, D. (2009). A note on fractal dimensions of biomedical waveforms. *Computers in Biology and Medicine*, *39*(11), 1006–1012.
236. Raichle, M. E., MacLeod, A. M., Snyder, A. Z., Powers, W. J., Gusnard, D. A., & Shulman, G. L. (2001). A default mode of brain function. *Proceedings of the National Academy of Sciences of the United States of America*, *98*(2), 676–682.
237. Rao, Y. L., Ganaraja, B., Murlimanju, B. V., Joy, T., Krishnamurthy, A., & Agrawal, A. (2022). Hippocampus and its involvement in Alzheimer's disease: a review. *3 Biotech*, *12*(2), 55.
238. Raport RPO, S. (2016). Sytuacja osób chorych na chorobę Alzheimera w Polsce. *Rzecznik Praw Obywatelskich*.
239. Raven, J. C., Court, J. H., & Raven, J. (1996). *Raven Manual: Section 3. Standard Progressive Matrices. 1996 edition with Adult US Norms*. Oxford Psychologist Press.
240. Régy, M., Dugravot, A., Sabia, S., Fayosse, A., Mangin, J.-F., Chupin, M., Fischer, C., Bouteloup, V., Dufouil, C., Chêne, G., Paquet, C., Hanseeuw, B., Singh-Manoux, A., Dumurgier, J., & MEMENTO cohort Study Group. (2022). Association of APOE ε4 with cerebral gray matter volumes in non-demented older adults: The MEMENTO cohort study. *NeuroImage*, *250*, 118966.
241. Riekkinen, P., Buzsaki, G., Riekkinen, P., Jr, Soininen, H., & Partanen, J. (1991). The cholinergic system and EEG slow waves. *Electroencephalography and Clinical Neurophysiology*, *78*(2), 89–96.
242. Ries, M., & Sastre, M. (2016). Mechanisms of Aβ Clearance and Degradation by Glial Cells. *Frontiers in Aging Neuroscience*, *8*, 160.
243. Robinson, Hayes, & Couch. (2023). *broom: Convert Statistical Objects into Tidy Tibbles* (R package version 1.0.5) [Computer software]. https://CRAN.R-project.org/package=broom
244. Robinson, Lee, B. Y., & Hanes, F. T. (2018). Recent Progress in Alzheimer's Disease Research, Part 2: Genetics and Epidemiology. *Journal of Alzheimer's Disease: JAD*, *61*(1), 459.
245. Rodriguez, G., Vitali, P., De Leo, C., De Carli, F., Girtler, N., & Nobili, F. (2002). Quantitative EEG changes in Alzheimer patients during long-term donepezil therapy. *Neuropsychobiology*, *46*(1), 49–56.
246. Rosenberg, M. (1989). *Society and adolescent self-image. Revised edition*. Wesleyan University Press.
247. Rosenthal, S. L., & Kamboh, M. I. (2014). Late-Onset Alzheimer's Disease Genes and the Potentially Implicated Pathways. *Current Genetic Medicine Reports*, *2*(2), 85–101.
248. Rossini, P. M., Di Iorio, R., Vecchio, F., Anfossi, M., Babiloni, C., Bozzali, M., Bruni, A. C., Cappa, S. F., Escudero, J., Fraga, F. J., Giannakopoulos, P., Guntekin, B., Logroscino, G., Marra, C., Miraglia, F., Panza, F., Tecchio, F., Pascual-Leone, A., & Dubois, B. (2020). Early diagnosis of Alzheimer's disease: the role of biomarkers including advanced EEG signal analysis. Report from the IFCN-sponsored panel of experts. *Clinical Neurophysiology: Official Journal of the International Federation of Clinical Neurophysiology*, *131*(6), 1287–1310.
249. Rusted, Evans, S. L., King, S. L., Dowell, N., Tabet, N., & Tofts, P. S. (2013). APOE ε4 polymorphism in young adults is associated with improved attention and indexed by distinct neural signatures. *NeuroImage*, *65*, 364–373.
250. Rusted, J., & Carare, R. O. (2015). Are the effects of APOE ϵ4 on cognitive function in nonclinical populations age- and gender-dependent? *Neurodegenerative Disease Management*, *5*(1), 37–48.
251. Satoh, J.-I., Kino, Y., & Niida, S. (2015). MicroRNA-Seq Data Analysis Pipeline to Identify Blood Biomarkers for Alzheimer's Disease from Public Data. *Biomarker Insights*, *10*, 21–31.

252. Saunders, J. B., Aasland, O. G., Babor, T. F., de la Fuente, J. R., & Grant, M. (1993). Development of the Alcohol Use Disorders Identification Test (AUDIT): WHO collaborative project on early detection of persons with harmful alcohol consumption--II. *Addiction* , *88*(6), 791–804.
253. Saunders, Strittmatter, W. J., Schmechel, D., George-Hyslop, P. H., Pericak-Vance, M. A., Joo, S. H., Rosi, B. L., Gusella, J. F., Crapper-MacLachlan, D. R., & Alberts, M. J. (1993). Association of apolipoprotein E allele epsilon 4 with late-onset familial and sporadic Alzheimer's disease. *Neurology*, *43*(8), 1467–1472.
254. Scarmeas, N., Stern, Y., Tang, M.-X., Mayeux, R., & Luchsinger, J. A. (2006). Mediterranean diet and risk for Alzheimer's disease. *Annals of Neurology*, *59*(6), 912–921.
255. Schliebs, R., & Arendt, T. (2006). The significance of the cholinergic system in the brain during aging and in Alzheimer's disease. *Journal of Neural Transmission* , *113*(11), 1625–1644.
256. Seghier M. L. (2013). The angular gyrus: multiple functions and multiple subdivisions. The Neuroscientist : a review journal bringing neurobiology, neurology and psychiatry, 19(1), 43–61.
257. Selkoe, D. J. (1991). The molecular pathology of Alzheimer's disease. *Neuron*, *6*(4), 487–498.
258. Shad, K. F., Aghazadeh, Y., Ahmad, S., & Kress, B. (2013). Peripheral markers of Alzheimer's disease: surveillance of white blood cells. *Synapse* , *67*(8), 541–543.
259. Shulman, G. L., Fiez, J. A., Corbetta, M., Buckner, R. L., Miezin, F. M., Raichle, M. E., & Petersen, S. E. (1997). Common Blood Flow Changes across Visual Tasks: II. Decreases in Cerebral Cortex. *Journal of Cognitive Neuroscience*, *9*(5), 648–663.
260. Silva, M. V. F., Loures, C. de M. G., Alves, L. C. V., de Souza, L. C., Borges, K. B. G., & Carvalho, M. das G. (2019). Alzheimer's disease: risk factors and potentially protective measures. *Journal of Biomedical Science*, *26*(1), 33.
261. Small, B. J., Rosnick, C. B., Fratiglioni, L., & Bäckman, L. (2004). Apolipoprotein E and cognitive performance: a meta-analysis. *Psychology and Aging*, *19*(4), 592–600.
262. Smits, F. M., Porcaro, C., Cottone, C., Cancelli, A., Rossini, P. M., & Tecchio, F. (2016). Electroencephalographic Fractal Dimension in Healthy Ageing and Alzheimer's Disease. *PloS One*, *11*(2), e0149587.
263. Snellman, A., Ekblad, L. L., Tuisku, J., Koivumäki, M., Ashton, N. J., Lantero-Rodriguez, J., Karikari, T. K., Helin, S., Bucci, M., Löyttyniemi, E., Parkkola, R., Karrasch, M., Schöll, M., Zetterberg, H., Blennow, K., & Rinne, J. O. (2023). APOE ε4 gene dose effect on imaging and blood biomarkers of neuroinflammation and beta-amyloid in cognitively unimpaired elderly. *Alzheimer's Research & Therapy*, *15*(1), 71.
264. Soares, H. D., Potter, W. Z., Pickering, E., Kuhn, M., Immermann, F. W., Shera, D. M., Ferm, M., Dean, R. A., Simon, A. J., Swenson, F., Siuciak, J. A., Kaplow, J., Thambisetty, M., Zagouras, P., Koroshetz, W. J., Wan, H. I., Trojanowski, J. Q., Shaw, L. M., & Biomarkers Consortium Alzheimer's Disease Plasma Proteomics Project. (2012). Plasma biomarkers associated with the apolipoprotein E genotype and Alzheimer disease. *Archives of Neurology*, *69*(10), 1310–1317.
265. Soininen, H., Partanen, J., Laulumaa, V., Helkala, E.-L., Laakso, M., & Riekkinen, P. J. (1989). Longitudinal EEG spectral analysis in early stage of Alzheimer's disease. In *Electroencephalography and Clinical Neurophysiology* (Vol. 72, Issue 4, pp. 290–297). https://doi.org/10.1016/0013-4694(89)90064-3
266. Soininen, Kosunen, O., Helisalmi, S., Mannermaa, A., Paljärvi, L., Talasniemi, S., Ryynänen, M., & Riekkinen, P. (1995). A severe loss of choline acetyltransferase in the frontal cortex of Alzheimer patients carrying apolipoprotein ε4 allele. *Neuroscience Letters*, *187*(2), 79–82.
267. Soldan, A., Pettigrew, C., & Albert, M. (2020). Cognitive Reserve from the Perspective of Preclinical Alzheimer Disease: 2020 Update. *Clinics in Geriatric Medicine*, *36*(2), 247–263.
268. Song, S., Stern, Y., & Gu, Y. (2022). Modifiable lifestyle factors and cognitive reserve: A systematic review of current evidence. *Ageing Research Reviews*, *74*, 101551.
269. Sorg, C., Riedl, V., Mühlau, M., Calhoun, V. D., Eichele, T., Läer, L., Drzezga, A., Förstl, H., Kurz, A., Zimmer, C., & Wohlschläger, A. M. (2007). Selective changes of resting-state networks in individuals at risk for Alzheimer's disease. *Proceedings of the National Academy of Sciences of the United States of America*, *104*(47), 18760–18765.
270. Spunt, B. (2016). *easy-optimize-x: fMRI Design Optimization Software*. https://doi.org/10.5281/zenodo.58616
271. Staehelin, H. B., Perrig-Chiello, P., Mitrache, C., Miserez, A. R., & Perrig, W. J. (1999). Apolipoprotein E genotypes and cognitive functions in healthy elderly persons. *Acta Neurologica Scandinavica*, *100*(1), 53–60.
272. Stern. (2009). Cognitive reserve. *Neuropsychologia*, *47*(10), 2015–2028.
273. Stern, Arenaza-Urquijo, E. M., Bartrés-Faz, D., Belleville, S., Cantilon, M., Chetelat, G., Ewers, M., Franzmeier, N., Kempermann, G., Kremen, W. S., Okonkwo, O., Scarmeas, N., Soldan, A., Udeh-Momoh, C., Valenzuela, M., Vemuri, P., Vuoksimaa, E., & the Reserve, Resilience and Protective Factors PIA Empirical Definitions and Conceptual Frameworks Workgroup. (2020). Whitepaper: Defining and investigating cognitive reserve, brain reserve, and brain maintenance. *Alzheimer's & Dementia: The Journal of the Alzheimer's Association*, *16*(9), 1305–1311.
274. Stern, Y., Gurland, B., Tatemichi, T. K., Tang, M. X., Wilder, D., & Mayeux, R. (1994). Influence of education and occupation on the incidence of Alzheimer's disease. *JAMA: The Journal of the American Medical Association*, *271*(13), 1004–1010.
275. Sternberg, S. (1966). High-speed scanning in human memory. *Science*, *153*(3736), 652–654.
276. Stock, A. J., Kasus-Jacobi, A., & Pereira, H. A. (2018). The role of neutrophil granule proteins in neuroinflammation and Alzheimer's disease. *Journal of Neuroinflammation*, *15*(1), 240.

277. Strittmatter, W. J., Saunders, A. M., Schmechel, D., Pericak-Vance, M., Enghild, J., Salvesen, G. S., & Roses, A. D. (1993). Apolipoprotein E: high-avidity binding to beta-amyloid and increased frequency of type 4 allele in late-onset familial Alzheimer disease. *Proceedings of the National Academy of Sciences of the United States of America*, *90*(5), 1977–1981.
278. Sun, Wang, B., Niu, Y., Tan, Y., Fan, C., Zhang, N., Xue, J., Wei, J., & Xiang, J. (2020). Complexity Analysis of EEG, MEG, and fMRI in Mild Cognitive Impairment and Alzheimer's Disease: A Review. In *Entropy* (Vol. 22, Issue 2, p. 239). https://doi.org/10.3390/e22020239
279. Surtees, P. G., Wainwright, N. W. J., Bowman, R., Luben, R. N., Wareham, N. J., Khaw, K.-T., & Bingham, S. A. (2009). No association between APOE and major depressive disorder in a community sample of 17,507 adults. *Journal of Psychiatric Research*, *43*(9), 843–847.
280. Tan, L., Nakanishi, E., & Lee, M. (2022). Association between exposure to air pollution and late-life neurodegenerative disorders: An umbrella review. *Environment International*, *158*, 106956.
281. Tang, M. X., Stern, Y., Marder, K., Bell, K., Gurland, B., Lantigua, R., Andrews, H., Feng, L., Tycko, B., & Mayeux, R. (1998). The APOE-epsilon4 allele and the risk of Alzheimer disease among African Americans, whites, and Hispanics. *JAMA: The Journal of the American Medical Association*, *279*(10), 751–755.
282. Tao, Z., Zhu, H., Zhang, J., Huang, Z., Xiang, Z., & Hong, T. (2022). Recent advances of eosinophils and its correlated diseases. *Frontiers in Public Health*, *10*, 954721.
283. The MathWorks Inc. (2022). *MATLAB* (9.12.10.01956245 (R2022a)) [Natick, Massachusetts].
284. Thompson, P. M., Martin, N. G., & Wright, M. J. (2010). Imaging genomics. *Current Opinion in Neurology*, *23*(4), 368–373.
285. Tuminello, E. R., & Han, S. D. (2011). The apolipoprotein e antagonistic pleiotropy hypothesis: review and recommendations. *International Journal of Alzheimer's Disease*, *2011*, 726197.
286. Van Hoesen, G. W., Hyman, B. T., & Damasio, A. R. (1986). Cell-specific pathology in neural systems of the temporal lobe in Alzheimer's disease. *Progress in Brain Research*, *70*, 321–335.
287. Vemuri, P., Jones, D. T., & Jack, C. R., Jr. (2012). Resting state functional MRI in Alzheimer's Disease. *Alzheimer's Research & Therapy*, *4*(1), 2.
288. Verfaillie, S. C. J., Tijms, B., Versteeg, A., Benedictus, M. R., Bouwman, F. H., Scheltens, P., Barkhof, F., Vrenken, H., & van der Flier, W. M. (2016). Thinner temporal and parietal cortex is related to incident clinical progression to dementia in patients with subjective cognitive decline. *Alzheimer's & Dementia: The Journal of the Alzheimer's Association*, *5*, 43–52.
289. Vermunt, L., Sikkes, S. A. M., van den Hout, A., Handels, R., Bos, I., van der Flier, W. M., Kern, S., Ousset, P.-J., Maruff, P., Skoog, I., Verhey, F. R. J., Freund-Levi, Y., Tsolaki, M., Wallin, Å. K., Olde Rikkert, M., Soininen, H., Spiru, L., Zetterberg, H., Blennow, K., … ICTUS/DSA study groups. (2019). Duration of preclinical, prodromal, and dementia stages of Alzheimer's disease in relation to age, sex, and APOE genotype. *Alzheimer's & Dementia: The Journal of the Alzheimer's Association*, *15*(7), 888–898.
290. Wang, Karp, A., Herlitz, A., Crowe, M., Kåreholt, I., Winblad, B., & Fratiglioni, L. (2009). Personality and lifestyle in relation to dementia incidence. *Neurology*, *72*(3), 253–259.
291. Wang, & Reddy, P. H. (2017). Role of Glutamate and NMDA Receptors in Alzheimer's Disease. *Journal of Alzheimer's Disease: JAD*, *57*(4), 1041–1048.
292. Wanliss, J. A., & Wanliss, G. E. (2022). Efficient calculation of fractal properties via the Higuchi method. *Nonlinear Dynamics*, *109*(4), 2893–2904.
293. Waring, S. C., Doody, R. S., Pavlik, V. N., Massman, P. J., & Chan, W. (2005). Survival among patients with dementia from a large multi-ethnic population. *Alzheimer Disease and Associated Disorders*, *19*(4), 178–183.
294. Waskom, M. (2021). seaborn: statistical data visualization. *Journal of Open Source Software*, *6*(60), 3021.
295. Weber, M. (2022). *Python package to add statistical annotations on an existing boxplot/barplot generated by seaborn*. https://github.com/webermarcolivier/statannot
296. Weiner, H., & Schuster, D. B. (1956). The electroencephalogram in dementia; some preliminary observations and correlations. *Electroencephalography and Clinical Neurophysiology*, *8*(3), 479–488.
297. Wellcome Centre for Human Neuroimaging. (2020). *SPM12 Software: Statistical Parametric Mapping*. https://www.fil.ion.ucl.ac.uk/spm/software/spm12/
298. Whalley, L. J., Deary, I. J., Appleton, C. L., & Starr, J. M. (2004). Cognitive reserve and the neurobiology of cognitive aging. *Ageing Research Reviews*, *3*(4), 369–382.
299. Whitfield-Gabrieli, S., & Nieto-Castanon, A. (2012). Conn: a functional connectivity toolbox for correlated and anticorrelated brain networks. *Brain Connectivity*, *2*(3), 125–141.
300. WHO. (2023). *Dementia*. World Health Organization. https://www.who.int/news-room/fact-sheets/detail/dementia
301. Wickham, H., Averick, M., Bryan, J., Chang, W., McGowan, L., François, R., Grolemund, G., Hayes, A., Henry, L., Hester, J., Kuhn, M., Pedersen, T., Miller, E., Bache, S., Müller, K., Ooms, J., Robinson, D., Seidel, D., Spinu, V., … Yutani, H. (2019). Welcome to the tidyverse. *Journal of Open Source Software*, *4*(43), 1686.
302. Wilson, R. S., Bienias, J. L., Berry-Kravis, E., Evans, D. A., & Bennett, D. A. (2002). The apolipoprotein E epsilon 2 allele and decline in episodic memory. *Journal of Neurology, Neurosurgery, and Psychiatry*, *73*(6), 672–677.
303. Wojciechowski, J., Jurewicz, K., Dzianok, P., Antonova, I., Paluch, K., Wolak, T., & Kublik, E. (2023). Common and distinct BOLD correlates of Simon and flanker conflicts which can(not) be reduced to time-on-task effects. *Human Brain Mapping*. https://doi.org/10.1002/hbm.26549

304. Wojsiat, J., Laskowska-Kaszub, K., Mietelska-Porowska, A., & Wojda, U. (2017). Search for Alzheimer's disease biomarkers in blood cells: hypotheses-driven approach. *Biomarkers in Medicine*, *11*(10), 917–931.
305. Wood, W. G., Li, L., Müller, W. E., & Eckert, G. P. (2014). Cholesterol as a causative factor in Alzheimer's disease: a debatable hypothesis. *Journal of Neurochemistry*, *129*(4), 559–572.
306. Worsley, K. J., Marrett, S., Neelin, P., Vandal, A. C., Friston, K. J., & Evans, A. C. (1996). A unified statistical approach for determining significant signals in images of cerebral activation. *Human Brain Mapping*, *4*(1), 58–73.
307. Wu, Z., Yang, Y., Song, Z., Ma, M., Feng, M., Liu, Y., Xing, H., Chang, Y., & Dai, H. (2022). PICALM rs3851179 Variants Modulate Left Postcentral Cortex Thickness, CSF Amyloid β42, and Phosphorylated Tau in the Elderly. *Brain Sciences*, *12*(12). https://doi.org/10.3390/brainsci12121681
308. Xia, M., Wang, J., & He, Y. (2013). BrainNet Viewer: a network visualization tool for human brain connectomics. *PloS One*, *8*(7), e68910.
309. Xie, J., Van Hoecke, L., & Vandenbroucke, R. E. (2021). The Impact of Systemic Inflammation on Alzheimer's Disease Pathology. *Frontiers in Immunology*, *12*, 796867.
310. Xu, W., Tan, L., & Yu, J.-T. (2015). The Role of PICALM in Alzheimer's Disease. *Molecular Neurobiology*, *52*(1), 399–413.
311. Yang, X., Li, J., Liu, B., Li, Y., & Jiang, T. (2016). Impact of PICALM and CLU on hippocampal degeneration. *Human Brain Mapping*, *37*(7), 2419–2430.
312. Yu, J.-T., Tan, L., & Hardy, J. (2014). Apolipoprotein E in Alzheimer's Disease: An Update. *Annual Review of Neuroscience*, *37*(1), 79–100.
313. Zawadzki, B., Strelau, J., Szczepaniak, P., & Śliwińska, M. (2010). *NEO-FFI. Inwentarz Osobowości Paula T. Costy Jr i Roberta R. McCrae. Adaptacja polska. Podręcznik* (A. Matczak, Ed.). Pracownia Testów Psychologicznych Polskiego Towarzystwa Psychologicznego.
314. Zhang, C., Kong, M., Wei, H., Zhang, H., Ma, G., Ba, M., & Alzheimer's Disease Neuroimaging Initiative. (2020). The effect of ApoE ε 4 on clinical and structural MRI markers in prodromal Alzheimer's disease. *Quantitative Imaging in Medicine and Surgery*, *10*(2), 464–474.
315. Zhang, Huang, H., Shen, D., & Alzheimer's Disease Neuroimaging Initiative. (2014). Integrative analysis of multi-dimensional imaging genomics data for Alzheimer's disease prediction. *Frontiers in Aging Neuroscience*, *6*, 260.
316. Zhang, Qin, W., Wang, D., Liu, B., Zhang, Y., Jiang, T., & Yu, C. (2015). Impacts of PICALM and CLU variants associated with Alzheimer's disease on the functional connectivity of the hippocampus in healthy young adults. *Brain Structure & Function*, *220*(3), 1463–1475.
317. Zhang, Wang, Z.-T., Liu, Y., Hu, H., Sun, Y., Hu, H.-Y., Ma, Y.-H., Tan, L., & Yu, J.-T. (2022). Peripheral Immune Cells and Cerebrospinal Fluid Biomarkers of Alzheimer's Disease Pathology in Cognitively Intact Older Adults: The CABLE Study. *Journal of Alzheimer's Disease: JAD*, *87*(2), 721–730.
318. Ziegler-Graham, K., Brookmeyer, R., Johnson, E., & Arrighi, H. M. (2008). Worldwide variation in the doubling time of Alzheimer's disease incidence rates. *Alzheimer's & Dementia: The Journal of the Alzheimer's Association*, *4*(5), 316–323.

Publications

[Publications directly underlying or related to this PhD thesis are marked with emphasis.]

[1] **Dzianok P**, Kublik E. (2023). Modified granulocyte count and erythrocyte measures in middle-aged, healthy carriers of *APOE* and *PICALM* risk genes for Alzheimer's disease. Acta Neurobiologiae Experimentalis. DOI: doi.org/10.55782/ane-2023-012.

[2] Wojciechowski J, Jurewicz K, **Dzianok P**, Antonova I, Paluch K, Wolak T, Kublik E. (2023). Common and distinct BOLD correlates of Simon and flanker conflicts which can(not) be reduced to time-on-task effects. Human Brain Mapping. DOI: 10.1002/hbm.26549.

[3] **Dzianok P**, Antonova I, Wojciechowski J, Dreszer J, Kublik E. (2022). The Nencki-Symfonia electroencephalography/event-related potential dataset: Multiple cognitive tasks and resting-state data collected in a sample of healthy adults. GigaScience. 7;11:giac015. DOI: 10.1093/gigascience/giac015.

[4] **Dzianok P**, Nagańska E. (2021). Genomika obrazowa – nowe narzędzie w diagnostyce chorób neurologicznych. Neurologia po Dyplomie, 4. ISSN: 2449-9641.

[5] **Dzianok P**, Kublik E. (2020). Commentary: Differential Signaling Mediated by ApoE2, ApoE3, and ApoE4 in Human Neurons Parallels Alzheimer's Disease Risk. Frontiers in Aging Neuroscience, 12, 127. DOI: 10.3389/fnagi.2020.00127.

[6] **Dzianok P**. (2020). Genomika obrazowa: nowy trend w badaniach nad chorobą Alzheimera (Imaging genomics: a new trend in Alzheimer's disease research). Kosmos. Problemy nauk biologicznych 69, 1. DOI: 10.36921/kos.2020_2636.

Conference publications

[7] **Dzianok P**, Kołodziej M and Kublik E. (2021). Detecting attention in Hilbert-transformed EEG brain signals from simple-reaction and choice-reaction cognitive tasks. 2021 IEEE 21st International Conference on Bioinformatics and Bioengineering (BIBE), 2021. DOI: 10.1109/BIBE52308.2021.9635187.

Preprints

[8] **Dzianok P**, Kublik E. (2023). Imaging genomics: Polish Electroencephalography, Alzheimer's Risk-genes, Lifestyle and Neuroimaging (PEARL-Neuro) Database, a cohort of non-demented middle-aged adults and initial results. Under the review process: Scientific Data.

[9] **Dzianok P**, Wojciechowski J, Wolak T, Kublik E. Effect of *APOE/PICALM* risk-genes on resting-state EEG/fMRI features in cognitively intact and healthy individuals is in-line with Alzheimer's disease EEG hallmarks. Under preparation.

Appendix

Table description that can be applied to all tables presented below: “Shapiro-Wilk *p*-value” and “QQ plot” columns corresponds to the testing of model residuals; “Factor normality” column corresponds to additional checking of normality assumption by groups by inspection of QQ plots and using Shapiro-Wilk test (where “+” means that that normality of distribution for all separate groups was confirmed, “-“ means that the distribution was not normal in all tested groups, and “+/-“ means that in some groups the distribution was not normal; “Leven’s test *p*-value” corresponds to checking the homogeneity of variances assumption. “QQ plot” values correspond to the visual evaluation of QQ plots, where “+” means that all the points fall approximately along the reference line, “-“ means that the normality cannot be assumed, and “+/-“ that based only on QQ plots normality of the data is difficult to determine.

Table 34. Demographic and health measures: test assumptions for one-way ANOVA

Parameter	**Shapiro-Wilk *p*-value**	**QQ plot**	**Factor normality**	**Leven's test *p*-value**
Age	< .05	-	+/-	.84
EHI	< .001	-	-	.82
AUDIT scores	< .001	-	+/-	.32
BMI	< .05	+/-	+	.55

Table 35. Psychometric tests assessment: test assumptions for two-way ANOVA and exact *p*-values for sex factor and interaction

Parameter	**Shapiro-Wilk *p*-value**	**QQ plot**	**Factor normality**	**Leven's test *p*-value**
BDI	< .001	-	+/-	.44
SES	.79	+	+	.12
Mini-Cope-1	.07	+/-	+/-	.76
Mini-Cope-2	< .05	-	+/-	.62
Mini-Cope-3	.27	+	+/-	.52
Mini-Cope-4	.39	+	+	.84
Mini-Cope-5	< .001	-	+/-	< .05
Mini-Cope-6	< .05	-	+/-	.45
Mini-Cope-7	.48	+	+/-	.77
NEO-NEU	< .01	-	+/-	.22

NEO-EXT	.07	+/-	+/-	.23
NEO-OPE	.97	+	+/-	.89
NEO-AGR	.24	+	+/-	.94
NEO-CON	< .05	-	+	.51
RAVEN	< .05	-	+	.12
CVLT-1	.15	+	+	.95
CVLT-2	.07	+	+/-	.51
CVLT-3	.17	+	+/-	.62
CVLT-4	< .001	-	+/-	.51
CVLT-5	< .001	-	+/-	.32
CVLT-6	< .001	-	+/-	.41
CVLT-7	< .001	-	+/-	.54
CVLT-8	< .001	-	+/-	.53
CVLT-9	< .001	-	-	.81
CVLT-10	< .001	-	-	.22
CVLT-11	< .001	-	-	.43
CVLT-12	< .001	-	-	.05

Table 36. Psychometric tests assessments: test assumptions for one-way ANOVA

Parameter	**Shapiro-Wilk *p*-value**	**QQ plot**	**Factor normality**	**Leven's test *p*-value**
BDI	< .001	-	+/-	.37
Mini-Cope-2	< .01	-	+/-	.99
Mini-Cope-5	< .001	-	+/-	< .01
Mini-Cope-6	< .001	-	+/-	.15
NEO-NEU	< .05	-	+/-	< .05
NEO-CON	.39	+	+	.61
RAVEN	< .05	-	+/-	< .05
CVLT-4	.06	+/-	+/-	.89
CVLT-5	< .001	-	-	.79
CVLT-6	< .001	-	-	.68
CVLT-7	< .001	-	-	.70
CVLT-8	< .001	-	-	.49
CVLT-9	< .001	-	-	.68
CVLT-10	< .001	-	-	.55
CVLT-11	< .001	-	-	.75
CVLT-12	< .001	-	-	.29

Table 37. miRNA: test assumptions for two-way ANOVA and exact *p*-values for sex factor and interaction

Parameter	**Shapiro-Wilk *p*-value**	**QQ plot**	**Factor normality**	**Leven's test *p*-value**	***p*-value sex**	***p*-value interaction**
miR-29b-3p	.45	+	+/-	.13	0.95	0.33
miR-30-5p	.36	+/-	+/-	.09	0.96	0.20
miR-34a-5p	< .05	-	+	.19	-	-
miR-125b-5p	.46	+	+	.19	0.27	0.62
miR-135a-5p	.15	+	+	.24	0.40	0.63
miR-142-3p	.11	+/-	+	< .05	-	-
miR-146-5p	< .01	+/-	+/-	.97	-	-
miR-200a-3p	.09	+/-	+/-	.87	0.82	0.11

miR-483-5p	< .01	+/-	+/-	.55	-	-
miR-486-5p	< .01	+/-	+/-	.86	-	-
miR-502-3p	0.35	+	+	.50	0.17	0.54

Table 38. miRNA: test assumptions for one-way ANOVA

Parameter	**Shapiro-Wilk *p*-value**	**QQ plot**	**Factor normality**	**Leven's test *p*-value**
miR-34a-5p	< .05	+/-	+/-	.43
miR-142-3p	0.11	+	+/-	< .05
miR-146-5p	<.01	+	+/-	0.96
miR-483-5p	< .01	-	+/-	.055
miR-486-5p	< .01	-	+/-	.80

Table 39. Behavioral results: test assumptions for two-way ANOVA and exact *p*-values for sex factor and interaction

Parameter	**Shapiro-Wilk *p*-value**	**QQ plot**	**Factor normality**	**Leven's test *p*-value**	***p*-value sex**	***p*-value interaction**
EEG experiment						
MSIT LD RT	.07	+	+	.87	-	-
log	.50	+	+	.92	< .05	.37
MSIT HD RT	< .01	-	+/-	.35	-	-
log	.43	+	+/-	.55	< .01	.11
STM LD RT	< .05	+/-	+	.61	-	-
log	.21	+	+	.72	.12	.19
STM HD RT	.06	+/-	+/-	.62	-	-
log	.34	+	+	.76	.22	.12
fMRI experiment						
MSIT LD RT	.40	+	+/-	.80	< .05	.28
MSIT HD RT	.11	+	+/-	.93	< .05	.39
STM LD RT	.12	+	+	.97	-	-
log	.87	+	+	.96	.45	.62
STM HD RT	< .05	-	+/-	.85	-	-
log	.12	+	+	.73	.55	.34

Table 40. Cortical thickness: test assumptions for two-way ANOVA and exact *p*-values for sex factor and interaction

Parameter	**Shapiro-Wilk *p*-value**	**QQ plot**	**Factor normality**	**Leven's test *p*-value**	***p*-value sex**	***p*-value interaction**
Parahippocampal gyrus left	.14	+	+/-	.89	.85	.22
Parahippocampal gyrus right	.78	+	+	.74	.83	.46
Supramarginal gyrus left	.71	+	+	.42	.07	.59
Supramarginal gyrus right	.18	+	+/-	.36	.94	.30
Temporal pole left	.06	+/-	+	.19	< .01	.28
Temporal pole right	.88	+	+	.34	.07	.11
Superior parietal lobule left	< .05	+/-	+/-	.66	-	-
Superior parietal lobule right	< .01	-	+/-	.44	-	-

Inferior temporal gyrus left	1.0	+	+	.81	0.48	0.41
Inferior temporal gyrus right	.31	+	+/-	.64	.43	.89

Table 41. Cortical thickness: test assumptions for one-way ANOVA

Parameter	**Shapiro-Wilk *p*-value**	**QQ plot**	**Factor normality**	**Leven's test *p*-value**
Superior parietal lobule left	.06	-	+/-	.59
Superior parietal lobule right	< .05	-	+/-	.37

Table 42. Blood measures: test assumptions for two-way ANOVA and exact *p*-values for sex factor and interaction

Parameter	**Shapiro-Wilk *p*-value**	**QQ plot**	**Factor normality**	**Leven's test *p*-value**	***p*-value sex**	***p*-value interaction**
Eosinophils	< .001	+/-	+/-	.74	-	-
Basophils	< .01	+/-	+/-	.63	-	-
Neutrophils	.22	+/-	+	.63	< .05	.81
Leukocytes	< .05	+/-	+	.26	-	-
Erythrocytes	.26	+	+	.90	< .001	.65
Hemoglobin	.96	+	+	.91	< .001	.20
Hematocrit	.58	+	+/-	.82	< .001	.49
MCV	.31	+	+/-	.30	.16	.89
MCH	< .05	+/-	+/-	.21	-	-
MCHC	< .01	+/-	+	.14	-	-
RDW-CV	< .001	-	+/-	.25	-	-
Platelets	.40	+	+	< .05	-	-
PDW	.05	-	+	.63	-	-
MPV	.13	+	+	.61	.85	.64
P-LCR	.13	+	+	.55	.77	.55
Lymphocytes	< .001	-	+/-	.52	-	-
Monocytes	.31	+	+/-	.22	< .001	.53
Total cholesterol	.06	+/-	+	.56	< .001	.61
HDL cholesterol	.10	+	+	< .05	< .001	.36
No-HDL cholesterol	< .05	+/-	+	.30	-	-
LDL cholesterol	< .05	+/-	+/-	.34	-	-

Table 43. Blood measures: test assumptions for one-way ANOVA

Parameter	**Shapiro-Wilk *p*-value**	**QQ plot**	**Factor normality**	**Leven's test *p*-value**
Eosinophils	< .001	-	+/-	.38
Basophils	< .01	-	+/-	.34
Leukocytes	< .05	+/-	+/-	.34
MCH	< .001	-	+/-	.67
MCHC	<.05	+/-	+	.07
RDW-CV	< .001	-	+/-	.49
Platelets	.06	-	+/-	.44

PDW	.01	-	+/-	.94
Lymphocytes	< .001	-	+/-	.39
No-HDL cholesterol	.15	+	+	.92
LDL cholesterol	.08	+/-	+/-	.63

Table 44. HFD measures: test assumptions for two-way ANOVA and exact *p*-values for sex factor and interaction

Parameter	Shapiro-Wilk *p*-value	QQ plot	Factor normality	Leven's test *p*-value	*p*-value sex	*p*-value interaction
Global	.84	+	+	.77	< .05	.06
MF	< .05	-	+/-	.24	—	—
FL	.70	+	+	.31	.88	< .01
FR	.62	+	+	.76	.21	< .01
C	.39	+	+/-	.40	.06	.16
CTL	.32	+	+	.73	.36	.12
CTR	.15	+	+	.48	< .05	.06
PC	.10	+	+	.49	.11	.64
PTL	.79	+	+/-	.67	< .05	.20
PTR	< .05	+/-	+	.55	—	—
OC	.12	+	+	.54	.10	.88
OL	.67	+	+	.85	< .01	.81
OR	< .05	+/-	+	.51	—	—

MF: midfrontal; FL: frontal-left; FR: frontal-right; C: central; CTL: central-left; CTR: central-right; PC: posterior-central; PTL: posterior-left; PTR: posterior-right; OC: occipital-central; OL: occpital-left; OR: occipital-right.

Table 45. HFD measures: test assumptions for one-way ANOVA

Parameter	Shapiro-Wilk *p*-value	QQ plot	Factor normality	Leven's test *p*-value
MF	< .001	-	+/- (A+P+ < .01)	.51
PTR	.12	+	+	.07
OR	.06	+/-	+	.52

MF: midfrontal; PTR: posterior-right; OR: occipital-right.

Table 46. Delta relative power: test assumptions for two-way ANOVA and exact *p*-values for sex factor and interaction

Parameter	Shapiro-Wilk *p*-value	QQ plot	Factor normality	Leven's test *p*-value	*p*-value sex	*p*-value interaction
Global	.38	+	+/-	.50	.37	< .05
MF	.22	+	+/-	.61	.95	.16
FL	< .05	-	+/-	.32	–	–
FR	< .01	-	+/-	.51	–	–
C	.71	+	+	.93	.36	< .05
CTL	< .01	-	+/-	< .01	–	–
CTR	.25	+	+/-	.08	.33	.06
PC	.24	+	+	.90	.46	.31
PTL	.20	+	+/-	.17	.06	< .05
PTR	.13	+	+/-	.15	.14	< .05

OC	.26	+	+	.96	.23	.16
OL	< .05	+/-	+/-	.61	–	–
OR	.25	+	+	.68	.08	.054

MF: midfrontal; FL: frontal-left; FR: frontal-right; C: central; CTL: central-left; CTR: central-right; PC: posterior-central; PTL: posterior-left; PTR: posterior-right; OC: occipital-central; OL: occpital-left; OR: occipital-right.

Table 47. Delta relative power: test assumptions for one-way ANOVA

Parameter	**Shapiro-Wilk *p*-value**	**QQ plot**	**Factor normality**	**Leven's test *p*-value**
FL	< .01	+/-	+/-	.64
FR	< .001	-	+/-	.55
CTL	< .001	-	+/-	.07
OL	< .01	-	+/-	.35

MF: midfrontal; PTR: posterior-right; OR: occipital-right.

Table 48. Theta relative power: test assumptions for two-way ANOVA and exact *p*-values for sex factor and interaction

Parameter	**Shapiro-Wilk *p*-value**	**QQ plot**	**Factor normality**	**Leven's test *p*-value**	***p*-value sex**	***p*-value interaction**
Global	.73	+	+	.41	< .05	.78
MF	.84	+	+/-	.10	< .05	.92
FL	.69	+	+	.71	< .05	.91
FR	.52	+	+/-	.19	< .05	.77
C	.92	+	+	.25	< .05	.84
CTL	.27	+	+	.26	< .05	.55
CTR	.24	+	+	.63	< .05	.21
PC	.64	+	+	.89	.06	.78
PTL	.56	+	+	.52	< .05	.38
PTR	.60	+	+	.71	< .05	.62
OC	.64	+	+	.28	< .05	.92
OL	.80	+	+	.34	< .01	.86
OR	.37	+	+	.62	< .01	.86

MF: midfrontal; FL: frontal-left; FR: frontal-right; C: central; CTL: central-left; CTR: central-right; PC: posterior-central; PTL: posterior-left; PTR: posterior-right; OC: occipital-central; OL: occpital-left; OR: occipital-right.

Table 49. Low alpha relative power: test assumptions for two-way ANOVA and exact *p*-values for sex factor and interaction

Parameter	**Shapiro-Wilk *p*-value**	**QQ plot**	**Factor normality**	**Leven's test *p*-value**	***p*-value sex**	***p*-value interaction**
Global	.07	+	+	.93	.15	< .01
MF	< .05	+/-	+/-	.94	–	–
FL	.16	+	+/-	.99	.12	< .01
FR	.07	+	+/-	.94	.17	< .01
C	< .05	+/-	+	.80	–	–
CTL	.11	+	+	.99	.13	< .01
CTR	.13	+	+	.92	.11	< .01
PC	.22	+	+/-	.75	.20	< .01
PTL	.17	+	+	.42	.22	< .01

PTR	.13	+	+	.75	.12	< .01
OC	.09	+	+/-	.89	.11	< .01
OL	.29	+	+	.76	.22	< .01
OR	.17	+	+	.86	.23	< .01

MF: midfrontal; FL: frontal-left; FR: frontal-right; C: central; CTL: central-left; CTR: central-right; PC: posterior-central; PTL: posterior-left; PTR: posterior-right; OC: occipital-central; OL: occpital-left; OR: occipital-right.

Table 50. Low alpha relative power: test assumptions for one-way ANOVA

Parameter	**Shapiro-Wilk *p*-value**	**QQ plot**	**Factor normality**	**Leven's test *p*-value**
MF	.14	+	+	.45
C	.46		+	.83

MF: midfrontal; PTR: posterior-right; OR: occipital-right.

Table 51. High alpha relative power: test assumptions for two-way ANOVA and exact *p*-values for sex factor and interaction

Parameter	**Shapiro-Wilk *p*-value**	**QQ plot**	**Factor normality**	**Leven's test *p*-value**	***p*-value sex**	***p*-value interaction**
Global	< .05	+/-	+	.97	–	–
MF	< .05	+/-	+/-	.94	–	–
FL	< .05	+/-	+	.88	–	–
FR	< .01	-	+/-	.93	–	–
C	.41	+	+	.94	.08	.48
CTL	.49	+	+/-	.91	< .05	.18
CTR	.12	+	+/-	.84	< .05	.32
PC	.07	+	+	.68	.22	.23
PTL	.14	+	+	.94	< .05	.32
PTR	< .05	+/-	+	.87	–	–
OC	.09	+	+/-	.78	< .05	.31
OL	.15	+	+	.86	< .01	.29
OR	.29	+	+	.59	< .01	.18

MF: midfrontal; FL: frontal-left; FR: frontal-right; C: central; CTL: central-left; CTR: central-right; PC: posterior-central; PTL: posterior-left; PTR: posterior-right; OC: occipital-central; OL: occpital-left; OR: occipital-right.

Table 52. High alpha relative power: test assumptions for one-way ANOVA

Parameter	**Shapiro-Wilk *p*-value**	**QQ plot**	**Factor normality**	**Leven's test *p*-value**
Global	.16	+	+	.92
MF	.08	+	+/-	.97
FL	< .05	-	+/-	.41
FR	< .05	-	+/-	.81
PTR	.09	+/-	+	.95

MF: midfrontal; PTR: posterior-right; OR: occipital-right.

Table 53. ERP MSIT: N2/P3 peak amplitudes and peak latencies and LSP average amplitude: test assumptions for one-way ANOVA in 00 condition

Parameter	**Shapiro-Wilk *p*-value**	**QQ plot**	**Factor normality**	**Leven's test *p*-value**
N2 peak amplitude: Cz	< .01	-	+/-	.90
N2 peak latency: Cz	.29	+	+	.38
P3 peak amplitude: Pz	< .001	-	+/-	.20
P3 peak latency: Pz	.17	+	+	.36
LSP average amplitude: Pz	< .001	+/-	+/-	.08

MF: midfrontal; PTR: posterior-right; OR: occipital-right.

Table 54. ERP MSIT: N2/P3 peak amplitudes and peak latencies LSP average amplitude: test assumptions for one-way ANOVA in FS condition

Parameter	**Shapiro-Wilk *p*-value**	**QQ plot**	**Factor normality**	**Leven's test *p*-value**
N2 peak amplitude: Cz	< .05	+/-	+/-	.83
N2 peak latency: Cz	.18	+	+/-	.47
P3 peak amplitude: Pz	<.01	-	+/-	.41
P3 peak latency: Pz	< .001	-	+/-	.39
LSP average amplitude: Pz	< .001	-	+/-	.27

MF: midfrontal; PTR: posterior-right; OR: occipital-right.

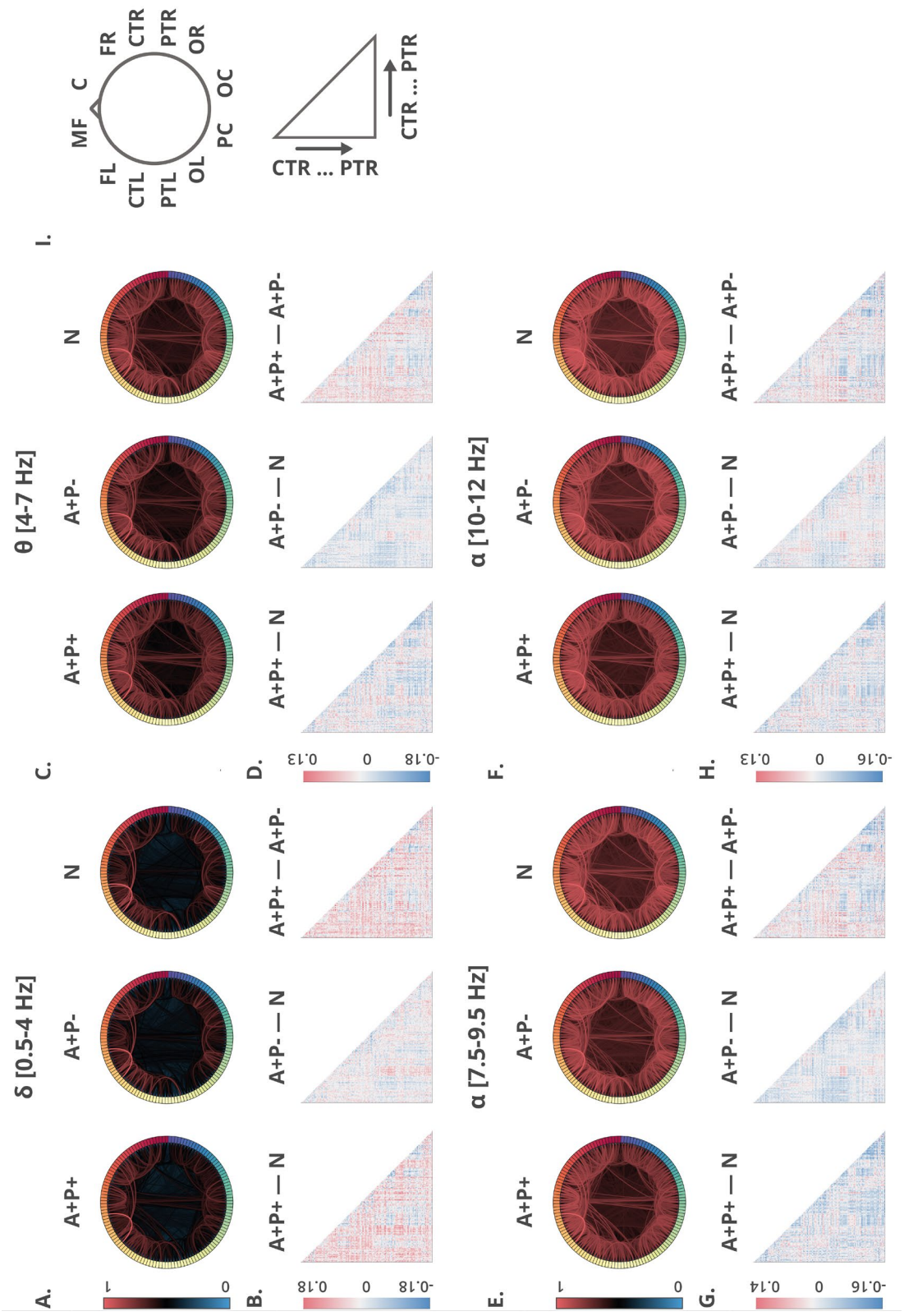

Figure 29. Connectivity (coherence) using high-density montage featuring all 128 electrodes. Connectograms are displayed for every group, with distinct frequency bands labeled as A., E., C., and F. in the graphs. Matrix representations showcasing group differences are presented in graphs B., D., G., and H. Graph I. shows as a legend with details about electrode placement in all the plots, arranged in alignment with previously defined clusters.